universität wien

DIPLOMARBEIT

Titel der Diplomarbeit

Contribution of Activin Signals to Progression of Malignant Pleural Mesothelioma and Evaluation of Therapeutic Implications

Verfasserin

Julia Münzker

angestrebter akademischer Grad

Magistra der Naturwissenschaften (Mag.rer.nat.)

Wien, 2011

Studienkennzahl lt. Studienblatt:	A 442
Studienrichtung lt. Studienblatt:	Diplomstudium Anthropologie
Betreuerin / Betreuer:	Priv. Doz. Dr. Michael Grusch

Danksagung

Mein besonderer Dank gilt meinem Betreuer Priv. Doz. Dr. Michael Grusch, für all seine Unterstützung und freundliche Betreuung.

Danke an Dr. Mir Ali Reza Hoda, für sein großes Engagement und Begeisterung für das Projekt, seine motivierenden Worte, freundliche Betreuung und Unterstützung.

Ein besonders herzlicher Dank gilt meinen beiden lieben Kolleginnen Emine Sahin und Sara Ghassemi, für die Hilfe und Unterstützung, die unzähligen Gespräche und Cafe-Pausen. Ich hätte mir keine besseren Kolleginnen wünschen können!

Danke an Dr. Walter Klepetko, dem Leiter der Thoraxchirurgie des AKH Wien, für die Administration dieser Studie. Dr. Bahil Ghanim für seine stets freundliche Unterstützung und die zahllosen lustigen Gespräche! Dr. Balazs Hegedus, Prof. Dr. Walter Berger und seiner ganzen Arbeitsgruppe, die mir gegenüber stets freundlich und hilfsbereit war!

Danke an meine Familie, für ihre Untersützung in jeglicher Hinsicht. Danke an meine lieben Freunde und Studienkollegen, die mich während des Studiums begleitet haben.

Mein größter und herzlichster Dank gilt meiner lieben Mutter, der ich diese Arbeit widmen möchte! Danke, dass du immer für mich da bist, immer ein offenes Ohr für mich hast, mich unterstützt und zu mir hältst. Danke für die stets liebevollen, ermutigenden und motivierenden Worte. Ohne dich wäre dieses Studium nicht möglich gewesen. Danke für alles!

Table of Contents

1 Abstract

Background: Malignant pleural mesothelioma (MPM) is an asbestos-related malignancy characterized by frequent resistance to chemo- and radiotherapy. Growth factors of the activin family are involved in malignant growth in several tumor types including non-small cell lung cancer (NSCLC) and esophageal cancer. The aim of the present study was to investigate activin signals in MPM cell models and their contribution to malignant growth and spreading.

Methods: The expression of the activin βA, βB, βC and βE subunits (encoded by the genes INHBA, INHBB, INHBC, INHBE), activin receptors (ACVR2, ACVR2B, ALK4 and ALK7) and activin antagonizing factors was analyzed in a panel of 9 MPM cell lines and in non-malignant mesothelial cells by RT- and qRT-PCR. Activin A expression was also analyzed by immunohistochemistry in paraffin embedded tissues. For functional analysis of activin signals, MPM cell lines were treated with exogenous activin A, activin receptor inhibitors or INHBA-targeting siRNA. Cell growth was assessed by MTT and clonogenic growth assays and cell migration by scratch and transwell assays. Phosphorylation of SMAD2 was analyzed by Western blotting as readout for activation of the canonical activin/TGF-β signaling pathway.

Results: Expression data in mesothelioma cell models obtained by real-time PCR revealed high expression of activin-βA and activin receptors in most cell lines compared to non-malignant mesothelial cells. Likewise, immunohistochemistry in paraffin embedded tissue sections of MPM patients showed intense cytoplasmic staining for activin A in the tumor cells of a subset of the cases analyzed. Treatment with exogenous activin A induced SMAD2 phosphorylation in all cell lines tested, thus demonstrating functionality of the activin signaling axis in mesothelioma cell models. In contrast to the human hepatocarcinoma cell line HepG2, which in agreement with previous reports was inhibited, proliferation of mesothelioma cell models was stimulated by activin A as observed by MTT assays and clonogenic assays. Treatment with two different kinase inhibitors of activin receptors (SB-431542, A8301) in contrast, clearly inhibited mesothelioma cell proliferation and clonogenicity as well as migration. As kinase inhibitors are not absolutely specific for activin receptors and also co-target TGF-β receptors, INHBA was also silenced with siRNA oligonucleotides. As expected, transfection with INHBA-targeting siRNA but not scrambled control siRNA decreased activin-βA expression level and impaired cell proliferation. Finally, the influence of Trichostatin A and 5-azacytidine on the expression of INHBA was tested as single agents, as well as in combination, but no clear trend towards up- or down-regulation could be observed.

Conclusions: The data generated during this investigation clearly suggest that deregulated activin A signaling contributes to the malignant phenotype of mesothelioma cells and might therefore represent a valuable candidate for therapeutic interference.

2 Zusammenfassung

Hintergrund: Das maligne Pleuramesotheliom (MPM) ist ein Asbest-bedingter bösartiger Tumor mit häufig auftretender Resistenz gegen Chemo- und Strahlentherapie. Wachstumsfaktoren aus der Aktivin Superfamilie spielen beim malignen Wachstum von verschiedenen Tumorerkrankungen, einschließlich dem Nicht-Kleinzelligen Bronchialkarzinom und Ösophaguskarzinom eine wichtige Rolle. Das Ziel dieser Studie war es zu untersuchten, welche Rolle Activin Signale in MPM Zellmodellen spielen und inwieweit diese zu Wachstum und Migration beitragen.

Methoden: Die Expression von Activin βA, βB, βC und βE (kodiert durch die Gene INHBA, INHBB, INHBC and INHBE), Aktivin-Rezeptoren (ACVR2, ACVR2B, ALK4 und ALK7) und Aktivin-Antagonisten wurde in 9 MPM Zelllinien und in nicht-malignen Mesothelzellen mittels RT- und qRT-PCR untersucht. Die Aktivin A Expression wurde weiters mittels Immunhistochemie in Paraffin-eingebetteten MPM-Gewebeproben untersucht. Zur funktionellen Analyse von Aktivin Signalen wurden MPM Zelllinien exogen mit Aktivin A, Aktivin-Rezeptor-Inhibitoren und INHBA-regulierenden siRNAs behandelt. Die Ermittlung der Zellproliferation erfolgte durch MTT und Clonogenic Assays und Zellmigration wurde durch Scratch und Transwell Assays ermittelt. Die Phosphorylierung von SMAD2 wurde mittels Western Blot untersucht als Nachweis für die Aktivierung des kanonischen Aktivin/TGF-β Signalweges.

Ergebnisse: Die mit PCR durchgeführten Expressionsanalysen zeigten eine hohe Expression von Aktivin A und Aktivin-Rezeptoren in den meisten Zelllinien im Vergleich zu nicht malignen Mesothelzellen. Immunhistochemisch konnte in Gewebeproben von MPM Patienten eine intensive zytoplasmatische Färbung der Tumorzellen gezeigt werden. Die Behandlung mit exogenem Aktivin A führte zu einer Phosphorylierung von SMAD2 in allen Zelllinien, was auf die Funktionalität der Aktivin-Signalachse in MPM Zelllinien schließen lässt. Im Gegensatz zur humanen Leberkrebszelllinie HepG2, die durch eine Behandlung mit Aktivin A inhibiert wird, konnte die Proliferation von Mesotheliom-Zelllinien durch Behandlung mit Aktivin A stimuliert werden, wie MTT Assays und Clonogenic Assays zeigten. Eine Behandlung mit zwei verschiedenen Kinase-Inhibitoren für Aktivin-Rezeptoren (SB-431542, A8301) führte hingegen zu einer klaren Inhibierung der Proliferation, Klonogenität und Migration von Mesotheliom-Zellen. Da diese Kinase-Inhibitoren jedoch nicht spezifisch für Aktivin-Rezeptoren sind und zusätzlich auch auf TGF-β Rezeptoren wirken, wurde die Expression von INHBA zusätzlich durch siRNA-Oligonukleotide reduziert. Wie erwartet wurde durch die Transfektion mit siRNA

spezifisch für Aktivin A, jedoch nicht durch Scrambled Kontroll-siRNA die Aktivin A Expression reduziert und die Zellproliferation geschwächt. Abschließend wurde der Einfluß von Trichostatin A und 5-Azacytidine als Einzelsubstanzen und als Kombination auf die Genexpression von INHBA getestet, allerdings konnte kein klarer Trend bezüglich einer Erhöhung oder Reduktion der Expression festgestellt werden.

Schlussfolgerung: Diese Daten zeigen, dass deregulierte Aktivin A Expression zum malignen Phänotyp von Mesotheliom-Zellen beiträgt und dass Aktivin-Signale als neues therapeutisches Target weiter untersucht werden sollten.

3 Introduction

3.1 Activins

Activins are members of the transforming growth factor-beta (TGF-β) superfamily of growth and differentiation factors (10) and were discovered in the 1980's as gonadal proteins that are able to stimulate the secretion of follicle stimulating hormone (FSH) from pituitary gonadotropes (11-13). Based on tsequence similarities, the TGF-βsuperfamily can be divided into three subfamilies: TGF-β *sensu stricto*, bone morphogenetic proteins (BMPs) and the activin subfamily (14). There are also many distant family members, like the Anti-Mullerian Hormone (AMH), which is also known as the Mullerian Inhibiting Substance (MIS), Lefty, Myostatin (also known as growth and differentiation factor 8 (GDF8)), Nodal and inhibin-α (INHA) (14).

3.1.1 Structure

Like other members of the TGF-βsuperfamily, activins consist of two subunits that are covalently linked via a single disulfide bond. In humans and other mammals, four different subunits have already been identified, called beta A, beta B, beta C and beta E, which are encoded by a single gene – INHBA, INHBB, INHBC and INHBE (15). There is also a fifth subunit, called beta D, that has not been identified in humans but in Xenopus laevis (16).
The four mammalian activin subunits can either form homodimers or heterodimers of two beta-subunits (a list of possible formations is presented in Table 1). So far, only little is known about the subunits activin beta C and E, whereas the best investigated subunit is activin beta A. The two activin heterodimers activin AB and AC have been described under physiological conditions in vivo (17, 18), whereas the formation of activin AE, BC and CE has only been found in in vitro systems (19-22).
All beta-subunits are synthesized as inactive proforms with 350-426 amino acids and a molecular weight ranging between 38 and 50 kDa (15). In order to gain biological activity, all activins need to be processed. The N-terminal prodomains are removed in the early Golgi by convertases of the subtilising/kexin family (23) to release mature peptides of 112 to 134 amino acids (15). Unprocessed forms of activin A do not show any biological activity (24).
Activins and other members of the TGF-βsuperfamily harbour nine conserved cysteines in the mature peptides, which are required for the 3-dimensional structure. The intermolecular disulfide bond, which is necessary for dimerization, is created by the sixth cysteine, whereas the other cysteines are involved in the formation of three intramolecular disulfide bonds, leading to the so-called cysteine knot, necessary for the correct folding of the protein and biological activity

(25). Cysteine mutations lead to an incorrect protein folding, resulting in reduced biological activity, the secretion of an unprocessed form of the protein, or no secretion at all (25).

Table 1. Possible Formations of Activin Subunits

Activin	***Composition of Activin Subunits***
Activin A	beta A and beta A
Activin B	beta B and beta B
Activin C	beta C and beta C
Activin E	beta E and beta E
Activin AB	beta A and beta B
Activin AC	beta A and beta C
Activin AE	beta A and beta E
Activin BC	beta B and beta C
Activin BE	beta B and beta E
Activin CE	beta A and beta E

3.1.2 Receptors and Signalling Mechanisms

Activin signals are transduced via a heterotetrameric receptor complex consisting of two different kinds of single-pass transmembrane serine threonine kinase receptors (type I and type II) (26). Both types of activin receptors consist of a small extracellular region, a large intracellular domain with serine threonine kinase activity and a transmembrane region, but vary in their structural and functional properties. For the mediation of activin signal transduction, the type II receptors (ActR-II/ACVR2 and ActR-IIB/ACVR2B) need to be activated by ligand binding. The activated type II receptors subsequently recruit and phosphorylate a type I receptor and form a receptor complex (14, 27). Activin A preferentially binds to the type I receptor ActR-IB/ACVR1B, also known as activin receptor-like kinase 4 (ALK4), whereas activin AB and activin B preferentially form a complex with the type I receptor ACVR1C (ALK7) (4, 28). The exact signalling mechanism and receptors for activin C and activin E have not been identified so far.

Within this complex of activin receptors, the activated type II receptor phosphorylates the type I receptor in the regulatory GS domain, also called GS-Box – a segment rich in glycine and serine that is located prior to the serine threonine kinase domain (27, 29, 30). The phosphorylation of the type I receptor leads to the activation of the downstream receptor-regulated SMAD proteins (R-SMADs), such as SMAD2 and SMAD3. There is also another group of R-SMADs (SMAD1,

SMAD5, SMAD8), which get phosphorylated by BMP-receptors (31, 32), whereas SMAD2 and SMAD3 are specific for activins and TGF-β (33).

Once the R-SMADs are activated, they recruit the so called common-mediator SMAD4 (Co-SMAD4) (34) and subsequently, this whole complex translocates to the nucleus where it is directly involved in the regulation of gene expression (35). A schematic diagram of the TGF-β and activin signalling mechanism via the SMAD-pathway is presented in Figure 1.

Beside the transduction of activin signals via SMAD proteins, there might be alternative independent signaling pathways for activins like the MAP kinases ERK1/2 (36, 37), the stress-activated kinase p38 (38), the PI3K/Akt pathway (39), or Rho and JNK (40).

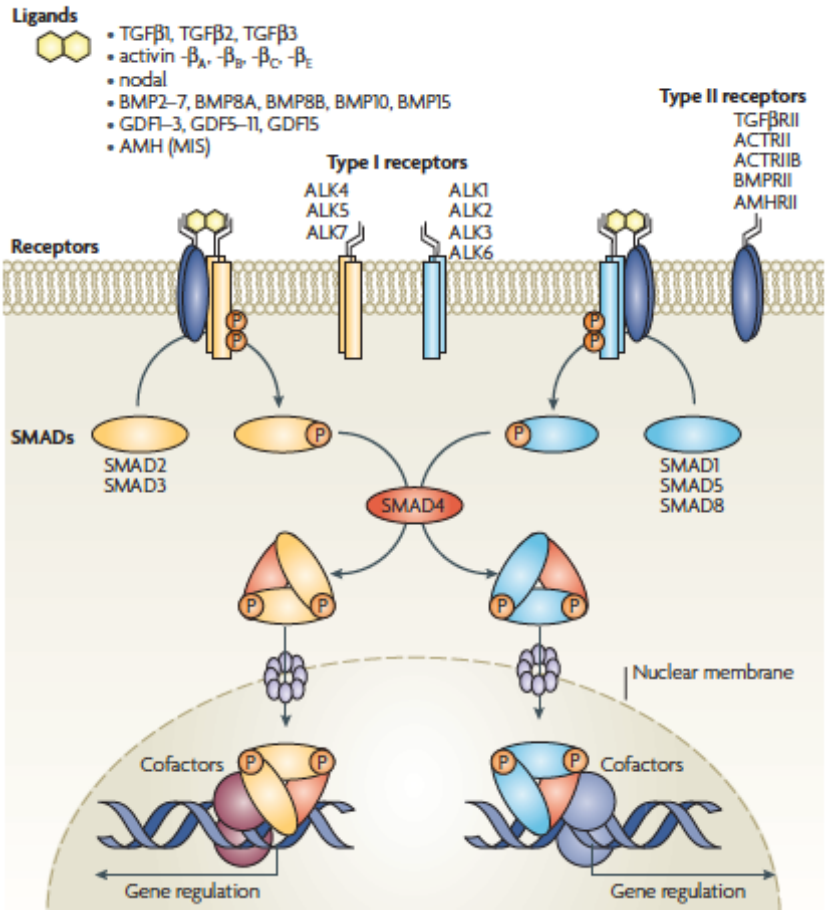

Figure 1. TGF-beta family signaling mechanism via the SMAD-pathway (4).

3.1.3 Expression and Biological Functions

The activin subunits beta A and beta B are expressed in multiple tissues and cell lines (20, 41), whereas activin beta C and beta E are expressed in a more restricted fashion in the human body. Increased expression of activin beta A was detected in association with inflammation (42, 43), wound repair (44-47) and also at earlier time points after partial hepatectomy (48, 49) and in many different kinds of cancers (for the role of activin A in tumors, see 3.3.). The healthy liver shows only a low expression of activin beta A and activin beta B (20), whereas elevated levels of

circulating activin beta A were detected in patients suffering from hepatitis, hepatocellular carcinoma, liver cirrhosis or acute liver failure (50-55). In vitro and also in vivo studies showed that activin A induces hepatocyte apoptosis and inhibits DNA synthesis (21, 56-58). Increased amounts of circulating activin A were also detected in patients with septicemia, interstitial pulmonary fibrosis or angina (59-62). Beside this, activin A plays an important role in reproductive biology (63), erythroid differentiation (64), mesoderm induction (65), stem cell biology (66) and cell death induction (67).

High expression of INHBB, the gene encoding for activin beta B, were found in human adipocytes, whereas diet-induced weight loss was reported to decrease the expression of activin beta B. Furthermore, it is suggested as a risk factor for the metabolic syndrom (68).

Activin beta C is expressed predominantly in the liver, but also in prostate, testes, ovary and pituitary gland (19, 56, 69-71). A reduced expression of activin beta C was found in the hepatoma cell lines HepG2 and Hep3B in contrast to normal liver tissue (21) and a transient down-regulated gene expression of activin beta C was detected in patients after partial hepatectomy (49, 72-74).

Another activin subunit that shows a significant high expression in the liver, is activin beta E. It is also expressed in other human organs like testis, placenta, heart and skeletal muscle (20, 75-77). A down-regulation of activin beta E expression was detected in hepatocellular carcinoma, whereas a transiently upregulated expression was found after partial hepatectomy (10, 78).

Knockout-mice for activin beta A show severe craniofacial defects and die shortly after birth (79-81), whereas knockout-mice for activin beta B are viable, but suffer from eyelid defects and abnormalities in the female reproduction (82, 83). Normal development without any effects on reproduction were found in knockout-mice for activin beta C or activin beta E (84).The functions of activin beta C and E are still unknown.

3.2 Modulation of Activin Signaling

3.2.1 Inhibins

Like activins, inhibins were discovered as gonadal proteins that influence the secretion of follicle-stimulating hormone (FSH) from pituitary glands. In contrast to activins, which have a stimulating effect, the secretion of FSH gets inhibited by inhibins (13). In males, inhibins get primarily synthesized in the Sertoli cells in the testes, whereas in females inhibins get synthesized in granulosa cells (85).

In contrast to activins, that consist of two beta subunits, inhibins are heterodimers of an alpha and a beta subunit, covalently linked by a single disulfide bond. The beta subunit can either be a beta A or beta B subunit, resulting in inhibin A (subunits alpha and beta A) or inhibin B

(subunits alpha and beta B). Overexpression of inhibin alpha is associated with some types of tumors, like ovarian and adrenal cancer (28).

Only little is known about the functions and the signaling mechanisms of inhibins, but inhibins may compete with activins for binding to the activin type II receptors (86). For many biological systems, antagonistic effects of inhibins and activins have been described so far (33).

3.2.2 Follistatin

Follistatin is a single-chain polypeptide with the ability to inhibit the release of the follicle-stimulating hormone (FSH) from the pituitary gland (87). It has no structural relation to activins or other members of the TGF-βsuperfamily but acts as modulator of the activity of activin A by preventing it from binding to the type II receptors and subsequently blocking activin signaling (Figure 2) (88). Follistatin is expressed in many tissues within the body, like the endocrine glands, liver, reproductive tissues, pituitary, pancreas and prostate (7, 89). In patients suffering from hepatocellular carcinomas, elevated levels of circulating follistatin and high expression in the tumor tissue were found (28, 51, 78, 90). About 24-48 hours after partial hepatectomy, expression of follistatin as well as hepatocyte DNA synthesis were increased (72).

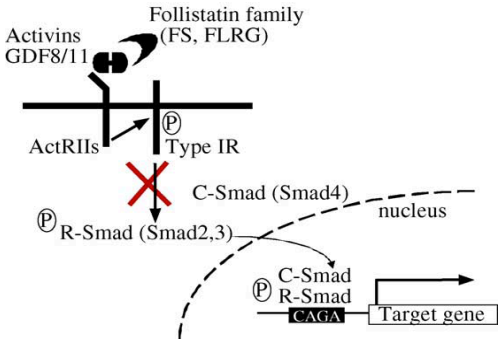

Figure 2. Inhibition of activin signaling via binding of follistatin or follistatin-related gene (FLRG) to activins (2).

The two major forms of follistatin, termed follistatin 288 (FS-288; consisting of 288 amino acids) and follistatin 315 (FS-315; consisting of 315 amino acids), result from a common precursor gene by alternative splicing at the 3' end (91, 92). A third form of follistatin (FS-303; consisting of 303 amino acids) results from proteolysis of the carboxy-terminal end of FS-315 (93, 94).

Structurally, follistatins contain an N-terminal activin-binding domain and three follistatin domains (FS domains) consisting of 73-75 amino acids (93, 95), which are also found in another protein, called follistatin-related gene (FLRG) or follistatin-like 3 (FSTL3). FLRG only consists of the first two FS domains and lacks the third one but has also the ability to modulate the activity of activin A (96-98). A deletion of either the first or the second FS domain eliminates the ability for activin binding, while loss of the third domain does not affect it (98). Both isoforms of follistatin bind secreted activin A with high affinity and almost irreversibly (91, 97, 99), though FS-288 seems to have a much higher affinity than FS-315 (100, 101).

The two isoforms of follistatin, FS-288 and FS-315, vary in their ability to bind heparan sulfate proteoglycans, since the shorter splice-variant FS-288 has a high affinity for heparin and the longer splice-variant FS-315 does not bind it (91, 102). Experiments with rat pituitary cells

demonstrated, that complexes of activin A and FS-288 can bind to heparan sulfate proteoglycans on the cell surface and subsequently undergo lysosomal endocytosis (Figure 3) (103, 104). Since FS-315 has no affinity for heparin, complexes of activin A and FS-315 do not undergo endocytosis but cannot bind to activin receptors either (7). FS-315 represents the predominant circulatory isoform of follistatin (105).

Beside activin beta A, follistatin has also an affinity for activin beta B, though it is about ten times lower than that for activin A (106). Modulation of the activity of activins containing the subunits beta C or beta E has not been described so far (16, 69, 76). Furthermore, inhibition of myostatin, growth and differentiation factor 11 (GDF11) and BMPs has also been reported (107-110).

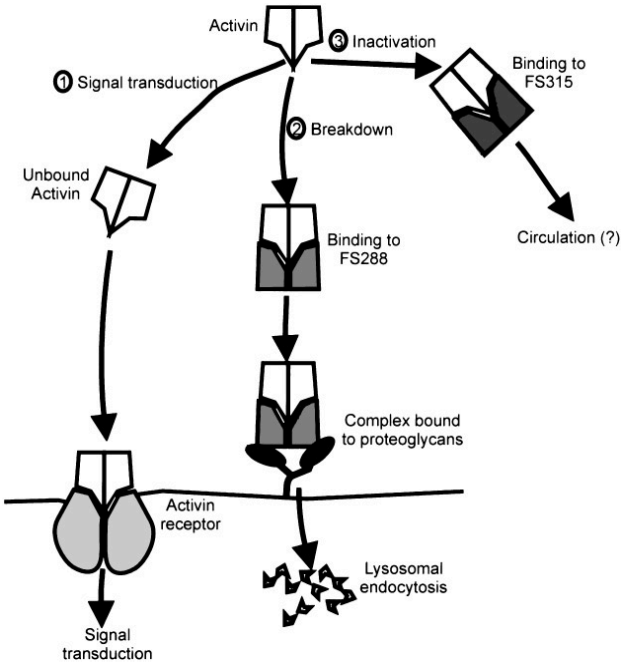

Figure 3. Possible interactions of activin A and the two follistatinisoforms FS-288 and FS-315 (7).

3.2.3 Follistatin-Related Gene (FLRG)

Another protein with the ability to bind activin A and thus prevent it from binding to type II receptors is the follistatin-related gene (FLRG), also known as follistatin-like 3 (FSTL3). Originally, it was identified in leukemia as a target of chromosomal rearrangement (111). The protein shows high structural similarity with follistatin, but only consists of two follistatin domains, while it has also the ability to modulate the activity of activin A (96-98). High expression of FLRG was detected in testis and placenta (33) and like follistatin, FLRG can also bind myostatin and growth and differentiation factor 11 (GDF11), but it does not interact with TGF-β (96, 112).

3.2.4 Inhibitory SMADs (I-SMADs)

Beside the receptor-regulated SMADs (R-SMADs; SMAD2 and SMAD3) and the Co-SMAD (SMAD4), there is also another group of SMAD-proteins, called inhibitory SMADs (I-SMADs; SMAD6 and SMAD7). SMAD7 is a negative regulator of the TGF-β and activin signaling, since it binds to activin type I receptors and subsequently prevents SMAD4 from binding to these receptors, thus blocking the signaling pathway (113, 114). The I-SMAD protein SMAD6 inhibits the signaling pathway of BMPs (32).

3.2.5 Cripto

The cell surface-protein Cripto is a member of the epidermal growth factor, Cripto, FRL-1 and Cryptic (EGF-CFC) protein family and is also known as teratocarcinoma-derived growth factor 1 (TDGF-1). Overexpression of Cripto was found in many cancers, like those of the breast, testicles, ovary, stomach, colon, lung or pancreas (115).

Cripto is able to bind to the activin type II receptors ActRII and ActRIIB and therefore prevents those receptors from phosphorylating the downstream type I receptor and blocks activin signaling (116). Overexpression of Cripto inhibits activin signaling in different cancer cell lines (116, 117). Furthermore, Cripto acts as a co-receptor and facilitates binding of the protein Nodal to the activin like kinase 4 (ALK4) and therefore promotes Nodal signaling (118, 119).

3.3 Activin A in Tumors

Like TGF-β, activin A has the ability to either inhibit or promote cell growth, depending on the type of tissue. Many different studies demonstrated a deregulation of activin signaling and that activin A inhibits cell proliferation of hepatocellular carcinoma cells (15, 28, 120), breast cancer (121-124), prostate cancer (125-127) and also of pituitary adenoma cells (128, 129). Elevated serum levels of activin A were found in patients suffering from hepatocellular carcinoma, endometrial carcinoma, cancers of the human breast or ovary, and are therefore discussed as serum markers (52, 130-133). In the liver, activin A is a negative regulator of proliferation. In vitro and in vivo experiments demonstrated an inhibition of mitogen-induced DNA synthesis, induction of apoptosis and a significant reduction of liver mass achieved by infusions with recombinant activin A (56-58).

In contrast, promotion of cell proliferation was detected in endometrial carcinomas (134, 135), testicular cancer (126, 136), gastric cancer (137, 138), head and neck squamous cell carcinoma (139), oral squamous cell carcinoma (140) and various thoracic tumors, like esophageal squamous cell carcinoma (141-143), esophageal adenocarcinoma (144) and lung

adenocarcinoma (145). Overexpression of activin A was measured in various cancer types and was associated with poor prognosis, metastasis and a shorter disease-free survival rate (139, 140, 144). Furthermore, exogenous treatment of cancer cells already overexpressing INHBA can further stimulate cell proliferation in vitro (144, 145). Moreover, it was shown that down-regulation of INHBA gene expression via RNA interference reduces cell proliferation and invasion of cancer cells (140, 144, 145), thus demonstrating the importance of activin A signaling for various carcinomas and suggesting INHBA as a valuable candidate for therapeutic application.

3.4 Malignant Pleural Mesothelioma

Malignant Pleural Mesothelioma (MPM) is a rare but highly lethal cancer with poor prognosis that arises from the serous linings of the lungs and was first described in 1960 (146). In most cases, there is a clear correlation with a past exposure to asbestos, but there are also other factors considered to contribute to the development of this tumor, like genetic alterations or the Simian virus 40 (SV40). So far, no effective treatment has been established. Current therapies for MPM often combine surgery, radiation and chemotherapy in a multimodality approach.

3.4.1 Epidemiology

Until the second half of the 20th century, Malignant Pleural Mesothelioma was an extremely rare kind of neoplasm. Since then, the incidence has increased significantly and is expected to peak within the next 20 years (147). Every year, there are about 2500 new cases in the United States and approximately 10000 cases worldwide (148).

The main risk factor for developing MPM is a past exposure to asbestos and due to occupational exposure, men are at much higher risk than women (149). About 80% of all U.S. patients suffering from MPM have a history of asbestos exposure, although only 5% of people with long-time asbestos exposure develop MPM (150). The time between the initial exposure to asbestos and the diagnosis of the cancer is between 20 and 40 years, leading to a mean age of the patients ranging from 50 to 70 years at the time of diagnosis (151, 152).

3.4.2 Histology

MPM is classified into three histological subtypes: epithelioid, sarcomatoid and biphasic, also often described as mixed subtype. The epithelioid form is the most common type, with approximately 50-60% of all cases, and is associated with a better prognosis than the sarcomatoid or biphasic form (153). Epithelioid mesotheliomas typically show tubopapillary

and glandular patterns with uniform shaped and well-defined epthelial structure, whereas the sarcomatoid form is characterized by spindle cells, typically elongated and not uniform in shape. The biphasic or mixed version consists of both structures and therefore it can be necessary taking multiple tumor tissue samples to verify a biphasic subtype of MPM (8).

3.4.3 Asbestos

Asbestos is considered to be the main risk factor for developing MPM. Until the second half of the 20th century, it was in worldwide use in the construction and shipbuilding industry because of its resistance to heat or electrical damage. Since 2005 the usage of Asbestos has been completely forbidden in the European Union, but it is still used in some parts of the world.

The term asbestos refers to a group of fibrous silicate minerals with two major types: the serpentine form, like chrysotile (also known as white asbestos), and the amphibole form, like crocidolite (also known as blue asbestos), amosite (also known as brown asbestos), antophyllite, actinolite and tremolite. Asbestos fibres get inhaled in the lung where they are able to cause DNA damage (e.g. by disrupting mitosis), release of reactive oxygen species (ROS) and reactive nitrogen species (NOS), local inflammation (based on mechanical damage of the mesothelial surface by the fibres) and diseases like lung cancer, fibrosis and MPM (150, 154-156). The amphibole forms, especially crocidolite, are considered to be much more oncogenic than serpentine, since amphiboles have long and thin fibres that can better accumulate in the lung with a longer biopersistence (157, 158).

3.4.4 Molecular Mechanisms and Alterations

The molecular mechanisms underlying the pathogenesis of MPM are still not clear. Inhaled asbestos fibres accumulate in the lung, damage the mesothelial cells and cause local inflammation (Figure 4). In vitro experiments with primary human mesothelial cells have shown that exposure to asbestos induces necrosis and the secretion of the high-mobility group protein-1 (HMGB-1) which causes inflammation, accumulation of macrophages and the secretion of tumor necrosis factor-alpha (TNF-α), further leading to an activation of the transcription factor NF-kB (159-162). Moreover, asbestos was described as being non-pathogenic in TNF-α receptor knockout mice (163).

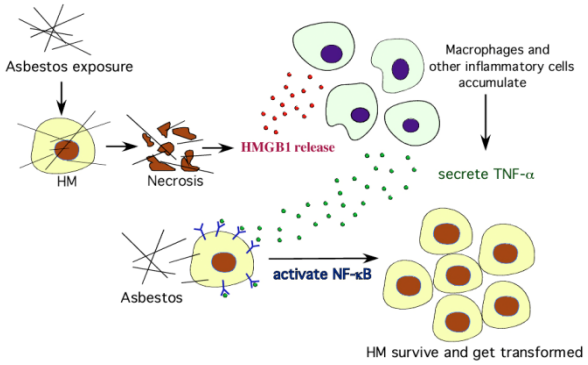

Figure 4. Asbestos exposure causes necrosis, release of HMGB-1, accumulation of macrophages, inflammation and secretion of TNF-alpha, further activating NF-kB and leading to survival of human mesothelioma (HM) cells (5).

Inflammation and the accumulation of macrophages further stimulates the release of cytokines and growth factors, giving MPM cells a growth advantage (Figure 5) (164). Various studies already demonstrated that MPM cells produce and respond to different growth factors, like the platelet-derived growth factor (PDGF) (164, 165), vascular endothelial growth factor (VEGF) (166, 167), epidermal growth factor (EGF) (168), hepatocyte growth factor (HGF) (169), insulin-like growth factor (IGF) (170) and the transforming growth factor β (TGF-β) (171, 172). In vitro and in vivo experiments with antisense oligodeoxynucleotides to TGF-β demonstrated inhibition of cell proliferation and tumor growth (172). Animal experiments with intraperitoneal injections of MPM cells into severe combined immunodeficient (SCID) mice showed increased levels of VEGF, IL-6, IL-8 and the basic fibroblast growth factor (bFGF, also known as FGF2) seven days after injection (173). Inhibition of angiogenesis by blocking VEGF resulted in reduced tumor growth in animal models (174).

At the chromosome level, multiple alterations, predominantly deletions, have been found so far. Inhaled asbestos fibres can interfere with mitosis by mechanically disrupting the mitotic spindle, resulting in DNA strand breaks, chromosomal abnormalities and aneuploidy (175). The most common numeric alteration in MPM is loss of a copy of chromosome 22 (176). In about 40-50% of all MPM cases, the gene NF2, which is located at 22q12 and coding for the tumor suppressor Merlin, is mutated or inactivated by homozygous deletion (177-179). Another frequent mutation is loss of CDKN2A/ARF due to homozygous deletion (180-182). The gene CDKN2A/ARF is located at 9p21 and coding for two proteins – $p16^{INK4a}$ and through an alternative transcript $p14^{ARF}$ – which are both important negative regulators of cell cycle progression. Previous in vitro studies with various established MPM cell lines demonstrated a loss of this gene locus by homozygous deletion in 90% of the tested cell lines (180, 183). Homozygous deletion of $p16^{INK4a}$ and $p14^{ARF}$ further affects the tumor suppressive pathways of retinoblastoma (Rb) and p53 which regulate the cell cycle (184, 185). In numerous cell lines without a homozygous deletion of CDKN2A/ARF, a downregulation at the expression level was found (180). Furthermore, re-expression of p16 in MPM cell lines, that were subsequently used for xenograft experiments, resulted in an inhibition of tumor growth, reduced tumor size and cell cycle arrest as well as cell death (186). Moreover, structural rearrangements of 1p, 3p, 6q and 9p are also often detected in MPM cells (187, 188).

Another molecular characteristic of MPM cells is the high expression of telomerase which was found in about 90% of all MPM cases, leading to cell immortalization (189, 190). MPM cells also show high expressions of Bcl-XL and Bax, two antiapoptotic molecules, which may be linked to the strong chemotherapy resistance of MPM cells (191, 192).

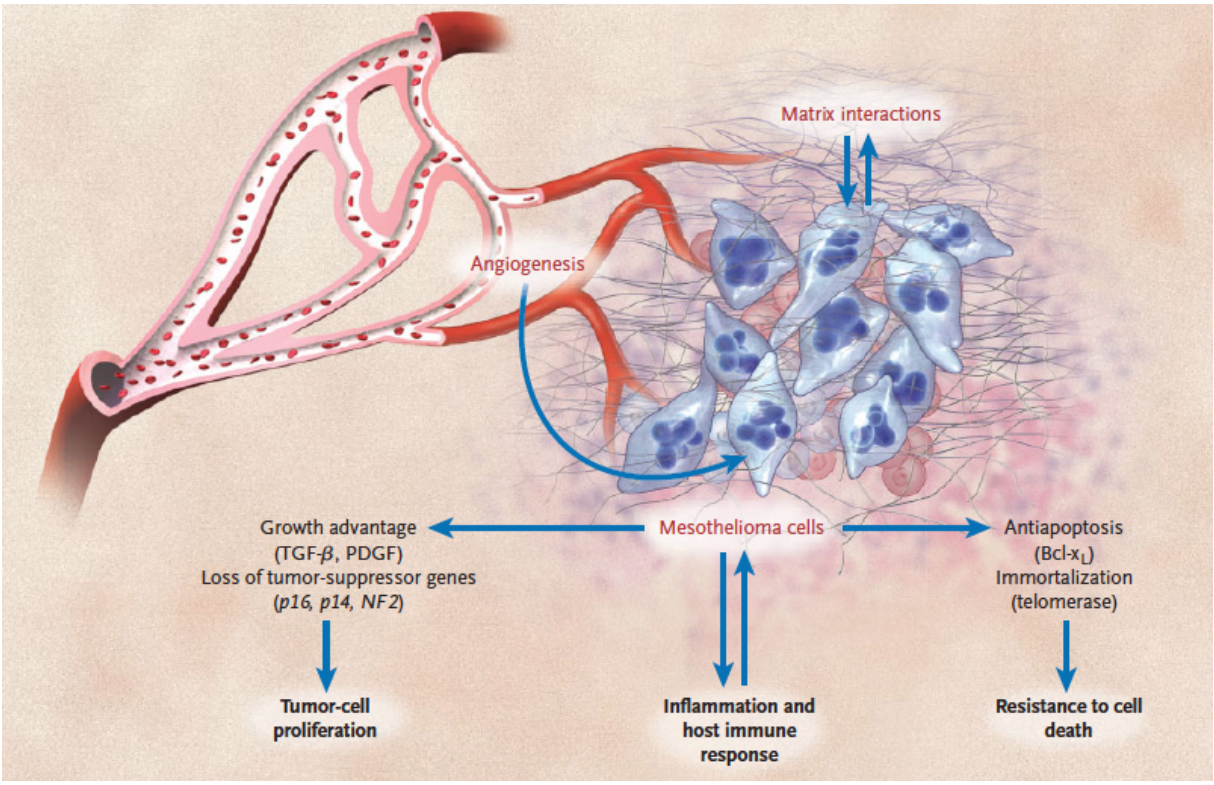

Figure 5. Molecular mechanisms involved in the development of MPM (193).

3.4.5 Simian Virus 40 (SV40)

The contribution of Simian Virus 40 (SV40), a double-strand DNA virus endogenous in rhesus monkeys, to the development of MPM is a very controversial issue. Animal models showed a clear association between exposure to SV40 and the development of MPM, since 60% of hamsters injected intracardially with the virus and 100% injected intrapleurally developed MPM within 4-9 months (194).

Inside of its host, the virus produces two proteins, called large T antigen (Tag; 90 kDa) and small t antigen (tag; 17kDa) (152). The large T antigen induces structural and numerical alterations of chromosomes, point mutations and inhibits p53 (195) and Rb (196) pathways, which have a regulatory function in the cell cycle. If SV40 infected MPM cells get treated with antisense Tag, p53 gets reactivated and growth arrest gets induced (195). SV40 was also described to induce telomerase activity in MPM cells, whereas this effect could not be shown for fibroblasts (197).

The transfer of the virus from monkeys to the human population may have occurred between 1955 and 1963, when polio vaccines were contaminated with SV40 (198). A multi-laboratory study in 1998 detected SV40 sequences and Tag expression in 83% of the tested MPM patients (199). Other studies reported, that SV40 sequences could only be detected in malignant mesothelioma cells, but not in nearby stromal cells (200, 201).

Furthermore, a synergistic relationship between the presence of SV40 and exposure to asbestos to the development of MPM is suggested. Eleven patients suffering from MPM were analyzed

regarding exposure to asbestos and SV40 and it turned out that five of seven patients with a past exposure to asbestos were positive for SV40, whereas none of the patients without a past asbestos exposure were positive for SV40 (202). Experiments with transgenic mice and hamsters also demonstrated a co-cancerogenic affect of SV40 with asbestos (203-205). However, the published numbers of SV40 DNA sequences found in patients suffering from MPM vary from 0% to 90% and it is suggested that high numbers of positive results may be due to contaminations with other laboratory plasmids (195).

3.4.6 Diagnosis

Patients usually suffer from breathlessness, often associated with chest wall pain due to a pleural effusion. If MPM is suspected, it is recommended to perform an endoscopic examination by thorascopy in combination with a biopsy. Computed tomography (CT; Figure 6), magnetic resonance tomography (MRT) and positron emission tomography (PET) can also be used for imaging, detection of invasion into the chest wall or the diaphragm and for confirming diagnosis. Histology helps to identify the subtype (epithelioid, sarcomatoid or biphasic) and immunohistochemical stainings provide the possibility to distinguish MPM from adenocarcinoma. Additionally, occupational history must be obtained.

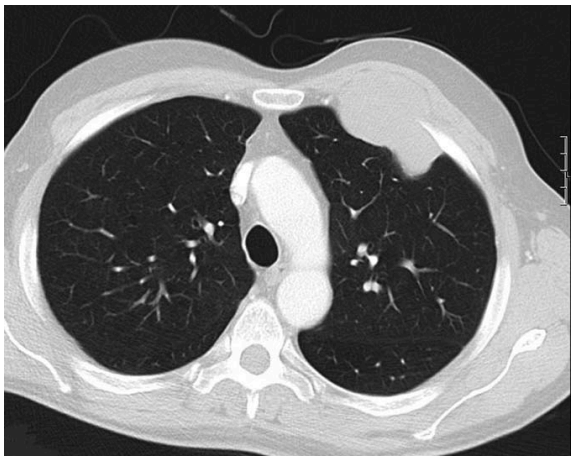

Figure 6. Computer tomography scan of a MPM invading the chest wall (3).

3.4.7 Staging

So far, no standard staging system for MPM has been established. The most common system used for the clinical staging of the progress of MPM (Table 3) is based on the TNM (tumor – node – metastasis) system (Table 2) (3). This system helps to describe the size of the tumor and whether it is resectable or not (T1-T4), the involvement of lymph nodes (NX, N1-N3) and the presence of metastasis (MX, M0, M1).

Table 2. TNM staging system for MPM (3).

T1	T1a	Tumour limited to the ipsilateral parietal pleura, including mediastinal and diaphragmatic pleura. No involvement of the visceral pleura
	T1b	Tumour involving the ipsilateral parietal pleura, including mediastinal and diaphragmatic pleura. Scattered foci of tumour also involving the visceral pleura
T2		Tumour involving each of the ipsilateral pleural surfaces (parietal, mediastinal, diaphragmatic and visceral pleura) with at least one of the following features: Involvement of diaphragmatic muscle Confluent visceral pleural tumour (including the fissures) or extension of tumour from visceral pleura into the underlying pulmonary parenchyma
T3		Describes locally advanced but potentially resectable tumour. Tumour involving all of the ipsilateral pleural surfaces (parietal, mediastinal, diaphragmatic and visceral) with at least one of the following features: Involvement of the endothoracic fascia Extension into the mediastinal fat Solitary completely resectable focus of tumour extending into the soft tissues of the chest wall Non-transmural involvement of the pericardium
T4		Describes locally advanced technically unresectable tumour. Tumour involving all of the ipsilateral pleural surfaces (parietal, mediastinal, diaphragmatic and visceral) with at least one of the following features: Diffuse extension or multifocal masses of tumour in the chest wall with or without associated rib destruction Direct transdiaphragmatic extension of tumour to the peritoneum Direct extension of tumour to the contralateral pleura Direct extension of tumour to one or more mediastinal organs Direct extension of tumour into the spine Tumour extending through to the internal surface of the pericardium with or without a pericardial effusion, or tumour involving the myocardium
N		Lymph nodes
NX		Regional lymph nodes cannot be assessed
N0		No regional lymph node metastases
N1		Metastases in the ipsilateral bronchopulmonary or hilar lymph nodes
N2		Metastases in the subcarinal or the ipsilateral mediastinal lymph nodes including the ipsilateral internal mammary nodes
N3		Metastases in the contralateral mediastinal, contralateral internal mammary, ipsilateral or contralateral supraclavicular lymph nodes
M		Metastases
MX		Presence of distant metastases cannot be assessed
M0		No distant metastasis
M1		Distant metastasis present

Table 3. Clinical staging system (3).

Stage	Description
Stage I	
Ia	T1aN0M0
Ib	T1bN0M0
Stage II	T2N0M0
Stage III	Any T3M0
	Any N1M0
	Any N2M0
Stage IV	Any T4
	Any N3
	Any M1

3.4.8 Prognosis

Usually, MPM gets diagnosed rather late, predominantly at stage II. The five-year survival rate of patients suffering from MPM is below 15% (206). The median survival time of MPM patients ranges between six and eighteen months after diagnosis because of the poor response to current therapies (8). A poor performance status, anemia, low haemoglobin, high white cell counts, an age of 65 years or older, a sarcomatoid histological subtype and high platelet counts, as well as hypermethylation of $p16^{INK4a}$ are factors predicting a poor prognosis (207-210). Patients with an epithelial histological subtype usually have a better prognosis and live a few months longer. Combination chemotherapy including antifolates seems to prolong the median survival for three to four months (211). Most MPM patients die from respiratory insufficiency and local extension.

3.4.9 Therapy

So far, no effective treatment for patients suffering from MPM has been found. Single therapies with either surgery, radiation therapy or chemotherapy show only low efficiency. Current therapies consist of surgery, adjuvant radiation and chemotherapy, combined in a multimodality approach and have already demonstrated an improved short-term and also long-term survival rate (212-215). In a recent follow-up study, patients with MPM of the epithelioid subtype and without any involvement of the lymph nodes had a 5-year survival rate of approximately 46% (213).

3.4.9.1 Surgery

Currently, there are two surgical methods used for the treatment of MPM. The extrapleural pneumonectomy (EPP) is a radical technique that involves the complete removal of the lung, the parietal and visceral pleura as well as involved diaphragm, pericardium and the phrenic nerve (Figure 7, right). Removed parts get replaced by synthetic materials, usually Gore-Tex. Lymph nodes are removed for further pathological analysis. Following EPP, adjuvant therapy involving radiation and chemotherapy has to be applied. Since the lung has been removed, higher doses can be used for adjuvant radiation. EPP is more effective in patients with epithelioid histology, good performance status and early stages (stage I or stage II) and prognosis for MPM patients is very poor if extrapleural lymph nodes are involved or for sarcomatoid or biphasic histology.
Another possible surgical method is pleurectomy, a less radical method, where only the pleura gets stripped off the lung from the apex to the diaphragm, whereas the lung is not removed (Figure 7, left). Removed parts get replaced by synthetic materials. However, complete pleurectomy could not show a prolonged survival in MPM patients (206).

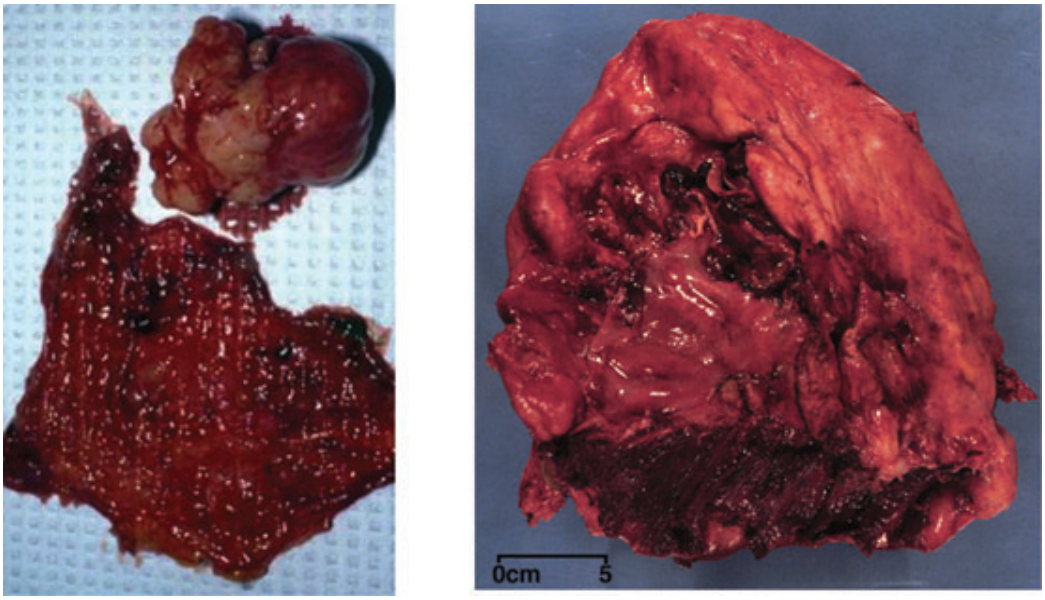

Figure 7. Removed tumor tissue after pleurectomy (left) versus extrapleural pneumonectomy (right) (8).

3.4.9.2 Radiation

The effects of radiation therapy alone on MPM patients are rather disappointing and a prolonged survival has not been achieved so far (216, 217). Within a multimodality approach, radiation is used after surgery as adjuvant therapy. The dose of radiation is limited due to nearby organs like the lung, esophagus, heart and also the liver. After EPP, higher radiation doses can be applied, since the lung has been removed.

3.4.9.3 Chemotherapy

Within the chemotherapeutical treatment of MPM, several single drugs and drug combinations have been tested so far, but MPM seems to be rather resistant against chemotherapy. In a meta-analysis of all clinical trials from 1965-2001, the platinum-compound cisplatin was the most active single drug in the chemotherapeutical treatment of MPM (218). Further studies showed, that even better results can be achieved with a combination of cisplatin and the antifolate pemetrexed (211).

Cisplatin

The biological and cytotoxic activity of cisplatin (cis-diammine-dichloro-platinum(II)) was already found in 1965, when Barnett Rosenberg discovered, that electrolysis of platinum electrodes produces cisplatin and inhibits cell division of E. coli (219). Further studies showed a potent anticancer activity of cisplatin and today, the drug is commonly used in the treatment of cervical, ovarian, testicular, bladder, small-cell lung cancer and non-small-cell lung cancer.

The antitumor activity of cisplatin is based on binding to the DNA and inducing inter- and intrastrand cross-link adducts. Once inside the cell, the chloride ligands of cisplatin get replaced by water molecules, leading to a positive charge of the platinum-compound, which can subsequently interact with the nucleophilic sites of nucleic acids or proteins and induce cross-link adducts (Figure 8) (6). These adducts inhibit DNA replication, RNA transcription, chain elongation, and cause cell arrest in the G2-phase of the cell cycle and apoptosis (220-223). Unfortunately, cisplatin is able to cause severe side effects, like nephrotoxicity, neurotoxicity, nausea, vomiting and myelosuppression (224).

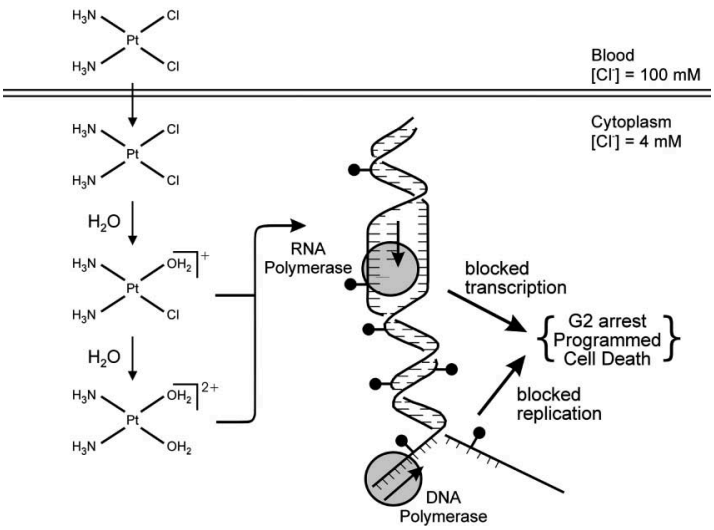

Figure 8. Schematic overview of the antitumor activity of cisplatin (6).

Pemetrexed

Pemetrexed (Alimta, LY231514; Figure 9) is a multitargeted antifolate, that inhibits different enzymes in the folate metabolism and further the synthesis of DNA. The drug is an analogue of folic acid and like folic acid, it is transported into the cell via the reduced folate carrier system and cell membrane transporters. Once inside the cell, pemetrexed gets polyglutamated and interferes with the folate-dependent enzymes thymidylate synthase (TS), glycinamide ribonucleotide formyltransferase (GARFT) and dihydrofolate reductase, which are all required for the synthesis of purine and thymidine nucleotides (Figure 10) (1).

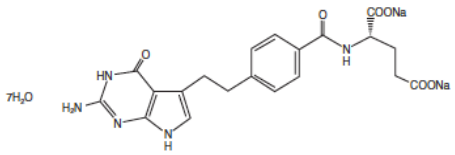

Figure 9. Pemetrexed sodium (Alimta), chemical structure (9).

Pemetrexed is the first FDA (Food and Drug Administration) approved chemotherapeutic agent for the treatment of MPM in combination with cisplatin. In a randomized trial, 456 patients suffering from MPM, but with a good performance status, were either treated with cisplatin, pemetrexed or a combination of both agents. In order to reduce the toxic side effects of the

chemotherapy, a subgroup of patients was additionally supplemented with folic acid and vitamin B12. The study demonstrated a survival benefit and improved quality of life of patients who were treated with the combination of cisplatin and pemetrexed in contrast to patients only treated with cisplatin (median survival of 12.1 months versus 9.3 months). Supplementation of folic acid and vitamin B12 achieved a further prolonged survival of the patients (13.3 months vs. 10 months) (9). The high efficiency of pemetrexed in the therapy of MPM may be based on the upregulated expression folate transporters in the cell membrane (225).

Beside MPM, pemetrexed is also commonly used in the chemotherapy of non-small-cell lung cancer, head and neck, breast, colon, pancreas and bladder carcinomas (226). Toxic side effects of pemetrexed are myelosuppression and elevated levels of hepatic transaminases.

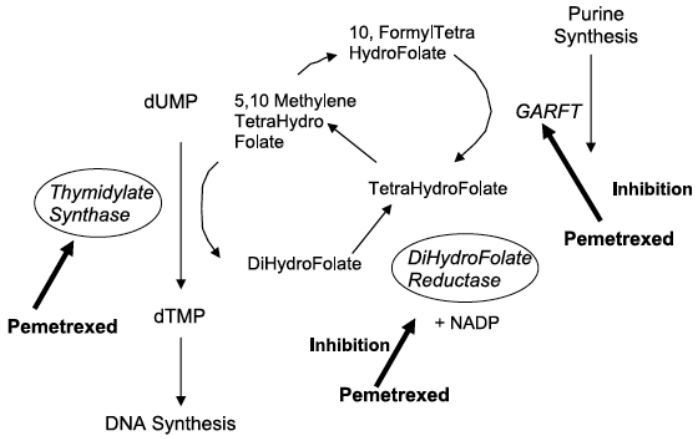

Figure 10. Enzyme targets of pemetrexed (1).

4 Aim of the Study

Malignant Pleural Mesothelioma is a highly aggressive tumor, strongly associated with past asbestos exposure, followed by chronic inflammation. Previous studies have already shown an implication of growth factors and cytokines like the platelet-derived growth factor (PDGF), epidermal growth factor (EGF), vascular endothelial growth factor (VEGF), hepatocyte growth factor (HGF), insulin-like growth factor (IGF) and the transforming growth factor β (TGF-β) in MPM cells. In vitro and in vivo experiments with antisense oligodeoxynucleotides to TGF-βalready demonstrated inhibition of cell proliferation and tumor growth.
Activin A is a member of the TGF-β superfamily and has already been described as a promoter of tumor aggressiveness and proliferation in other tumors, especially thoracic tumors. High levels of circulating activin A have previously been associated with chronic inflammation.

The aim of the here presented study was to investigate whether deregulation of activin A signalling contributes to progression of Malignant Pleural Mesothelioma and whether this pathway can be exploited for therapeutic implications. For this purpose, the contribution of activin signals and their impact on malignant growth and spreading was analysed in nine MPM cell models in contrast to the non-malignant SV40 Tag-immortalized mesothelial cell line Met5a (196). Gene expression patterns of activins, their receptors and antagonists were analysed and cells were exogenously stimulated with recombinant activin A. Furthermore, the effects of down-regulating activin activity via small molecule inhibitors (SB-431542, A8301) as well as siRNA targeting human INHBA were investigated with respect to cell proliferation, cell invasion and clonogenicity. Treatment with Trichostatin A and 5-azacytidine was performed to examine the role of epigenetic regulation in INHBA expression. Paraffin embedded tissues derived from surgical biopsies and specimens of patients at the Department of Surgery of the Medical University of Vienna suffering from Malignant Pleural Mesothelioma were used for immunohistochemical stainings of activin A, further confirming activin expression in patients.

5 Material und Methods

5.1 Cell Culture

All cell lines were maintained in a humidified atmosphere at 37°C and 5% CO_2. Cells were grown in Roswell Park Memorial Institute medium (RPMI), Minimum essential Eagle medium (MEME), Minimum essential Eagle medium - containing 1 mM sodium pyruvate and 1% non-essential amino acids - (MNP) containing 10% fetal calf serum (FCS). For a complete list of all used cell lines, their standard growth medium, histological subtype and source of the cell lines, see Table 4.

Table 4. Cell lines used for in vitro analyses.

Cell line	***Standard Growth Medium***	***Histological Subtype***	***Source***
Met5a	RPMI + 10% FCS	SV40 Tag-immortalized mesothelial cell line	ATCC
SPC111	RPMI + 10% FCS	biphasic	R. Stahel University of Zurich
SPC212	RPMI + 10% FCS	biphasic	R. Stahel University of Zurich
CRL5820/NCI-H28	RPMI + 10% FCS	epithelial	ATCC
p31	MEME + 10% FCS	epithelial	K. Grankvist Umeå University
p31cis	MEME + 10% FCS	epithelial	K. Grankvist Umeå University
I2	RPMI + 10% FCS	epithelial	A. Catania Milano
M38K	RPMI + 10% FCS	biphasic	V L Kinnula University of Helsinki
VMC6	RPMI + 10% FCS	epithelial	W. Klepetko Medical University Vienna
VMC20	RPMI + 10% FCS	epithelial	W. Klepetko Medical University Vienna
HepG2	MNP + 10% FCS	Hepatoblastoma	ATCC

5.2 Tissue Samples

Between 01/1993 and 01/2010, 70 tumor tissue samples were derived from patients suffering from Malignant Pleural Mesothelioma at the Division of Thoracic Surgery at the Medical University of Vienna. All samples are histological proven as Mesothelioma, fixed in formalin and embedded in paraffin. Sections for immunohistochemical stainings were cut at 4 µm and presence of tumor tissue was assessed by hematoxylin and eosin (H&E) stainings.

5.3 RNA Interference

5.3.1 Basic siRNA Resuspension

Malignant Pleural Mesothelioma (MPM) cell lines were transiently transfected with small-interfering RNA targeting human INHBA, purchased from Dharmacon, using Oligofectamine (Invitrogen) as transfection reagent. According to the manufacturer's instructions, 5.0 nmol siRNA were resuspended in 250 µl nuclease-free water (Fermentas) to obtain a 20 µM stock solution and were afterwards stored frozen at -20°C. A further dilution with nuclease-free water was made in order to obtain a 5 µM working stock, also stored frozen at -20°C. Final concentration used for the knock-down of INHBA expression and for cell proliferation and vitality assays was 50 nM in all experiments. Cells treated with the same concentration of scrambled siRNA (Dharmacon) instead of INHBA-targeting siRNA were used as control.

5.3.2 Knock-down of INHBA in MPM cell lines

Gene knock-down using INHBA-targeting siRNA was done in duplicates, using scrambled siRNA as negative control. The day before transfection, cells were seeded in a 6-well plate (IWAKI) at a density of 2 x 10^5 cells per well in 1 ml growth medium containing 10% FCS. The next day 10 µl siRNA (5 µM working stock) targeting INHBA or, respectively, 10 µl scrambled siRNA (5 µM working stock) were mixed with 240 µl FCS-free medium in a 1.5 ml Eppendorf reaction tube. In a separate tube 10 µl Oligofectamine were mixed with 240 µl FCS-free medium. Solutions were vortexed and incubated for 5 minutes at room temperature. Subsequently both solutions were mixed, vortexed and incubated at room temperature for additional 20 minutes. In the meantime, the old medium in the wells was aspirated and cells were washed once with phosphate buffered saline (PBS) (PAA). Finally the siRNA mixture was added dropwise into the well and 500 µl complete medium containing 10% FCS were added to the cells, leading to a final siRNA concentration of 50 nM. Cells were harvested 48 hours after transfection for expression analyses.

5.4 Cell Treatment

5.4.1 Recombinant Activin A

For different kinds of in vitro assays, cell lines were treated with recombinant protein of activin A (R&D Systems). The cytokine was dissolved in PBS containing 0.1% BSA (New England Biolabs) and stored frozen at -20°C. In all experiments, activin A was further diluted in the respective growth medium to a final concentration of 10 ng/ml. Cells treated with equal amounts of PBS instead of activin A were used as negative control. During long-term experiments, culture medium and cytokine were refreshed every 72 hours.

5.4.2 Small Molecule Inhibitors

SB-431542 and A 8301 are two selective inhibitors for type I receptors of activin-like kinases (197, 198). They were both purchased from Tocris Bioscience, dissolved in DMSO (Amresco) to a concentration of 10 mM and stored frozen in small aliquots of 15 µl at -20°C. For all experiments the inhibitors were diluted in the respective culture medium to final concentrations of 20 µM. During long-term experiments, culture medium and inhibitors were refreshed every 72 hours.

5.4.3 Trichostatin A (TSA) and 5-Azacytidin (5-AZA)

The histone deacetylase inhibitor Trichostatin A was purchased from Sigma and dissolved in DMSO to a concentration of 3.3 mM. The demethylating reagent 5-azacytidin was purchased from Sigma and dissolved in DMSO to a concentration of 1 mM. Both substances were stored frozen at -20°C in small aliquots and further diluted in the respective growth medium before application.

Cells were seeded in 12-well plates (IWAKI) at a density of 15 x 10^4 cells per well in 1 ml medium containing 10% FCS and incubated at 37°C for 24 hours. All experiments were done in duplicates and cells treated with equal amounts of DMSO were used as negative control. The next day, medium was discarded, cells were washed once with PBS and 1 ml FCS-free medium was added to the cells. After 24 hours of incubation, a single treatment of cells with either Trichostatin A or 5-azacytidin, or a combination treatment of both substances was performed. Medium and the desired treatment were renewed every 48 hours.

For single treatment, cells were either treated with Trichostatin A at a final concentration of 300 nM or 5-azacytidin at a concentration of 5 µM in 1 ml growth medium containing 10% FCS. Cells

were harvested for expression analysis after 12 and 24 hours in case of treatment with TSA or after 48, 72 and 96 hours in case of 5-azacytidin.

For a combination treatment with TSA and 5-azacytidin, cells were simultaneously exposed to 300 nM TSA and 5 µM 5-azacytidin and were harvested for expression analysis 48, 72 or 96 hours after treatment.

5.5 Expression Analysis

5.5.1 Isolation and Quantification of RNA

For the isolation of RNA, cells were either seeded at the desired cell numbers in 6- or 12-well plates (IWAKI) or a confluent tissue culture flask (T25 (=25cm^2)) was directly used. After discarding the medium, 500 µl TRIzol (Invitrogen) in case of a 6- or 12-well plate or 1000 µl TRIzol in case of a tissue culture flask (T25) were added onto the cell layer. Following incubation for 5 minutes, cells were transferred into 1.5 ml Eppendorf tubes and chloroform was added at a quantity of 1/5 volume of TRIzol used (e.g. 200 µl chloroform to 1000 µl TRIzol). The reaction tubes were inverted for about 15 seconds and then incubated for additional 5 minutes at room temperature. Subsequently, the samples were centrifuged for 20 minutes at 15000 g at 4°C in an Eppendorf Centrifuge 5417R. The upper, aqueous phase was transferred into a fresh reaction tube, carefully avoiding the transfer of any interphase. Isopropanol (Merck) was added at half the amount of TRIzol previously used. After vortexing the tubes for a few seconds and an additional incubation for 15 minutes at room temperature, samples were again centrifuged for 10 minutes at 15000 g at 4°C. Supernatant was discarded and for washing the precipitated RNA pellet, 75% ethanol (Merck) was added at an equal amount of TRIzol used at the beginning. Samples were centrifuged for a last time for 7 minutes at 15000 g at 4°C. The supernatant was again discarded, the pellet air-dried and finally dissolved by pipetting up and down several times in 15 µl nuclease-free water.

The concentration of the purified RNA was quantified by measuring the optical density (OD_{260}) on a NanoDrop 1000 spectrophotometer (Peqlab) and the quality of the isolated RNA was checked by agarose gel electrophoresis. For further analyses, only intact RNA of high quality, showing sharp bands of 28S and 18S eukaryotic rRNA in the gel electrophoresis, was used. All RNAs were stored frozen at -80°C.

5.5.2 Synthesis of cDNA

For the synthesis of cDNA, 2 µg RNA were diluted with nuclease-free water to 13 µl and heated up for denaturation to 70°C for 10 minutes. After incubation on ice for 5 minutes, 7 µl of the cDNA Master-Mix were added to each sample. The reverse transcription was performed at 42°C for 60 minutes and stopped by incubating the samples at 70°C for additional 10 minutes. Finally 20 µl nuclease-free water were added to each cDNA solution and samples were either directly used for a quality check by RT-PCR of a housekeeping gene (e.g. glyceraldehyde-3 phosphate dehydrogenase (GAPDH) or 18s rRNA) or stored frozen at -20°C.

1 x cDNA Master-Mix:

Reagents (Concentration)	***Volume (µl)***
M-MLV RT buffer (5 x; Fermentas)	4
Random Hexamer Primer (0.5 µg/µl; Fermentas)	0.5
dNTPs (10 mM; Fermentas)	1
Reverse Transcriptase (Fermentas)	1
RiboLock RNase-Inhibitor (40 units/µl; Fermentas)	0.5
total Master-Mix volume	*7*

5.5.3 Reverse Transcriptase – Polymerase Chain Reaction (RT-PCR)

RT-PCR reactions were performed in a MyCycler Thermal Cycler (Bio-Rad) and all previous sample preparations were done on ice. For each sample, 1 µl cDNA solution was mixed with 24 µl RT-PCR Master-Mix and shortly spinned down in a centrifuge before the RT-PCR was started. Reactions were conducted according to the required conditions of the primers (Table 5 and Table 6). The correct RT-PCR products were afterwards identified by the specific size of the amplified fragment using gel electrophoresis.

1 x RT-PCR Master-Mix:

Reagents (Concentration)	***Volume (µl)***
GoTaq Green Master-Mix (Promega)	12.5
Nuclease-free water (Fermentas)	9.5
Primer forward (20 µM)	1
Primer reverse (20 µM)	1
total Master-Mix volume	*24*

Table 5. Standard RT-PCR cycling parameters.

	Temperature	***Time (minutes)***	***Repetitions***
Initial Denaturation	95°C	02:30	1 x
Denaturation	95°C	00:30	30 x
Annealing	49°C - 56°C	00:30	
Elongation	72°C	01:00	
Final Elongation	72°C	07:00	1 x

Table 6. List of primers used for RT-PCR.

Gene of Interest	***Sequences of Primers sense/antisense***	***Expected Size of Amplicon (bp)***	***Annealing Temperature***	***NM Numbers***
INHBA	AAGAAGAGACCCGATGTCAC/ AGCCGATGTCCTTGAAACTG	798	49°C	NM_002192
INHBB	GTGAAGCGGCACATCTTG/ TCACACTGCACGTCTAGG	526	52°C	NM_002193
INHBC	GTGTCCAGAGCTGCTTTGAGG/ CCAGCCAATCTCACGGAAGTC	584	53°C	NM_005538
INHBE	GAGACTACAGCCAGGGAGTG/ CCCAGTTCCTGGAAGTCTAC	548	53°C	NM_031479
INHA	TTCCGGCCATCCCAGCATAC/ CAGCCCACAACCACCATGAC	548	53°C	NM_002191
ACVR2 = ActR2	TGGCTCCAGAGGTATTA/ CGCAACCATCATAGACT	454	50°C	NM_001616
ACVR2B = ActR2B	CTCATCACGGCCTTCCAT/ AGCGAGCCTCTGCATCAT	619	56°C	NM_001106
ACVR1B = ALK4	CCGGTACACAGTGACAAT/ CACTCTCGCATCATCTTC	619	53°C	NM_020328
ACVR1C = ALK7	CTCCCTTCCAGAACTGAATG/ CCACACCTCACCAAATCTAC	438	55°C	NM_145259
Follistatin	GGAGGACGTGAATGACAAC/ AGGCTCATCCGACTTACTG	645	51°C	NM_006350
Follistatin [199]	CCAGCGAGTGTGCCATGAAG/ TCATCTTCCTCCTCTTCCTCG	114 (FS-315) 378 (FS-288)	61°C	NM_006350
FSTL1	AGACCACGATGTGGAAACG/ CCTCCTCATTAGATCTCTTTG	943	55°C	NM_007085

FSTL3	CTGGTGCTCCAGACTGATG/ CATGTGGCACGAGGAGATG	649	55°C	NM_005860
TGF-β1	GCGTGTCCAGGCTCCAAATG/ TGGCGATACCTCAGCAACCG	468	55°C	NM_000660
TDGF1 = Cripto	GGGCTGGGCCATCAGGAATTTG/ TGGAAGCCACGAGGTGCTCATC	396	55°C	NM_003212
Nodal	GTTGCTCTGCCCACCAGAAC/ CAACCCAGCCTGAGGCAATG	399	55°C	NM_018055
GAPDH	CTGGCGTCTTCACCACCAT/ GCCTGCTTCACCACCTTCT	499	49°C	NM_002046
18s rRNA	GTATTGCGCCGCTAGAGGTG/ GGTGCCCTTCCGTCAATTCC	274	49°C	

5.5.4 SYBR-Green quantitative RT-PCR (qRT-PCR)

The Master-Mix for SYBR-Green quantitative RT-PCR was prepared on ice. All reactions were done in duplicates and an additional reaction with nuclease-free water (Fermentas) instead of cDNA was used as negative control. For each sample, 2 µl cDNA solution were mixed with 23 µl SYBR-Green Master-Mix, gently vortexed, spinned down and divided into two wells of a 0.1 ml MicroAmp Fast Optical 96-well Reaction Plate (Applied Biosystems). Plates were sealed with a MicroAmp Optical Adhesive Film (Applied Biosystems) and expression analyses were performed using an ABI Prism 7500 Fast SDS thermocycler (Applied Biosystems). For cycling parameters and a list of primers used see Table 6 and Table 8). All experiments were performed two times. To validate the results of the SYBR-Green qRT-PCR, the sizes of the amplified fragments were afterwards checked by agarose gel electrophoresis.

1 x SYBR-Green qRT-PCR Master-Mix:

Reagents (Concentration)	***Volume (µl)***
2 x Maxima SYBR Green qPCR Master-Mix (Fermentas)	12.5
Nuclease-free water (Fermentas)	8.5
Primer forward (20 µM)	1
Primer reverse (20 µM)	1
total Master-Mix volume	*23*

5.5.5 TaqMan quantitative RT-PCR (qRT-PCR)

The Master-Mix for quantitative RT-PCRs using TaqMan probes (Applied Biosystems) were prepared on ice and all reactions were performed in duplicates. For each sample, 2 µl cDNA solution were mixed with 23 µl Master-Mix, gently vortexed and spinned down. Each sample was divided into 2 wells of a 0.1 ml MicroAmp Fast Optical 96-well Reaction Plate (Applied Biosystems) and plates were afterwards sealed with a MicroAmp Optical Adhesive Film (Applied Biosystems). The qRT-PCR reactions were performed in an ABI Prism 7500 Fast SDS thermocycler (Applied Biosystems) and fluorescence was measured after every cycle. Standard conditions and TaqMan probes used for expression analysis are listed in Table 7 and Table 8. The housekeeping genes beta-2 microglobulin (B2M), glyceraldehyde-3 phosphate dehydrogenase (GAPDH) and beta-actin (ACTB) were used for normalization and evaluation of gene expression was performed by applying the 2^(-ΔΔCT) method (227). All expression analyses were performed two times.

1 x TaqMan qRT-PCR Master-Mix:

Reagents (Concentration)	***Volume (µl)***
2 x Maxima Probe qPCR Master-Mix (Fermentas)	12.5
Nuclease-free water (Fermentas)	9.25
TaqMan probes (Applied Biosystems)	1.25
total Master-Mix volume	*23*

Table 7. TaqMan probes used for qRT-PCR.

Gene of Interest	***TaqMan Probe Assay ID***	***Gene of Interest***	***TaqMan Probe Assay ID***
INHBA	Hs00170103_m1	**FSTL3**	Hs00610505_m1
INHBB	Hs00173582_m1	**TGF-β1**	Hs00998133_m1
INHBC	Hs00173745_m1	**TDGF1/Cripto**	Hs02339499_g1
INHBE	Hs00368884_g1	**GAPDH**	Hs99999905_m1
INHA	Hs00171410_m1	**ACTB**	Hs99999903_m1
Follistatin	Hs00246256_m1	**B2M**	Hs00984230_m1
FSTL1	Hs00200053_m1		

Table 8. Standard TaqMan and SYBR-Green qRT-PCR conditions.

	Temperature	***Time (minutes)***	***Repetitions***
Initial Denaturation	95°C	10:00	1 x
Denaturation	95°C	00:15	40 x
Annealing	60°C	00:30	
Elongation	72°C	00:30	

5.5.6 Gel Electrophoresis of Nucleic Acids

In order to check the quality of isolated RNA and the size of the amplified fragments in PCR reactions, samples were separated using agarose gel electrophoresis (GenXpress). For the gel preparation, 1% (w/v) agarose (StarLab) was solubilised in 1 x Tris-borate-EDTA (TBE) buffer. Samples were mixed with the appropriate amount of a 6 x loading buffer, loaded into the agarose gel and separated by electrophoresis. Depending on the expected fragment sizes, a 100 bp or 1000 bp marker (Fermentas), mixed with the appropriate amounts of nuclease-free water and loading buffer, was additionally loaded onto the gel. As running buffer, TBE was used at the same concentration as used for the agarose gel. Gels were run at 50 volts for 10 minutes, and then run at 90 volts until the desired separation of the nucleic acids was achieved. Finally a Typhoon Trio (GE Healthcare) was used for gel imaging and visualisation of the fragment bands.

10 x Tris-borate-EDTA (TBE) buffer stock solution:

108 g trizma base (Sigma)
55 g boric acid (Sigma)
40 ml 0.5 M EDTA, pH = 8.0
ad 1 L bd H_2O

1 x TBE working stock:

100 ml 10 x TBE
ad 1 L bd H_2O

6 x loading buffer:

333 µl 6 x loading dye (Fermentas)

250 µl 80% glycerol (Merck)

66.5 µl 0.5 M EDTA

0.5 µl Vistra Green 10000 x (GE Healthcare)

ad 1 ml bd H_2O

5.6 Cell Proliferation and Cell Vitality Assays

5.6.1 Scratch Assay

Cells were seeded in 6-well plates and incubated at 37°C until they reached full confluence. Then four parallel scratches were made in the middle of the well using a yellow tip. The start and the end of every scratch were marked at the underside of the well with a pen. Medium was removed, and 1500 µl fresh culture medium, containing 10% FCS and the desired cell treatment, were added into the well. To monitor the migration of the cells, every scratch was photographed with an Eclipse TE300 microscope (Nikon) immediately after the scratch and also 4, 8, 24 and 48 hours later. Scratches without any treatment in the medium were used as a control. The distance of the cell migration was measured using Image-J.

5.6.2 Transwell Migration Assay

Another method to test cell migration and invasion is the transwell migration assay. 25 000 cells were seeded in 500 µl of the respective growth medium, containing 10% FCS and the desired treatment, onto the porous membrane of a transwell-chamber (24 well-plate format (BD Falcon)). Another 500 µl medium, also containing 10% FCS and the desired treatment, were added into the well resulting in a total volume of 1 ml. After an incubation of 24 hours, transwell-chamber and growth medium were removed and migrated cells attached to the well were washed carefully with PBS. 1 ml fresh medium without any treatment was added into the well and cells were incubated for another week in the incubator. The resulting colonies were finally fixed with 1 ml methanol/acetic acid (3:1) for 20 minutes and afterwards stained with crystal violet (stock: 10% crystal violet in ethanol, diluted 1:1000 in PBS) for 30 minutes. Colonies were washed once with PBS and air dried over night. All experiments were performed in duplicates and cells treated with equal amounts of DMSO were used as negative control.

5.6.3 MTT Assay

Cells were seeded in triplicates in a 96-well plate at a density of 2 x 10^3 cells per well in 100 µl growth medium and allowed to recover for 24 hours. The next day, medium was aspirated and replaced by 100 µl fresh medium containing the desired treatment and cells were incubated for 72 hours at 37°C.

To determine the proportion of viable cells after a combination treatment with small-interfering RNA targeting human INHBA and the cytotoxic drug cisplatin, cells were seeded in microtiterplates as described before. After an incubation of 24 hours, cells were transfected with siRNA targeting INHBA or, respectively, with scrambled-siRNA as negative control, at a final concentration of 50 nM in 100 µl of the respective growth medium and allowed to rest for 24 hours. Then the cytotoxic drug cisplatin was added to the medium at different concentration ranges and cells were incubated at 37°C for additional 72 hours.

The proportion of viable cells was determined by using the EZ4U reagent (Biomedica) according to the manufacturer's instructions. Absorbance was measured at 450 nm and 620 nm as reference using a SynergyHT plate reader (BioTEK) and Gen5 software (BioTEK) after an incubation of 1-4 hours, depending on the cell's metabolic capacity. All experiments were performed three times.

5.6.4 Clonogenic Assay

To study the influence of exogenous treatment with recombinant cytokines or inhibitors on the capacity to form colonies, 1000 cells per well were seeded in 6-well plates. After incubation for 24 hours, the medium was removed, cells were washed once with PBS and 1.5 ml fresh growth medium containing the desired treatment was added into the wells.

The effect of siRNA targeting INHBA on the cell capability to form colonies was tested in 12-well plates. 1000 cells were seeded per well, incubated for 24 hours and transfected with siRNA at a final concentration of 50 nM in 1 ml of the respective growth medium. Cells transfected with scrambled-siRNA were used as negative control.

After incubation for 10 days, the medium was removed and cells were washed once with PBS. Colonies were fixed with 1 ml methanol/acetic acid (3:1) for 20 minutes and afterwards stained with crystal violet (stock: 10% crystal violet in ethanol, diluted 1:1000 in PBS) for 30 minutes. Finally colonies were washed with PBS for a last time and air dried over night.

For a photometric quantification, fixed and stained colonies were incubated with 1.5 ml of 2% sodium dodecylsulfate (SDS) for 45 minutes. The solution was afterwards pipetted in triplicates into a microtiterplate and absorbance was measured at 562 nm using a SynergyHT plate reader (BioTEK) and Gen5 software (BioTEK). Unstained wells without any cells were also incubated with 2% SDS for blank measurements.

5.7 Cell Cycle Analysis

For cell cycle analysis using flow cytometry, cells were seeded in 6-well plates at a density of 250000 cells per well in 1 ml growth medium containing 10% FCS, and were allowed to rest for 24 hours. After this incubation period, medium was removed and replaced by 1 ml fresh medium and the desired treatment. Cells without any treatment were used as negative control. After an incubation for 24 hours, cells were washed once with PBS, suspended in 5 ml cold PBS and transferred into a 15 ml round-bottom tube (BD Falcon) and centrifuged at 800 rpm at 4°C for 10 minutes. The supernatant was discarded, cells were resuspended carefully in 3 ml cold 70% ethanol and fixed for 30 minutes at 4°C. Subsequently cells were centrifuged for 10 minutes at 800 rpm at 4°C and supernatant was again discarded. The cell pellet was resuspended in 2 ml cold PBS and centrifuged for a last time at 800 rpm at 4°C for 10 minutes. The supernatant was discarded again and cells were finally resuspended in 0.5 ml staining solution and transferred into 5 ml round-bottom tubes (BD Falcon). After incubation for 10 minutes at 4°C, fluorescence was measured by flow cytometry (FACS Calibur – Becton Dickinson). Each experiment was performed in duplicates.

1 x flow cytometry staining solution:

0.5 ml PBS (PAA)
25 µg RNase A (10 mg/ml) (Sigma)
25 µg propidiumiodide (2.5 mg/ml) (Calbiochem)

5.8 Protein Analysis

5.8.1 Total Protein Isolation

In order to test whether different cell signaling pathways like the SMAD2 pathway can get phosphorylated in Malignant Pleural Mesothelioma cells by an exogenous treatment with recombinant activin A (201-203), total cell proteins were collected after a treatment for 30

minutes. For every tested cell line, total proteins of cells treated with equal amounts of PBS were used as negative control.

For the isolation of non-secreted proteins, cells were seeded in 6-well plates at a density of 500000 cells per well in 1 ml growth medium containing 10% FCS. After incubation for 24 hours, culture medium was removed, cells were washed with PBS and 1 ml FCS-free medium containing recombinant activin A at a final concentration of 20 ng/ml was added into the wells. After an additional incubation for 30 minutes in the incubator, total cell proteins were isolated by lysis buffer for further analysis.

Culture plates were put on ice, medium was removed, cells were washed once with cold PBS and afterwards collected by scraping into 1.5 ml fresh PBS. Suspension was transferred into a 1.5 Eppendorf tube and centrifuged for 5 minutes at 200 g at 4°C. Supernatant was discarded and the cell pellet was carefully resuspended in 45 µl lysis buffer by pipetting up and down several times. The suspension was incubated on ice for 5 minutes and after a sonification for 5 minutes (Bandelin) centrifuged for a last time for 5 minutes at 12000 g at 4°C in order to remove insoluble components. Finally the aqueous supernatant was transferred into a fresh 1.5 Eppendorf tube and stored frozen at -20°C.

Lysis buffer:

1 mM EDTA
150 mM NaCl (Merck)
0.5 mM Na_3VO_4 (Sigma)
1.5 mM $MgCl_2$ (Fluka)
10% glycerol (Merck)
50 mM HEPES (USB)
10 mM NaF (Sigma)
1% Triton X-100 (Serva)

5.8.2 Determination of Protein Concentration

The concentration of isolated proteins was determined by Bradford Assay (Bio-Rad Protein Assay). Therefore a series of protein standards using bovine serum albumin (BSA), lysis buffer and distilled water were pipette in duplicates into a microtiterplate (Greiner) according to the scheme shown in Table 9. For each sample, 1 µl of the protein solution and 9 µl of distilled water were also pipetted in duplicates into the microtiterplate. Bradford Solution (Bio-Rad) was diluted at a ratio of 1:5 with distilled water and added as well into the microtiterplate at an

amount of 200 µl per well. After an incubation of at least 5 minutes, absorption was measured at 595 nm using a SynergyHT plate reader (BioTEK) and Gen5 software (BioTEK). The results obtained from the protein standards were used to finally calculate the protein concentrations of the samples.

Table 9. Pipetting scheme for determination of protein concentrations according to Bradford Assay.

	Distilled Water (µl)	***Lysis Buffer (µl)***	***BSA (µg/µl)***	***Concentration (µg/µl)***
Blank	9	1	0	0
Standard 1	8	1	1	0.1
Standard 2	7	1	2	0.2
Standard 3	6	1	3	0.3
Standard 4	5	1	4	0.4
Standard 5	4	1	5	0.5
Standard 6	3	1	6	0.6

5.8.3 SDS-PAGE

For SDS-Page (sodium dodecyl sulphate polyacrylamide gel electrophoresis), isolated proteins were loaded on discontinuous polyacrylamide gels consisting of 10% separating gel and 5% stacking gel. For each sample, 40 µg of protein lysate were mixed with a 5 x SDS-Page loading buffer and heated at 95°C for 5 minutes for denaturation and loaded on the polyacrylamide gel. 5 µl of a Page Ruler Plus Prestained Protein Ladder (Fermentas) were additionally loaded on the gel as a marker. A Mini Protean 3 system was used for gel electrophoresis. The gel was run in running buffer at 60 V until the bromophenol blue tracking dye had reached the separation gel and then run at 110 V until the running front reached the end of the gel.

10% SDS-Page separating gel:

3.92 ml bd H_2O

2.5 ml 1.6 M Tris-HCl, pH = 8.8

3.35 ml 30% Acrylamid/Bis; 29:1 (Bio-Rad)

200 µl 20% SDS

25 µl 10% APS (Merck)

10 µl Temed (Amresco)

5% SDS-Page stacking gel:

3.6 ml bd H_2O

0.625 ml 0.5 M Tris-HCl, pH = 6.8

0.625 ml 30% Acrylamid/Bis; 29:1 (Bio-Rad)

100 µl 20% SDS

50 µl 10% APS (Merck)

7.5 µl Temed (Amresco)

5 x SDS-Page loading buffer:

300 nM Tris, pH = 6.8

60% (w/v) glycerol (Merck)

10% SDS

0.025% bromophenolblue

7% β-Mercaptoethanol (Aldrich)

10 x SDS-Page running buffer:

30.3 g trizma base (Sigma)

144 g glycine (Bio-Rad)

0.1% SDS

1 x SDS-Page running buffer:

100 ml 10 x SDS-Page running buffer

ad 1 L bd H_2O

5.8.4 Western Blotting

The polyacrylamide gels were blotted onto a PVDF membrane (Hypond-P, GE Healthcare) for further analyses by Western blotting. Blotting was performed by using a Mini Protean 3 system according to the manufacturer's instructions (228). Before blotting was started, the PVDF membrane was shortly activated with methanol, washed with distilled water and equilibrated in Towbin Buffer, which was also subsequently used as transfer buffer. The transfer of the proteins onto the PVDF membrane was performed over night in a fridge at 4°C at 18 V.

The next day, staining of the membrane with Ponceau S Solution was performed in order to check the quality of the transfer of the proteins. After incubating the membrane in the staining solution for about 10 minutes, the background was removed by rinsing the membrane with distilled water. The membrane was air dried and staining was subsequently documented using a

photocopier.

The membrane was again activated in methanol, washed with distilled water and afterwards blocked with 5% skim milk powder (Fluka) in1 x Tris buffered saline with 0.1% Tween-20 (TBST) for 60 minutes on a shaker at room temperature. The membrane was then washed with TBST three times for 10 minutes and subsequently incubated in a primary antibody solution (Table 10) over night at 4°C.

On the following day, the membrane was washed 3 times with TBST for 10 minutes and afterwards incubated in the secondary antibody solution (Table 11) for at least 60 minutes at room temperature on a shaker. After washing the membrane again 3 times for 10 minutes with TBST and once with 1 x Tris buffered saline (TBS), proteins were visualized using Immun-Star WesternC Kit (Bio-Rad) and x-ray film. For every membrane a monoclonal Anti-β-Actin antibody (Sigma) was used as loading control.

10 x Tris buffered saline (TBS):

80 g NaCl (Merck)
2 g KCl (Merck)
30 g trizma base (Sigma)
ad 1 L bd H_2O, pH = 7.4

1 x Tris buffered saline (TBS):

100 ml 10 x TBS
ad 1 L bd H_2O

1 x Tris buffered saline with 0.1% Tween-20 (TBST):

100 ml 10 x TBS
900 ml bd H_2O
1 ml Tween-20 (Sigma)

Ponceau S Solution:

0.5 g/l Ponceau S (Sigma)
1 ml/l glacial acetic acid (Merck)
ad 1 L bd H_2O

Table 10. Primary antibody solutions used for Western Blotting.

Antibody	***Dilution***	***Supplier***	***Diluent***	***Size of Protein of Interest (kDa)***
Anti-Smad2/3	1:1000	Cell Signaling	M	60
Anti-Phospho-Smad2/3	1:1000	Cell Signaling	BSA	60
Anti-p38	1:1000	Santa Cruz Biotechnology	BSA	38
Anti-phospho-p38	1:1000	Santa Cruz Biotechnology	BSA	38
Anti-β-Actin	1:4000	Sigma	BSA	42
M … 5% milk powder in TBST; BSA … 3% bovine serum albumin in TBST				

Table 11. Secondary antibody solutions used for Western Blotting.

Antibody	***Dilution***	***Supplier***	***Diluent***
Polyclonal Goat Anti-Rabbit Immunglobulins/HRP	1:10000	Dako	M
Anti-Mouse-HRP	1:10000	Dako	M
M … 5% milk powder in TBST			

5.9 Immunohistochemistry

Tissue sections of formalin-fixed and paraffin-embedded tumor samples were incubated at 65°C for 10 minutes. Deparaffination and rehydration was performed by incubating the slides twice in xylol, 100% ethanol, 70% ethanol and distilled water for 1 minute each and afterwards 10 minutes in 0.3% H_2O_2/PBS at room temperature. Slides were additionally washed two times in PBS for 3 minutes. For epitope retrieval, tissue sections were heated for 10 minutes in citrate buffer (10 mmol/l, pH = 6.0) in a pressure cooker. Sections were allowed to cool down for about 15 minutes and afterwards washed in PBS containing 0.1% Tween-20 for 3 minutes. Slides were incubated in Ultra V Block (UltraVision LP) for 5 minutes at room temperature and subsequently incubated with an antibody against activin A (Serotec, clone E4) at a dilution of 1:100 for 1 hour. Then, slides were washed two times with PBS containing 0.1% Tween-20 and incubated with Primary Antibody Enhancer (UltraVision LP) for 10 minutes and again washed two times with PBS containing 0.1% Tween-20. After incubating the slides with horseradish peroxidase (HRP) polymer (UltraVision LP) for 15 minutes, colour was developed by 3,3'-diaminobenzidine

tetrahydrochloride (DAB) reagent (Dako) and counterstaining was performed using hematoxylin. Finally, entellan was used to coverslip the slides.

5.10 Construction of a Lentivirus Overexpressing INHBA

5.10.1 Gateway Recombination Cloning

The construction of a lentivirus expression vector for overexpressing human INHBA was conducted using the Gateway recombination technology (Invitrogen). The first step in the Gateway cloning strategy is the amplification of the gene of interest via RT-PCR, which gets subsequently ligated into an entry vector, containing attL binding sites and a kanamycin resistance cassette, for the generation of the entry clone. There is also another vector, the so called destination vector, which harbours attR binding sites and an ampicillin resistance cassette. As a next step, the LR recombination reaction is carried out in order to transfer the gene of interest from the entry clone into the destination vector, resulting in the generation of the expression clone. This procedure occurs via homolog recombination between the attL and attR binding sites.

The generated expression clone will subsequently be co-transfected with helper plasmids (Vira Power packaging mix, Invitrogen) into 293FT cells for the production of lentiviral particles, that can be harvested as viral supernatants 48 hours after transfection.

5.10.2 Amplification of the Gene of Interest

The gene of interest, INHBA, was amplified using reverse transcriptase polymerase chain reaction and a Pfu polymerase, which posseses a proofreading activity. 1 μl of cDNA was used as template for the reaction. Conditions and cycle parameters are presented in Table 12.

1 x Master-Mix for Pfu-PCR:

Reagents (Concentration)	***Volume (µl)***
Pfu DNA polymerase (Fermentas)	0.5
PCR buffer with $MgSO_4$ (Fermentas)	5
Nuclease-free water (Fermentas)	40.5
dNTPs (10 mM; Fermentas)	1
Primer forward (20 µM)	1
Primer reverse (20 µM)	1
total Master-Mix volume	*24*

Table 12. Temperature conditions and cycle parameters for RT-PCR with Pfu polymerase.

	Temperature	***Time (minutes)***	***Repetitions***
Initial Denaturation	94°C	03:00	1 x
Denaturation	94°C	00:50	33 x
Annealing	49°C	00:50	
Elongation	72°C	02:00	
Final Elongation	72°C	05:00	1 x

5.10.3 Nucleotide Phosphorylation of the PCR Product

For a direct integration of the PCR product into a linear vector backbone with blunt ends, the PCR product was phosphorylated with a T4 polynucleotide kinase (Fermentas). 15 µl of the PCR reaction were mixed with 2 µl of a 10 x Reaction Buffer A for PNK (Fermentas), 2 µl 10 mM ATP (Promega) and 1 µl T4 polynucleotide kinase (10 units/µl), resulting in a total reaction volume of 20 µl. The mixture was incubated at 37°C for 20 minutes and the reaction was afterwards stopped by incubating the mixture at 75°C for 10 minutes.

5.10.4 Gel Elution and DNA Purification of the PCR Product

For purification of the PCR product the reaction mixture was subjected to agarose gel electrophoresis. The agarose gel elution and the subsequent DNA purification were performed using a Wizard SV Gel and PCR Clean-Up System (Promega), according to the manufacturer's instructions. First of all, the DNA fragments were cut from the gel with a scalpel and weighed. Then 1 µl Membrane Binding Solution was added for every mg of the gel slice. The mixture was incubated at 60°C until the whole gel slice was dissolved. The solution was afterwards pipetted onto the membrane of a SV Minicolumn that had previously been inserted into a Collection Tube.

After an incubation for 60 seconds at room temperature, the reaction tube was centrifuged at 16000 g for 60 seconds at room temperature. The resulting flow through was discarded and 700 µl Membrane Wash Solution (containing ethanol) were pipetted onto the membrane. Reaction was again centrifuged at 16000 g at room temperature for 60 seconds and the flow through was also again discarded. Then another 500 µl of the Membrane Wash Solution (containing ethanol) were pipetted onto the membrane and the reaction was centrifuged for 5 minutes at 16000 g at room temperature. The flow through was discarded and the reaction was again centrifuged for 60 seconds at 16000 g at room temperature. Subsequently, the Minicolumn was added onto a fresh 1.5 ml Eppendorf reaction tube, 30 µl nuclease-free water (Fermentas) were added onto the membrane and the reaction was incubated at room temperature for 60 seconds. The DNA was finally eluted by centrifugation for 60 seconds at 16000 g at room temperature and stored frozen at -20°C.

5.10.5 Determination of DNA Concentration

For the determination of purified DNA concentrations, a NanoDrop 1000 spectrophotometer (PeqLab) was used. Blank measurements were done using the same water that was previously used for the resuspension of the DNA.

5.10.6 Ligation

The ligation of the insert into the vector backbone was done using the Rapid DNA Ligation Kit (Fermentas). For the ligation approach, the DNA solution of the vector backbone was mixed with a 3 times and a 5 times molar excess of the insert DNA, T4 DNA Ligase (5 units/µl), Rapid Ligation Buffer (5 x) and distilled water, resulting in a total volume of 10 µl. Reactions were incubated at 25°C for 10 minutes and afterwards transformed into competent E. Coli cells.

5.10.7 Transformation of Competent E. Coli

Competent E. coli were slowly thawed on ice. Then 3 µl of the ligation mix were mixed with 100 µl competent cells and incubated on ice for 20 minutes. The heat-shock was performed at 42°C for 60 seconds, followed by an addition of 1 ml cold SOC medium and an incubation on a shaking thermo-block at 37°C and 400 rpm for at least 1.5 hours. Then the suspension was centrifuged at 4000 rpm at room temperature for 3 minutes. The supernatant was discarded and bacteria were finally plated on LB agar plates containing 50 µg/ml kanamycin (Fluka). Plates were incubated over night at 37°C in a humidified incubator (Heraeus).

LB agar plates (Lysogeny Broth):

20 g LB Broth (Sigma)

15 g agar (Fluka)

ad 1 L bd H_2O

SOB medium (Super Optimal Broth):

20 g tryptone (Fluka)

5 g yeast extract (Oxoid)

0.5 g NaCl (Merck)

ad 1 L bd H_2O

SOC medium (Super Optimal Broth with glucose):

SOB medium

20 mM glucose (Merck)

5.10.8 Boiling Lysis Plasmid Preparation

Colonies were picked from the LB agar plates and grown in 5 ml LB medium containing 50 μg/ml kanamycin (Fluka) in round-bottom tubes (BD Falcon) on a shaker at 37°C and 200 rpm. On the following day, 1.5 ml cell suspension were transferred to a 1.5 ml Eppendorf reaction tube and centrifuged at 16000 g for 60 seconds at room temperature. The supernatant was discarded and the pellet resuspended in 700 μl STET-buffer. Then 13 μl lysozyme (10 mg/ml; Sigma) were added to the solution, the reaction tube was inverted several times and heated to 100°C for 2 minutes. After this the suspension was centrifuged again at 16000 g for 10 minutes at room temperature and the resulting pellet was carefully removed with a toothpick that had previously been tipped into RNase A (10 mg/ml; Sigma). For the DNA precipitation, 700 μl isopropanol (Merck) were added to the solution and the whole mixture was incubated at -20°C for 20 minutes. The DNA was pelleted by centrifugation for 15 minutes at 16000 g at 4°C. The supernatant was discarded, the DNA pellet was washed with 500 μl of 70% ethanol and pelleted again at 16000 g for 5 minutes at room temperature. The supernatant was removed carefully and the DNA pellet was air dried and finally resuspended in 15 μl TE-buffer.

LB medium:

20 g LB Broth (Sigma)

ad 1 L bd H_2O

STET-buffer:

25 ml 1 M Tris/HCl (pH = 8.0)
50 ml 0.5 M EDTA (pH = 8.0)
40 g sucrose (USB)
25 ml Triton-X 100(Serva)
ad 500 ml bd H_2O

TE-buffer:

100 mM Tris
10 mM EDTA, pH = 8.0

5.10.9 Glycerol Stocks

For a long-term storage of transformed bacterial cultures, cells were stored frozen at -80°C as glycerol stocks. For this, 700 µl of the overnight bacterial culture were mixed with 300 µl 80% glycerol (Merck) and immediately stored frozen at -80°C.

5.10.10 Diagnostic Restriction Digest

A diagnostic restriction digest was performed to identify a plasmid, either using one or two restriction enzymes. If only one enzyme was used for the digest, 1 µl of the DNA solution was mixed with 7.5 µl nuclease-free water, 0.5 µl of the restriction enzyme and 1 µl of the respective buffer (10 x), resulting in a total volume of 10 µl. The mixture was incubated at 37°C for about 2 hours, or in case of Fast-Digest reagents, the mixture was incubated for about 20 minutes.

If two restriction enzymes were used in combination, 0.5 µl of both enzymes, 1 µl of a 10 x Tango buffer for double digest (Fermentas) were used and the amount of nuclease-free water was reduced to 7 µl. The mixture was incubated at 37°C for 2 hours. For the verification of the correct plasmid, the whole approach was afterwards subject to gel electrophoresis.

5.10.11 Plasmid Minipreps for DNA Purification

For the isolation of high-quality plasmid DNA, a Wizard Plus SV Minipreps DNA Purification System (Promega) was used according to the manufacturer's constructions. First of all, 1.5 ml of overnight bacterial culture were transferred into an Eppendorf tube and centrifuged for 5 minutes at 16000 g at room temperature. The supernatant was discarded, another 1.5 ml of the same overnight bacterial culture were added into the tube and centrifugation was repeated. The

resulting supernatant was discarded and the pellet was resuspended in 250 µl Cell Resuspension Solution. 250 µl Cell Lysis Solution was additionally added into the solution and the tube was inverted several times. Then 10 µl Alkaline Protease Solution was added and the whole mixture was incubated at room temperature for 5 minutes, after inverting the tube several times. As a next step, 350 µl Neutralization Solution was added and the reaction tube was again inverted several times and centrifuged at 16000 g for 10 minutes at room temperature. The supernatant was pipetted onto the membrane of the spin column that had previously been inserted into the Collection tube, and centrifuged at 16000 g for 1 minute at room temperature. The flow through was discarded and 750 µl of the Wash Solution (containing ethanol) was pipetted onto the membrane. The reaction was centrifuged for 1 minute at 16000 g at room temperature, flow through was discarded and centrifugation was repeated for 2 minutes after pipetting 250 µl Wash Solution (containing ethanol) onto the membrane. The Spin column was afterwards inserted into a new 1.5 ml Eppendorf tube and centrifuged at room temperature for 1 minute at 16000 g. Finally the DNA was collected by adding 50 µl nuclease-free water into the Spin Column and a centrifugation for 1 minute at 16 000 g.

5.10.12 LR Recombination Reaction

For the LR recombination Reaction 50 ng of the entry clone were mixed with 75 ng of the destination vector and TE to a total volume of 4 µl. After the addition of 1 µl of Gateway LR Clonase II enzyme mix, the reaction was incubated at 25°C for 1 hour. Then 1 µl proteinkinase K (Invitrogen) was added and reaction was incubated at 37°C for 10 minutes und subsequently transformed into Stbl3 E. coli cells (Invitrogen).

5.10.13 Transformation of Stbl3 E. coli

Stbl3 E. coli cells (Invitrogen) were slowly thawed on ice. 2.5 µl of the LR recombination reaction were mixed with 25 µl Stbl3 E. coli cells and incubated on ice for 30 minutes. The heat-shock was performed at 42°C for 60 seconds and cells were afterwards put on ice for 2 minutes. Subsequently, 250 µl SOC medium (Invitrogen) were added and reaction was incubated on a shaking thermo-block for 1 hour at 37°C and 300 rpm. Subsequently, cells were centrifuged at 2000 g for 3 minutes and finally plated on LB agar plates containing 50 µg/ml ampicillin (Roche) and incubated over night at 37°C. The next day, colonies were picked and the plasmid DNA was isolated using a Wizard Plus SV Minipreps DNA Purification System (Promega) as described before. The result of the LR recombination reaction was controlled using diagnostic restriction digests of the isolated plasmids.

5.11 Statistical Analysis

Statistical analysis and calculations were performed using GraphPad Prism 5.0 software (GraphPad Software Inc.). For the evaluation of significance, t-tests were performed and a p-value of 0.05 was set as threshold significance level. P-values below 0.001 were regarded as *highly significant* (labelled as ***), p-values from 0.001 to 0.01 as *very significant* (labelled as **) and p-values between 0.01 and 0.05 were regarded as *significant* (labelled as *). All p-values higher 0.05 were seen as *not significant*.

6 Results

6.1 Activin Family Proteins are Expressed in MPM Cell Lines

6.1.1 Reverse Transcriptase Polymerase Chain Reaction (RT-PCR)

The mRNA transcript levels of all four mammalian activin subunits (beta A, beta B, beta C and beta E), activin type I and type II receptors (ALK4, ALK7, ACVR2, ACVR2B), activin antagonists (Follistatin, FSTL1, FSTL3, INHA, Cripto) as well as related related TGF-β family members (TGF-β, Nodal), were analyzed using RT-PCR (Figure 11). Analyses were performed in nine MPM cell lines, in contrast to the SV40 Tag immortalized non-malignant cell line Met5a. The activin subunit beta C, encoded by the gene INHBC, and the activin type I receptor ALK7 could not be detected at 30 cycles in any of the tested cell line, whereas the other activin subunits were detected in almost all cell lines. TGF-beta, the activin type I receptor ALK4 and the type II receptors ACVR2 and ACVR2B were expressed in all cell lines. Concerning the activin antagonists, both splice variants of Follistatin, as well as FSTL1 and Cripto were detected in nearly all cell lines, whereas FSTL3 could only be detected in some of them.

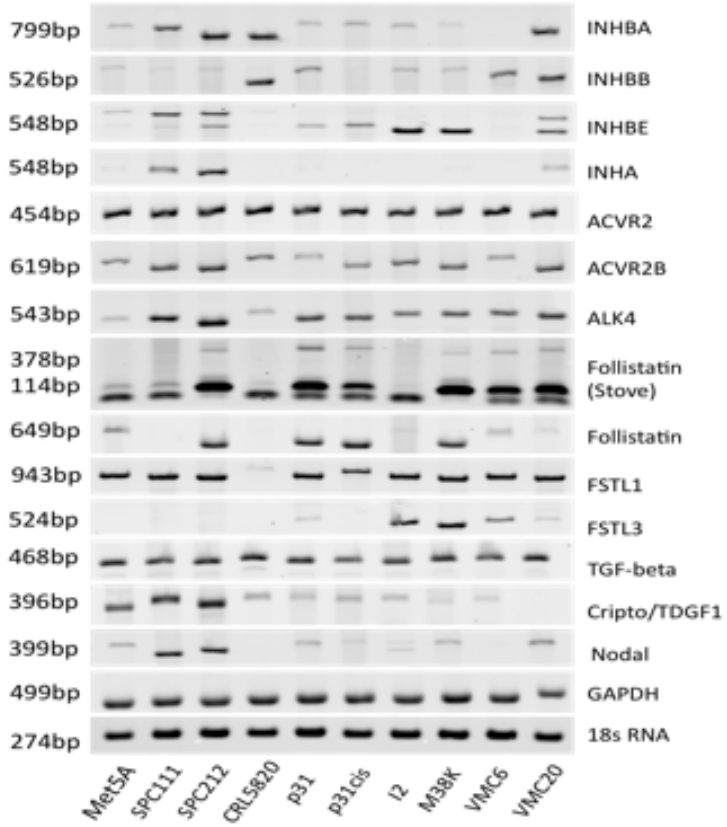

Figure 11. Expression analysis of activin family members and receptors by RT-PCR in nine MPM cell lines and the SV40 Tag immortalized non-malignant cell line Met5a.

6.1.2 TaqMan & SYBR-Green Quantitative RT-PCR

As a next step, the relative expression levels of the genes previously analyzed by RT-PCR analyzed genes were determined using TaqMan and SYBR-Green quantitative RT-PCR and the 2^(-ΔΔct) method. For each analyzed gene, the expression level of the non-malignant cell line Met5a was taken as reference. The average expression levels of two house-keeping genes (GAPDH, ACTB) was calculated and used for normalization (Figure 12).

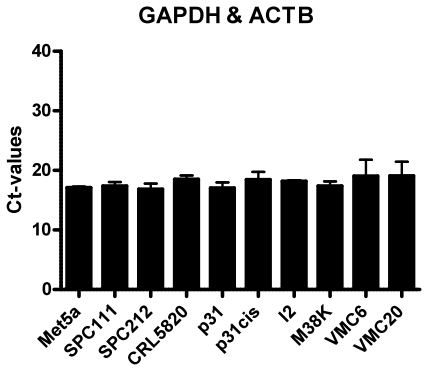

Figure 12. Avarage expression levels of GAPDH and ACTB.

6.1.2.1 Expression of the Activin Subunits

The expression analysis of the activin subunits by quantitative RT-PCR using TaqMan probes revealed, that there is a high expression of INHBA and INHBC in all MPM cell lines, in comparison to the Met5a. The activin subunit beta B was found to be highly expressed in nearly all tested cell lines, except the cisplatin resistant cell line p31cis, which showed a lower expression in comparison to the Met5a. The expression of INHBE was downregulated in the majority of the MPM cell lines, but also upregulated in contrast to the Met5a in some of them (Figure 13).

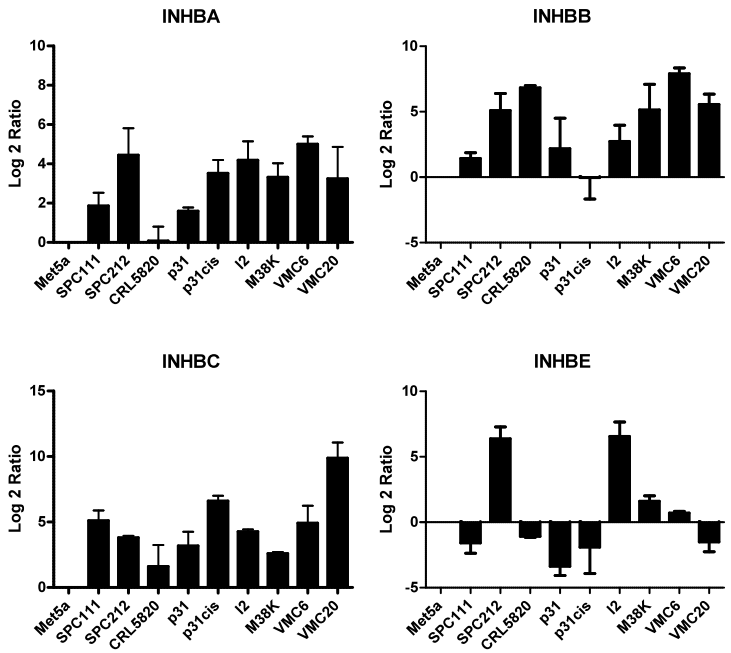

Figure 13. Expression levels of the four mammalian activin subunits determined by qRT-PCR.

6.1.2.2 Expression of the Activin Antagonists

The expression of the activin antagonist follistatin was found to be upregulated in five tested MPM cell lines and downregulated in four cell lines, in contrast to the Met5a. The follistatin related genes FSTL1 and FSTL3 were downregulated in the majority of the cell lines. Upregulated expression levels of INHA and TGF-beta were found in almost all MPM cell lines (Figure 14).

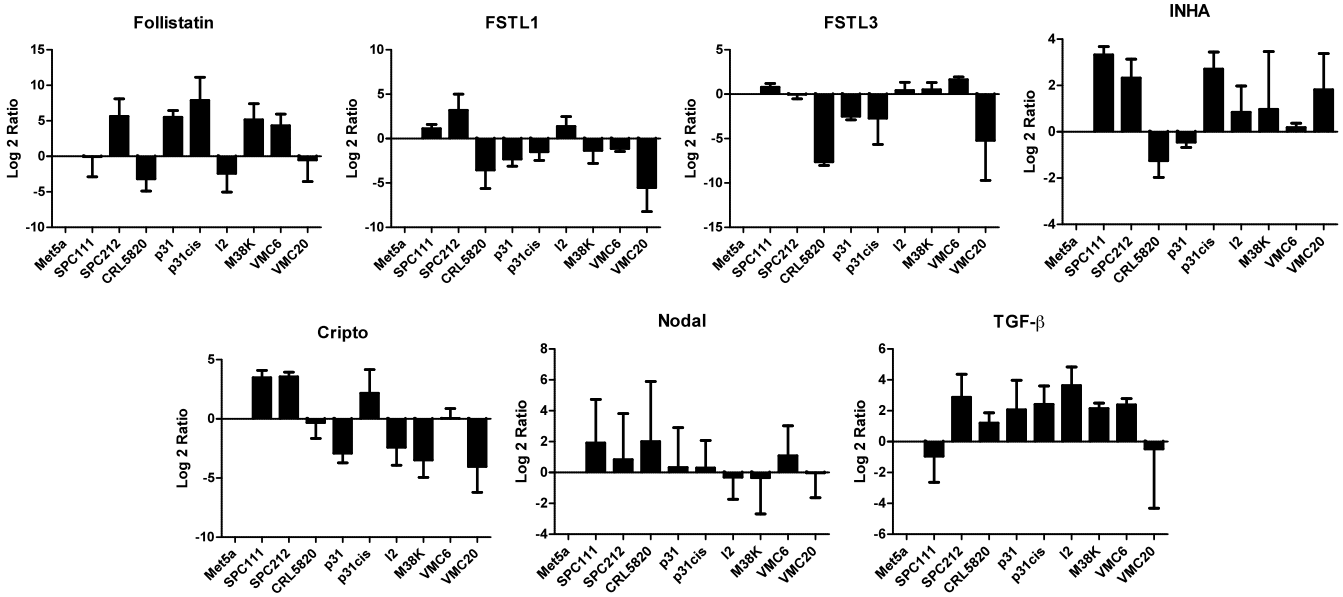

Figure 14. Relative expression levels of the activin antagonists Follistatin, FSTL1, FSTL3, INHA, Cripto, and of Nodal and TGF-beta determined by qRT-PCR (TaqMan and SYBR-Green).

6.1.2.3 Expression of the Activin Receptors Type I and Type II

The expression levels of the activin type I and type II receptors (type I: ALK4 and ALK7; type II: ACVR2 and ACVR2B) were determined by SYBR-Green qRT-PCR (Figure 15). The gene expression levels of the non-malignant cell line Met5a was used as reference and set as 1. In contrast to the Met5a, we measured a downregulation in the gene expression of ALK4 in all cell lines, except the cisplatin resistant cell line p31cis, whereas the other type I receptor, ALK7, was downregulated in all tested cell lines. Concerning the type II receptors, an upregulation in the gene expression of ACVR2 was measured in all cell lines, whereas the expression of ACVR2B was upregulated in five cell lines, but also downregulated in four cell lines.

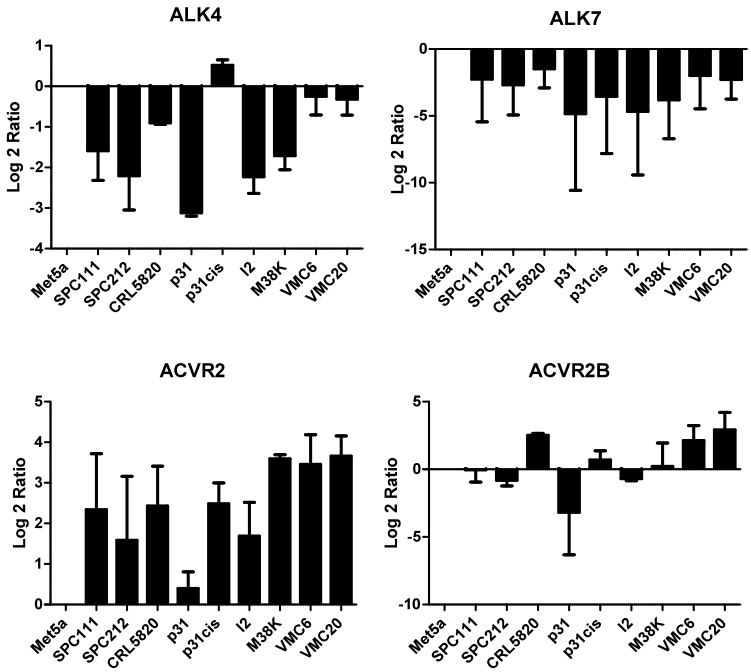

Figure 15. Expression levels of the type I and type II receptors in MPM cell lines.

6.2 Activin Signaling Pathways are Active in MPM Cell Lines

6.2.1 Activin A Phosphorylates SMAD-Pathway in MPM Cells

In a previous study with HepG2 cells, it was demonstrated that exogenous treatment with recombinant activin A at a final concentration of 20 ng/ml leads to the phosphorylation of SMAD2 (229). We could show that in all four tested MPM cell lines (p31, I2, M38K and VMC20), incubation of cells with recombinant activin A (20 ng/ml) for 30 minutes also activates the SMAD-pathway via phosphorylation of SMAD2 (Figure 16). Only in VMC20, an autogenous phosphorylation of SMAD2 could also be detected by Western blotting.

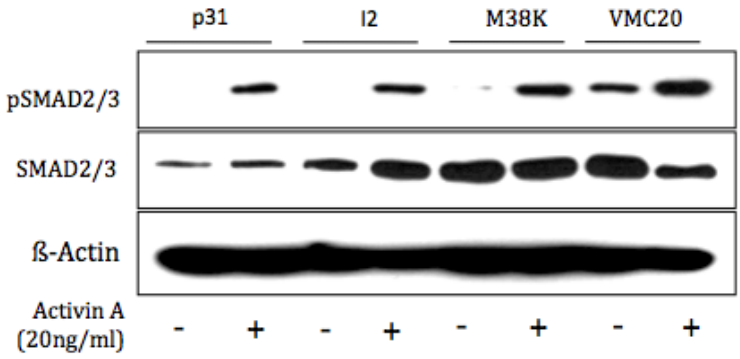

Figure 16. Exogenous treatment with recombinant activin A (20 ng/ml) leads to the phosphorylation of SMAD2 in MPM cell lines.

6.2.2 Activin A Does Not Activate p38 Kinase Pathway in MPM Cells

Previous studies reported activation of other pathways than the canonical SMAD-pathway, like the p38 kinase pathway. Within this study we wanted to determine whether an exogenous treatment of MPM cell lines with recombinant activin A at a final concentration of 20 ng/ml for 30 minutes can also activate the MAPK pathway p38 by phosphorylation. In the four tested cell lines, we could not see any phosphorylation of the p38 mitogen activated protein kinase pathway and could only detect the unphosphorylated form of p38 (Figure 17).

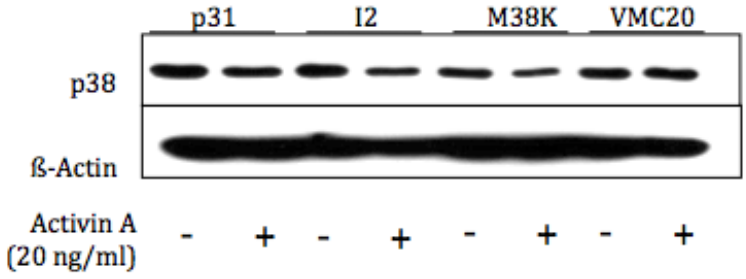

Figure 17. Immunodetection of p38 kinase pathway in MPM cells.

6.2.3 Activin A Increases Migration of MPM Cells in Vitro

Next it was tested, how efficiently MPM cell lines are able to close a scratch in the cell monolayer and whether treatment with recombinant activin A (20 ng/ml) can further stimulate migration. Figure 18 shows an example of two MPM cell lines (SPC212, p31cis) with an obvious upregulation of migration by an exogenous treatment with activin A. In both cell lines, the scratch was completely closed much earlier when simulated with activin A in contrast to the cells treated with equal amounts of PBS that were used as control. The scratch in the monolayer

of SPC212 cells stimulated with activin A was already closed after eight hours, whereas the scratch used as control was not closed until 24 hours after the scratch was initially performed. The scratch in the monolayer of non-treated p31cis cells was still not closed after 48 hours, whereas the scratch stimulated with activin A was already entirely closed 24 hours after the scratch was performed. The quantification of the migration of MPM cells through the scratch is presented in Figure 19in percent.

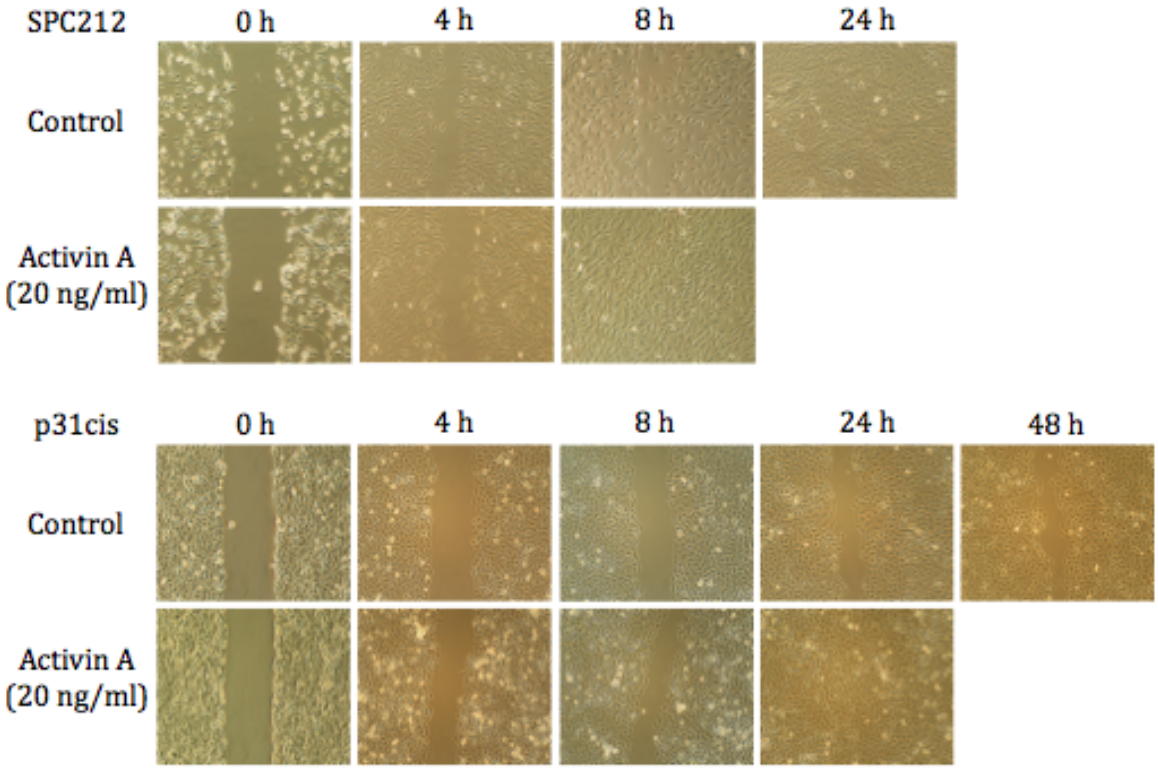

Figure 18. Example of two MPM cell lines (SPC212, p31cis) with an increased migration after exogenous treatment with recombinant activin A (20 ng/ml) in vitro.

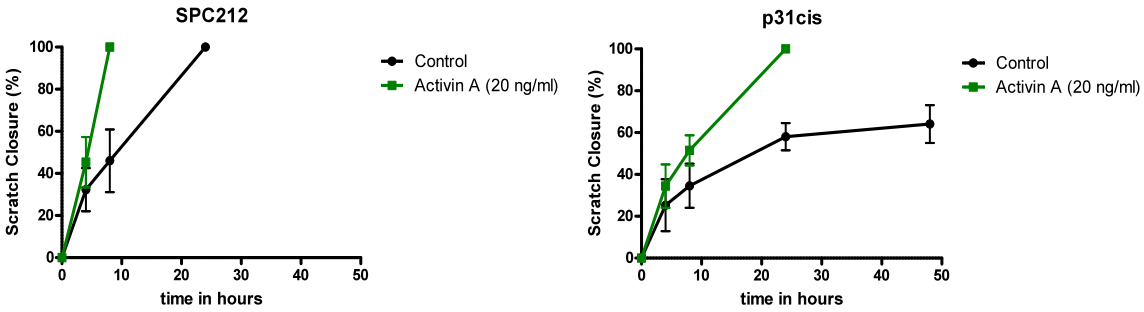

Figure 19. Quantification of cell migration of MPM cell lines (SPC212, p31cis).

6.2.4 Cell Proliferation Is Increased by Stimulation with Recombinant Activin A

Beside the effects on cell migration of MPM cells, we also tested whether cell treatment with recombinant activin A (20 ng/ml) can stimulate the cell proliferation rate in vitro. For this, cells were treated with activin A in culture medium containing 10% FCS or respectively 0.1% FCS and allowed to proliferate for 72 hours. Figure 20 gives an example of two MPM cell lines (I2, M38K) with an increase of cell proliferation in culture medium containing 10% FCS and an even stronger effect when the concentration of FCS was reduced down to 0.1% FCS.

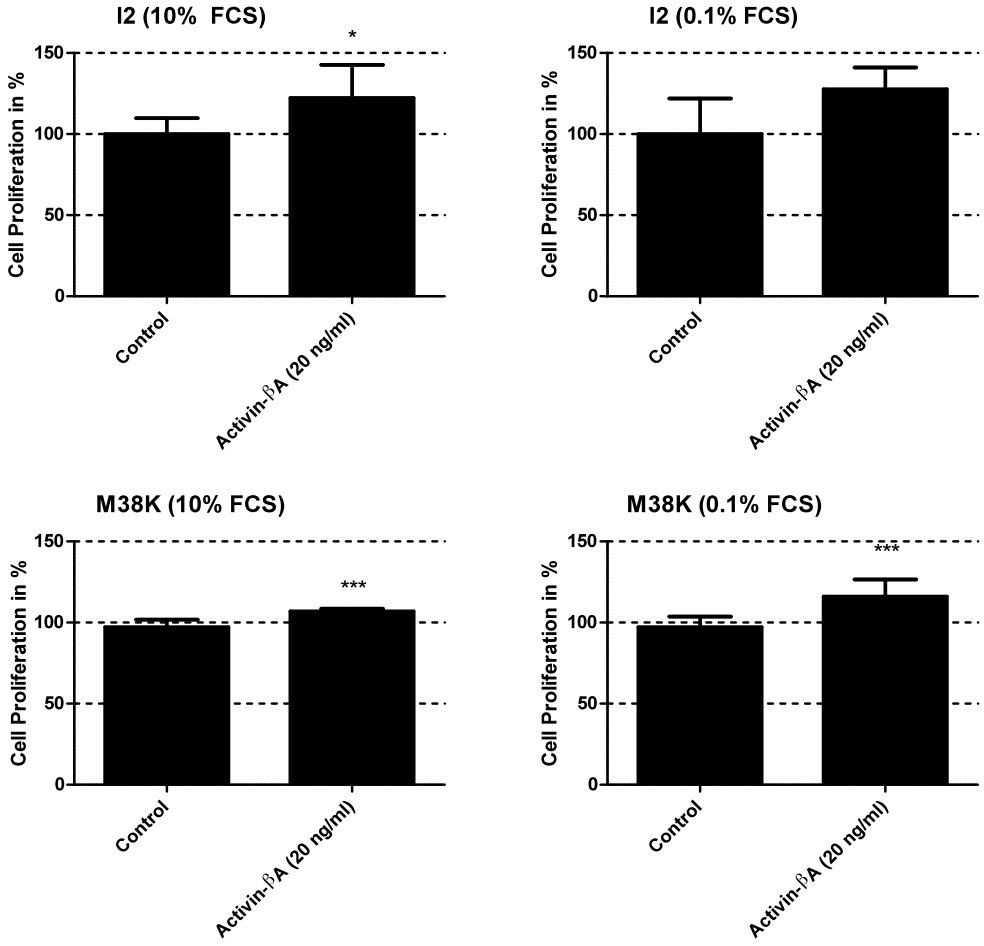

Figure 20. Example of two MPM cell lines with increased cell proliferation after treatment with recombinant activin A (20 ng/ml) and incubation for 72 hours. The cell line I2 shows a significantly increased proliferation rate only in growth medium containing 10% FCS, whereas a significantly increased cell proliferation was achieved in the cell line M38K in 10% FCS as well as in 0.1% FCS

6.2.5 Activin A Stimulates Clonogenicity in MPM Cells

MPM cells were seeded at a low density (1000 cells per well) and treated with recombinant activin A at a final concentration of 20 ng/ml. Figure 21 shows an example of four MPM cell lines (SPC111, M38K, VMC6 and VMC20) with increased clonogenicity after stimulation with activin A

in comparison to cells treated with equal amounts of PBS. These results can be quantified when crystal violet is solubilized with SDS and measured photometically (Figure 22). In three of the tested cell lines (SPC111, VMC6 and VMC20), the ability of the cells to survive and form colonies is upregulated to about 150% in contrast to the cells treated with equal amounts of PBS which were used as control, and even a slight stimulation of clonogenicity with activin A can be achieved in the cell line VMC6.

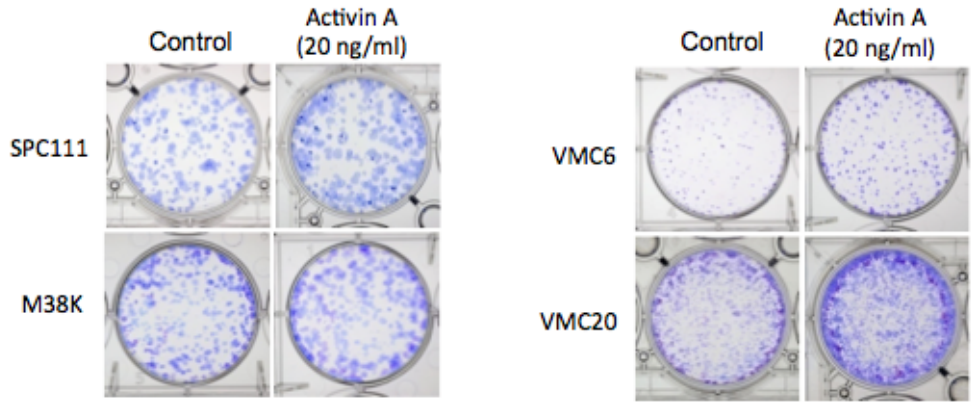

Figure 21. Stimulation with recombinant activin A (20 ng/ml) increases clonogenicity in MPM cell lines in contrast to cells treated with equal amounts of PBS.

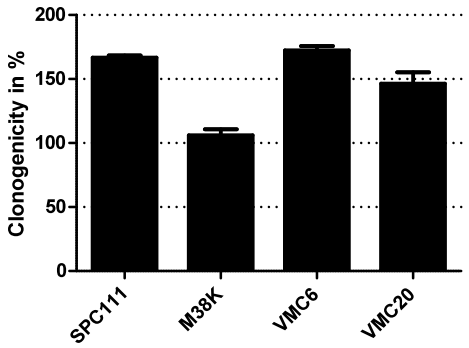

Figure 22. Photometical quantification of the stimulation of clonogenicity by exogenous treatment with recombinant activin A (20 ng/ml). Extinction values of cells treated with equivalent amounts of PBS were set as 100% and used for normalization.

Stimulation of clonogenicity by activin A is cell type specific, since the contrary effect can be achieved when the hepatocarcinoma cell line HepG2 is treated with activin A of the same concentration (20 ng/ml). In contrast to cells treated with equal amounts of PBS, cells incubated with recombinant activin A show a reduced ability to survive and form colonies (Figure 23).

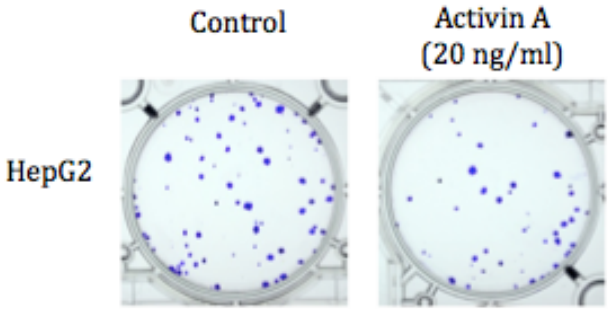

Figure 23. Treatment of the hepatocarcinoma cell line HepG2 with recombinant activin A (20 ng/ml) results in reduced clonogenicity.

6.3 Inhibition of Activin Receptor Signals Blocks Growth and Migration of MPM Cells

6.3.1 Treatment with SB-431542 Reduces Cell Migration

SB-431542 is a selective small molecule inhibitor for type I receptors of activin-like kinases, specifically ALK4, ALK5 and ALK7. Since the receptors ALK4 and ALK7 are part of the activin A signalling pathway, we wanted to determine whether the blockage of those receptors reduces the ability of MPM cells to close a scratch in the cell monolayer. Cells were treated with SB-431542 at a final concentration of 20 μM and already four hours after the scratch was performed, a decrease of migration was detected (an example of two MPM cell lines (p31, VMC6) is presented in Figure 24 and Figure 25). All tested cell lines failed at closing the scratch entirely by migration when treated with SB-431542, whereas the control-scratch of p31 for example was already closed 24 hours after the scratch was initially performed.

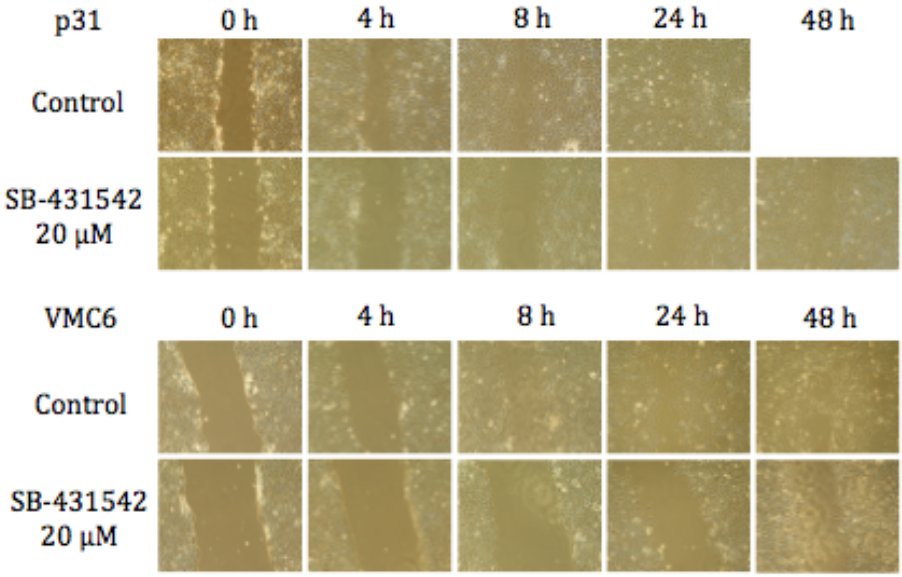

Figure 24. Example of a decreased cell migration of MPM cell lines (p31, VMC6) after treatment with the small molecule inhibitor SB-431542 at a final concentration of 20 µM.

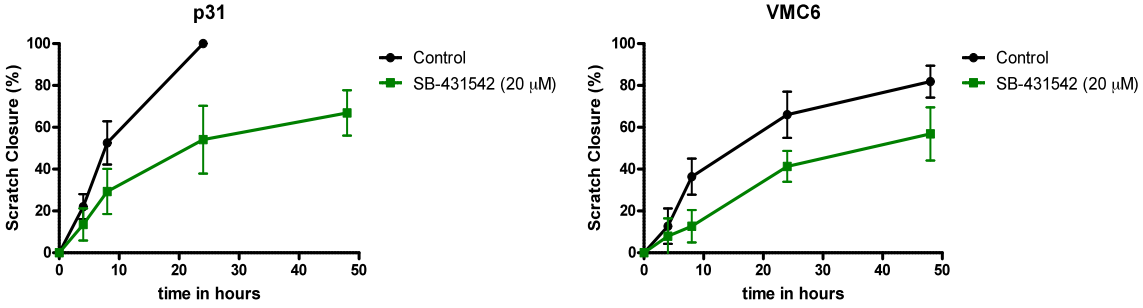

Figure 25. Quantification of cell migration of two MPM cell lines (p31, VMC6).

6.3.2 Migration Through Transwell Chambers Is Affected by SB-431542

Since we could show that the closure of a scratch in the cell monolayer by migration is clearly reduced when cells were treated with the small molecule inhibitor SB-431542, we wanted to determine whether the migration through a porous membrane could also be reduced by SB-431542. For this purpose, cells were seeded onto a transwell chamber, treated with SB-431542 at a final concentration of 20 µM and were allowed to migrate through the membrane for 24 hours. Figure 26 gives an example for two MPM cell lines (M38K, p31), which showed reduced migration through transwell chambers after treatment with the small molecule inhibitor SB-431542.

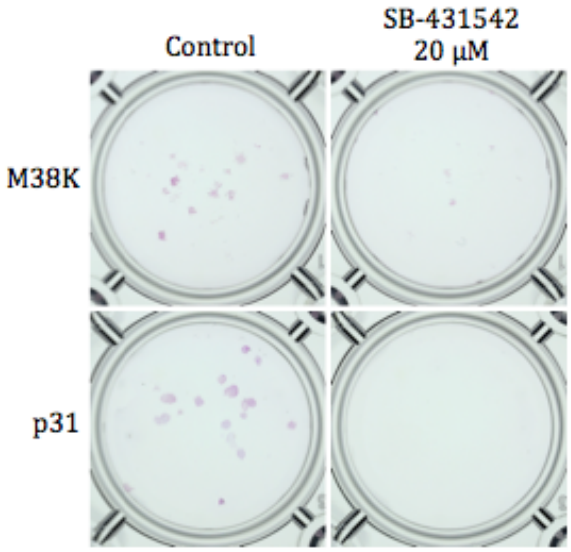

Figure 26. Example of two MPM cell lines with reduced ability for migrating through a porous membrane of a transwell chamber after treatment with SB-431542 at a final concentration of 20 µM in comparison to the control cells, which were treated with equal amounts of DMSO.

6.3.3 SB-431542 Impairs Cell Viability of MPM Cells

As a next step, we tested whether the blockage of activin type I receptors can also impair cell proliferation in MPM cell lines. For this purpose, we treated cells with the inhibitor SB-431542 at a final concentration of 20 µM and let them proliferate for 72 hours. Figure 27 gives an example of three tested MPM cell lines (I2, M38K and VMC20), which show a decrease of cell proliferation after cell treatment in culture medium containing 10% FCS. This effect was further increased when the concentration of FCS in the medium was reduced down to 0.1%. Cell lines I2 and VMC20 showed a reduction of the cell proliferation rate of about 50% in 0.1% FCS conditioned medium. Cell line M38K was only slightly impaired in cell proliferation at 10% FCS, but showed a strong impact on cell viability at 0.1% FCS.

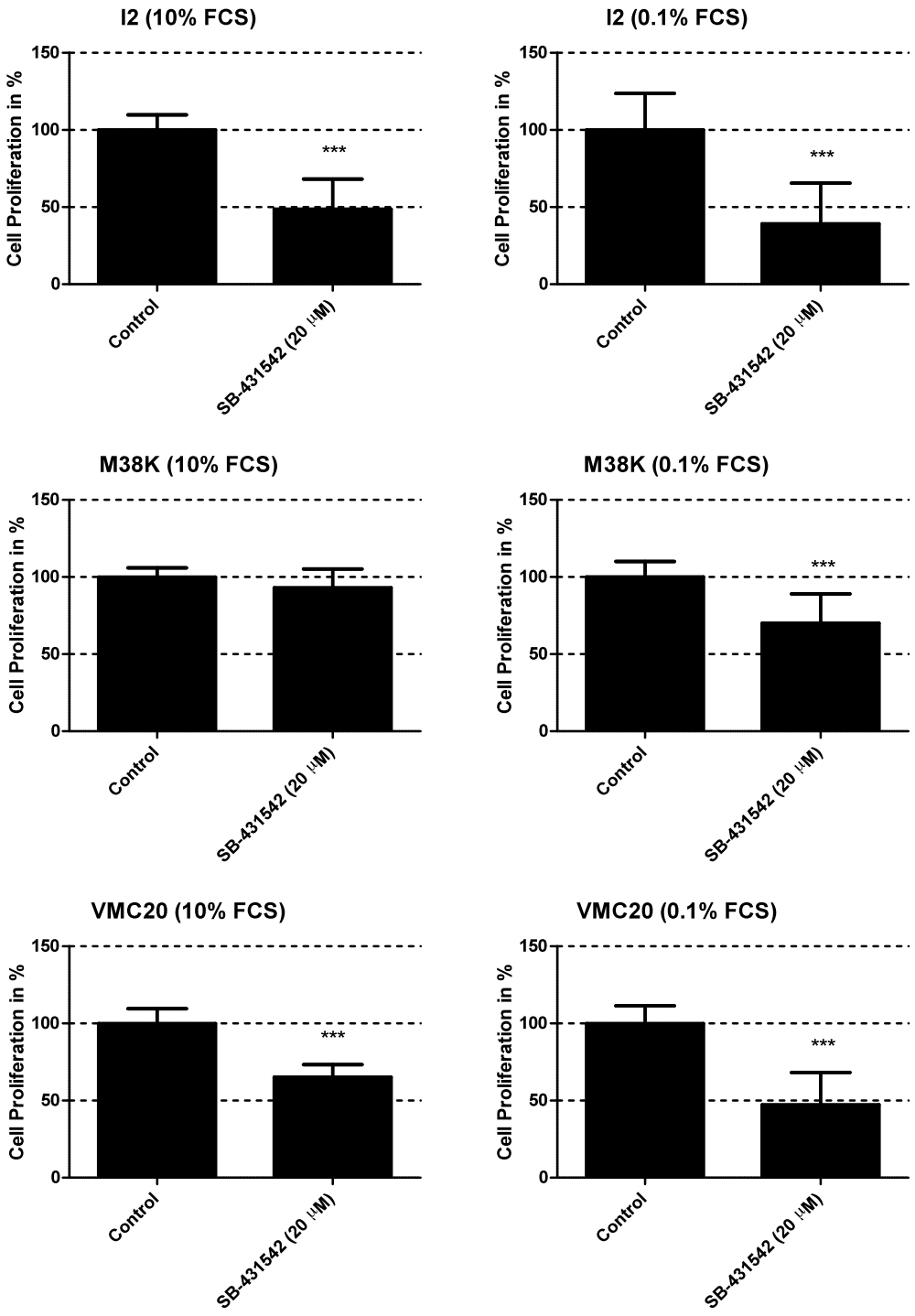

Figure 27. Small molecule inhibitor SB-431542 strongly inhibits cell proliferation in MPM cell lines. The graphs on the left show the effect of the inhibitor in medium containing 10% FCS, whereas the graphs in the right panel show the even stronger effects in 0.1% FCS containing medium.

6.3.4 SB-431542 Reduces Clonogenicity of MPM Cells

The ability of MPM cell lines to survive and form colonies is reduced by exogenous treatment with the small molecule inhibitor SB-431542 in vitro. We could demonstrate, that even at low concentrations of the inhibitor, the clonogenicity of the tested MPM cell lines (p31, p31cis, I2,

M38K, and VMC6) is clearly reduced. A dose-response relationship of SB-431542 in MPM cell lines is presented in Figure 28. Not only the number of colonies gets reduced by increasing the concentration of the inhibitor added to the growth medium, but also the size of the formed colonies gets smaller. The cell line I2 showed the strongest effect of SB-431542 on clonogenicity, since the ability to survive and form colonies was already completely blocked at a final concentration of 5 µM.

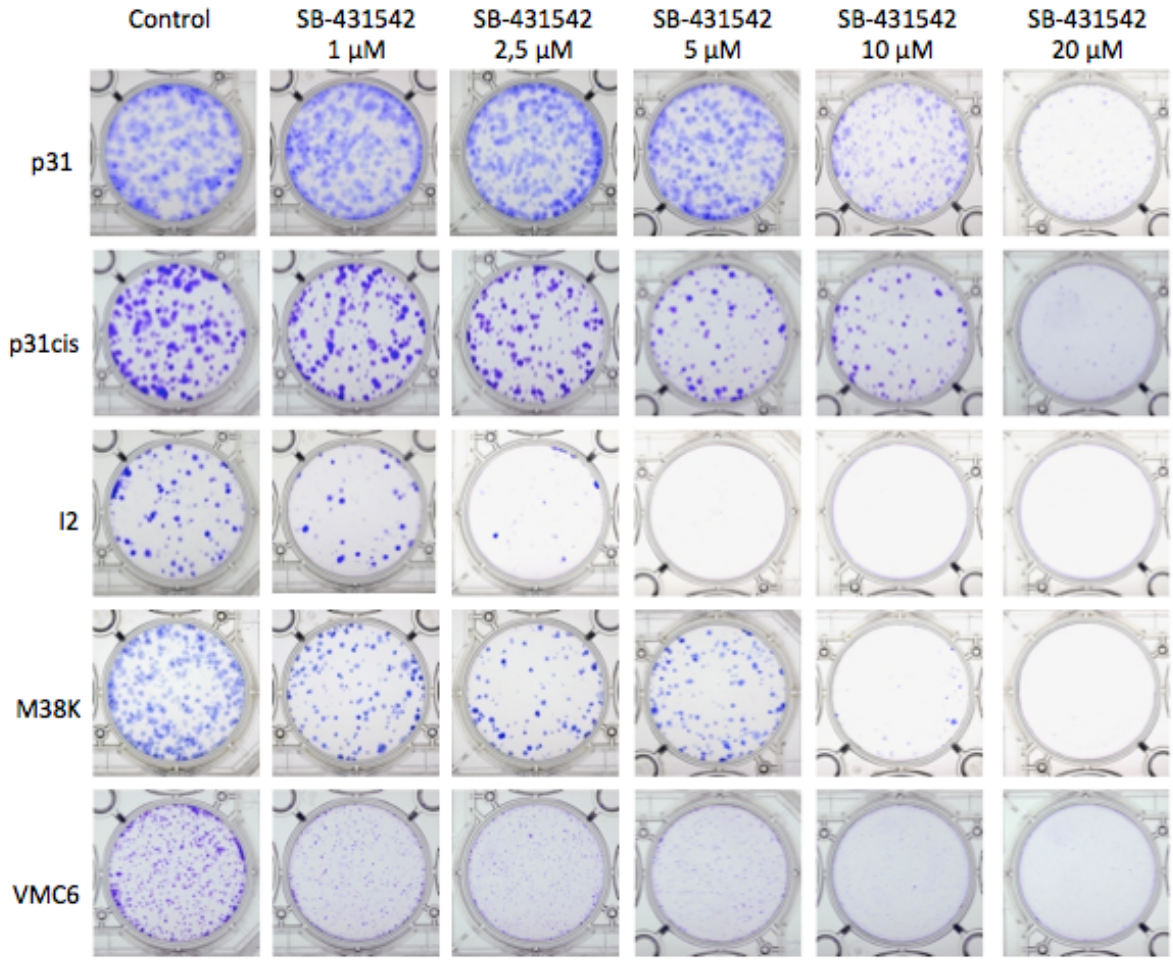

Figure 28. Dose-response relationship of the small molecule inhibitor SB-431542 in MPM cell lines. Even at low concentrations, SB-431542 reduces clonogenicity in MPM cell lines.

6.3.5 A8301 Reduces Clonogenicity of MPM Cells

Like SB-431542, the small molecule inhibitor A8301 targets type I receptors of activin-like kinases, specifically ALK4, ALK5 and ALK7. In our experiments, this inhibitor seemed to have a lower efficiency in MPM cell lines. Although an impairment of clonogenicity could be achieved by treating the MPM cells with A8301 in vitro, the effects were less pronounced in comparison to the treatment with SB-431542. A dose-response relationship of A8301 in MPM cell lines is presented in Figure 29.

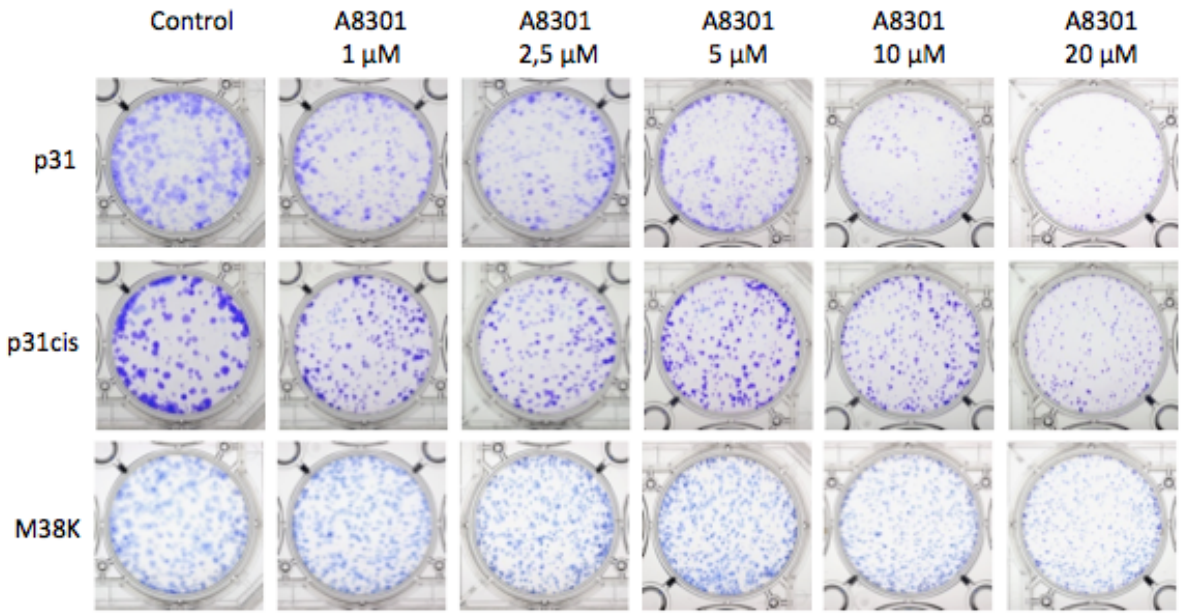

Figure 29. Dose-response relationship of the small molecule inhibitor A8301 in MPM cell lines. A8301 slightly reduces the cells ability to survive and form colonies.

6.3.6 Cell Cycle Alterations Induced by Small Molecule Inhibitors

In four cell lines (p31, I2, M38K and VMC20) the effects of the small molecule inhibitors SB-431542 and A8301 on cell cycle distribution were tested as single agents (final concentration: 20 µM) and in combination (final concentration for each of the two substances: 20 µM). After incubating the cells with the inhibitors for 24 hours, a cell cycle analysis by PI staining and flow cytometry was performed. All tested cell lines showed a different response on the cell cycle distribution (Figure 30).

The cell line p31, which had a high level of cells in the G0-G1-phase in the control, showed an increase of the S-phase and a strong reduction of the G0-G1-phase after the treatment with SB-431542 for 24 hours. A similar effect was seen when cells were treated with A8301 and a slight increase of the effect was achieved by combining both substances.

SB-431542 and A8301 did not show an effect on the cell cycle distribution of the cell line I2, but when both inhibitors where combined, the percentage of cells in G2-M-phase increased, whereas the percentage of cells in the S-phase decreased. Cell treatment of the cell lines M38K and VMC20 only showed slight alterations in cell cycle distribution.

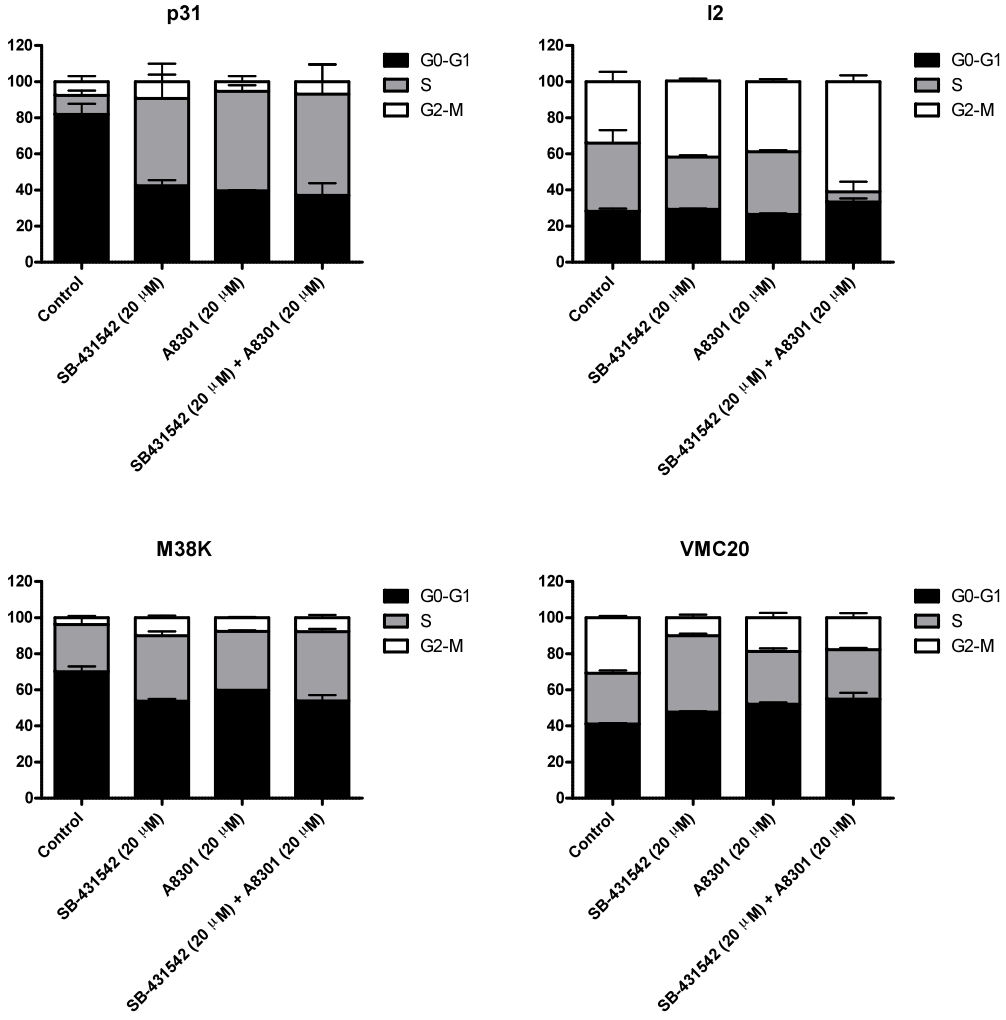

Figure 30. Cell Cycle distribution of MPM cell lines after treatment with the small molecule inhibitors SB-431542 and A8301 as single agents as well as in combination for 24 hours. Proportions of the different cell cycle phases are given in percent.

6.4 Silencing of Activin-βA Expression Blocks Growth and Migration of MPM Cells

6.4.1 siRNA Targeting Human INHBA Reduces Gene Expression in MPM Cells

For a specific silencing of INHBA in MPM cell lines, cells were subject to siRNA targeting human INHBA at a final concentration of 50 nM, since the tested small molecule inhibitors do not discriminate between activin receptors (ALK4, ALK7 and TGF-beta receptors (ALK5). The efficiency of the knockdown of INHBA was measured using qRT-PCR and cells treated with scrambled-siRNA of the same concentration were taken as reference. In all tested cell lines, a knockdown of at least two cycles (equivalent to about 75% reduction) was achieved 48 hours after transfection (Figure 31 and Figure 32).

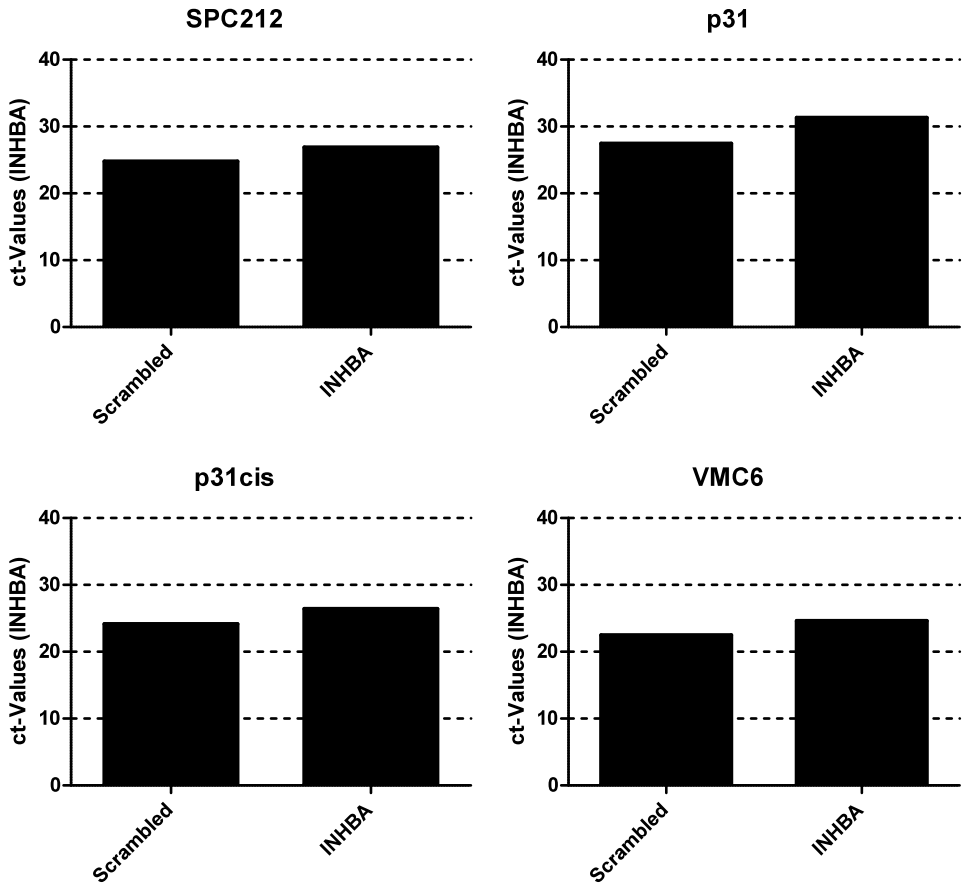

Figure 31. Ct-values of four cell lines transfected with 50 nM scrambled-siRNA or siRNA targeting human INHBA. In all cell lines, a knockdown of at least two cycles was achieved 48 hours after transfection.

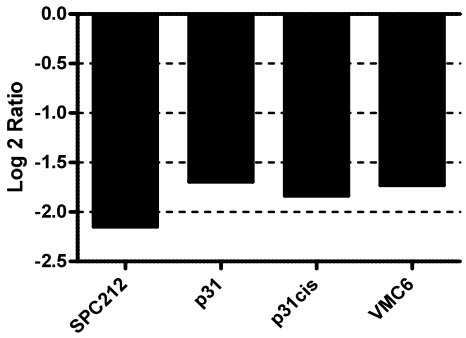

Figure 32. Log 2 ratios of the knockdown of INHBA in MPM cell lines was quantified using qRT-PCR. Cells treated with scrambled-siRNA at the same concentration were used as reference.

6.4.2 INHBA-Targeting siRNA Reduces Cell Viability

A reduced gene expression of INHBA via siRNA (final concentration: 50 nM) reduces cell proliferation in MPM cell lines (Figure 33). The viability of cells transfected with scrambled-siRNA was set as 100% and used for normalization. Even with 10% FCS added to the medium, a reduced cell proliferation was detected via MTT assay. This effect was further increased when the percentage of FCS added to the medium was reduced down to 0.1%. A v*ery significant* impairment of cell proliferation was achieved in the cell line p31cis and also in cell line VMC6, when the concentration was reduced to 0.1%. Only a slight effect on cell viability was measured in the cell line p31.

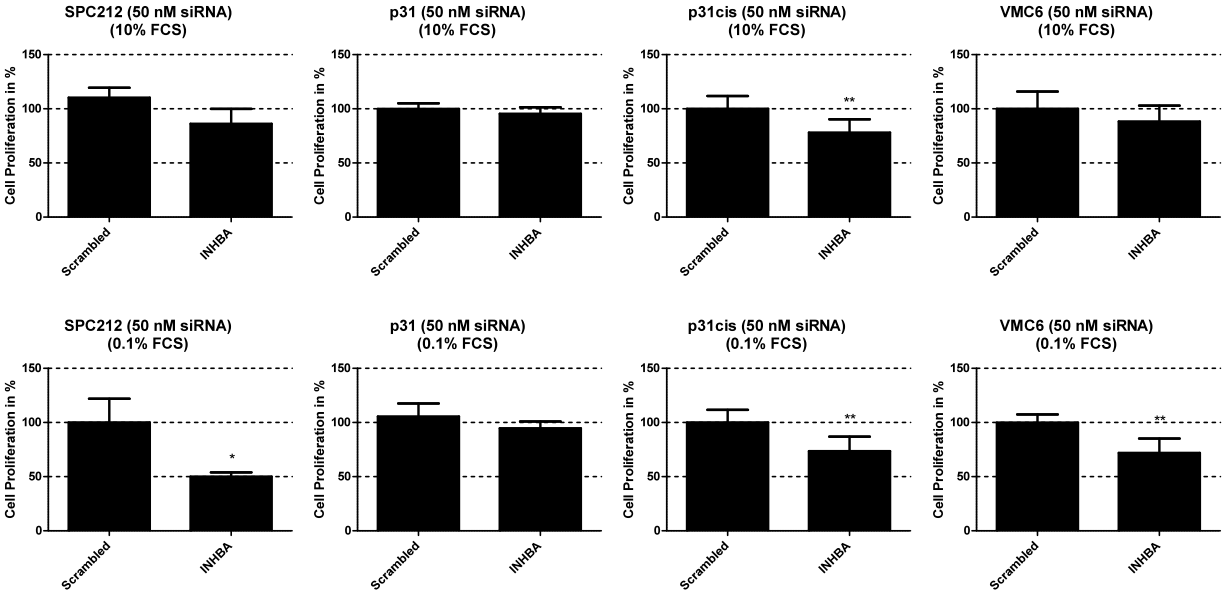

Figure 33. Reduced cell proliferation of MPM cell lines after transfection with 50 nM siRNA targeting human INHBA in contrast to transfection with scrambled-siRNA. The graphs in the upper panel show the effects of transfection in culture medium containing 10% FCS, whereas the graphs in the lower panel show the effects on cell proliferation after transfection with 0.1% FCS added to the culture medium.

6.4.3 INHBA-Targeting siRNA Impairs Clonogenicity

Beside the reduced cell proliferation rate induced by transfection of MPM cell lines with siRNA targeting INHBA, an impairment of the cells ability to survive and form colonies can also be achieved by silencing INHBA. An example of two cell lines with a reduced clonogenicity after transfection with siRNA targeting human INHBA in contrast to scrambled-siRNA transfected MPM cells is presented in Figure 34.

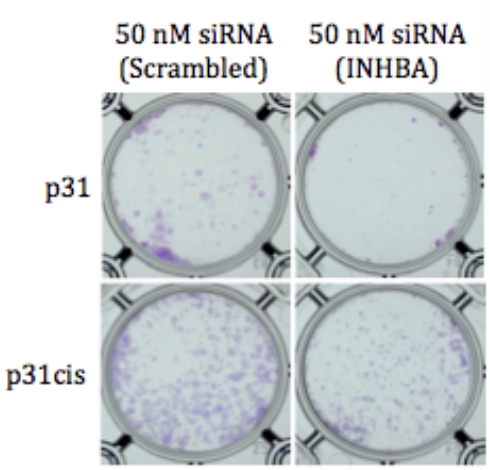

Figure 34. siRNA targeting human INHBA (final concentration: 50 nM) reduces clonogenicity in MPM cell lines in contrast to scrambled-siRNA transfected cells.

6.5 Influence of Activin A on Cisplatin Sensitivity

Since the results of our in vitro analysis showed a strong influence of activin A on MPM cell lines and high effects on cell proliferation and clonogenicity when the expression of INHBA gets reduced by siRNA, we wanted to determine whether a downregulation of the INHBA-expression can stimulate the efficiency of the chemotherapeutic agent cisplatin. For this purpose siRNA targeting human INHBA and cisplatin were used in combination for the treatment of MPM cell lines, whereas scrambled siRNA in combination with cisplatin was taken as control. An example for the synergistic effect of siRNA targeting human INHBA (final concentration: 50 nM) and cisplatin at different concentration levels is presented in Figure 35.

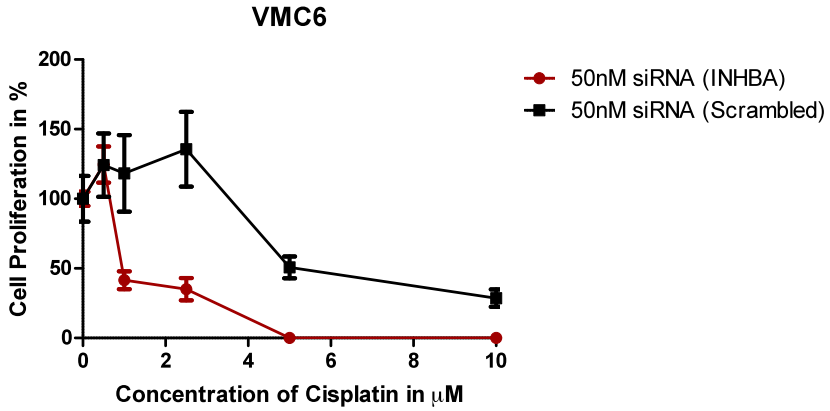

Figure 35. Example of a synergistic effect of siRNA targeting human INHBA (final concentration: 50 nM) and cisplatin at different concentration.

6.6 Regulation of Activin Expression by Methylation or Histone Acetylation

6.6.1 Regulation of Activin Expression by the Demethylating Agent 5-Azacytidine

The DNA methyltransferase inhibitor 5-azacytidine was reported to alter gene expression by demethylation of the DNA. For our study, we wanted to determine whether the expression of INHBA can be modified in MPM cell lines by treatment with 5-azacytidine at a final concentration of 5 µM. Cells treated with equivalent amounts of DMSO were taken as reference. Three MPM cell lines were tested, but the results differed from cell line to cell line (Figure 36). Cell line SPC212, which has a high baseline expression of INHBA, showed an upregulated gene expression of INHBA 24 hours and 48 hours after cell treatment, but a downregulation of the gene expression after 72 hours and 96 hours. The INHBA-expression of the cell line CRL5820, which has a rather low baseline INHBA expression, was decreased after 24 hours, but increased after 48, 72 and 96 hours. The last tested cell line with also a high baseline INHBA expression, VMC20, showed an upregulation in the expression of INHBA after 24 and 96 hours, but a reduced expression after 48 and 72 hours.

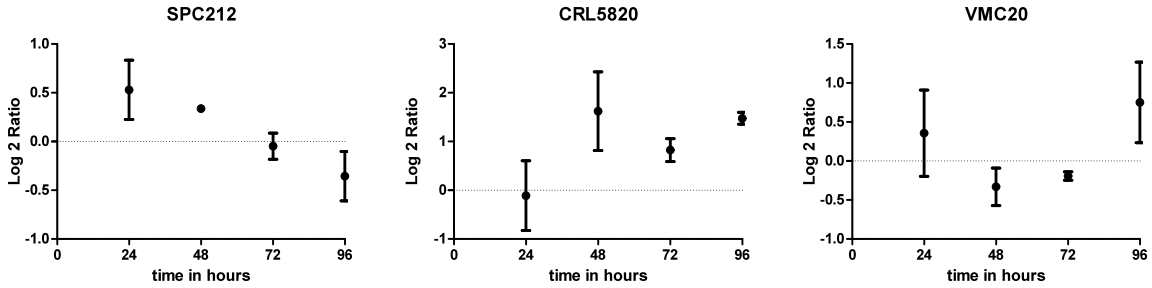

Figure 36. Expression of INHBA in MPM cell lines 24, 48, 72 and 96 hours after cell treatment with 5-azacytidine at a final concentration of 5 µM.

6.6.2 Modulation by Histone Deacetylase Inhibitor Trichostatin A

Trichostatin A is an organic compound that acts as a histone deacetylase inhibitor. For our study, TSA was used for cell treatment at a final concentration of 300 nM for 12 hours and 24 hours in order to determine whether modification of DNA acetylation alters the gene expression of INHBA in MPM cell lines (Figure 37). Four of the tested cell lines show a high baseline INHBA expression (SPC212, p31, p31cis, I2), but we also tested a fifth cell line with a rather low baseline INHBA expression (CRL5820). Again, cells treated with equal amounts of DMSO were taken as reference.

Cell lines CRL5820 and I2 showed a downregulation of the INHBA gene expression after 12 hours and 24 hours of incubation with TSA, whereas cell line p31 showed an upregulation. The

expression of INHBA was downregulated after 12 hours of incubation, but upregulated after 24 hours in the cell lines SPC212 and p31cis.

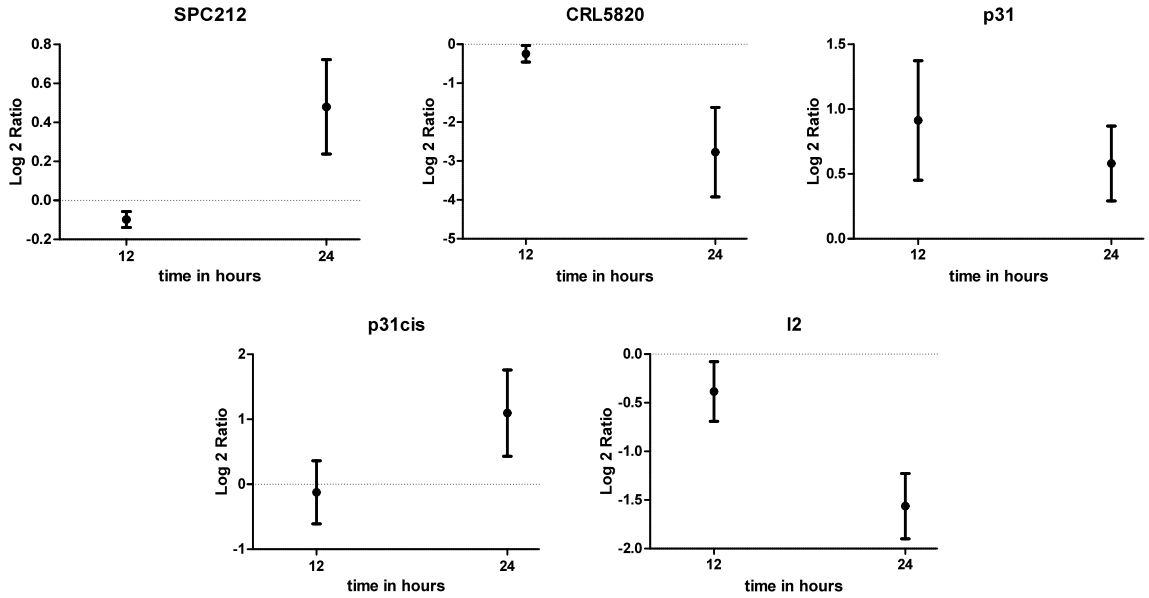

Figure 37. Expression of INHBA in MPM cell lines 12 hours and 24 hours after cell treatment with Trichostatin A at a final concentration of 300 nM.

6.7 Intense Immunohistochemical Staining of Activin A in MPM Tumor Tissue Samples

About 70 tumor tissue samples derived from patients suffering from MPM were subject to immunohistochemical staining for activin A. The evaluation of the stainings were performed by two independent authors and mean values of these scorings were calculated, resulting in scores from 0 (no staining for activin A) to 3 (intense cytoplasmatic staining). Figure 38 shows an example for a MPM tumor tissue sample of the epithelioid subtype with an intense cytoplasmatic staining (score 3) for activin A in the tumor cells, but not in the surrounding cells.

The results of the immunohistochemistry suggest an important role of activin A in MPM tumors and further correlation of the results with the clinical data from the patients.

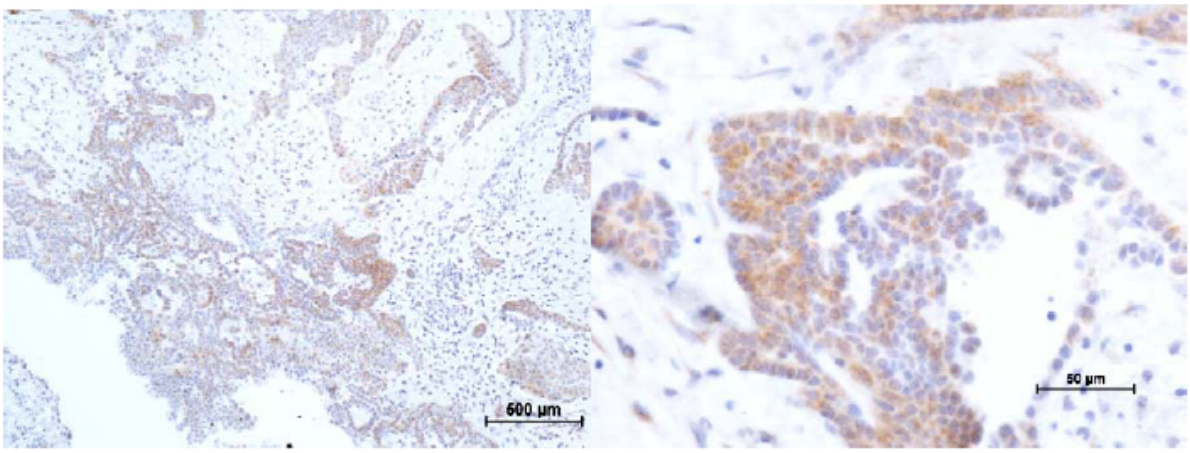

Figure 38. Immunohistochemical staining of a formalin-embedded MPM tumor tissue sample of the epithelioid subtype, showing an intense cytoplasmatic staining (score 3) for activin A in the tumor cells, but not in the surrounding cells.

6.8 Construction of a Lentivirus Overexpressing INHBA

6.8.1 Construction of the Entry Clone

For further investigations concerning the role of activin A in Malignant Pleural Mesothelioma cells, the construction of a lentivirus overexpressing INHBA was started. The cloning strategy is based on the Gateway Cloning Technology (Invitrogen) and involves the cloning of an entry vector containing the gene of interest flanked by attL recombination sites, which is subsequently inserted into a destination vector containing attR sites via homolog recombination (LR recombination reaction) between the attL and attR binding sites.

For the amplification of our gene of interest (INHBA) a RT-PCR based cDNA cloning with Pfu polymerase was performed. The PCR product was afterwards phosphorylated with a T4 polynucleotide kinase (Fermentas) and subsequently analyzed by agarose gel electrophoresis in order to confirm the correct size of the amplified fragments. As seen in Figure 39, we obtained a sharp band of approximately 1400 bp, which correlates with the size of the gene INHBA (1406 bp).
As a next step, the fragment was cut out and purified out of the agarose gel with the Wizard SV Gel and PCR Clean-up System Kit from Promega. The concentration of the purified DNA was measured via NanoDrop and resulted in 14.45 ng/µl.

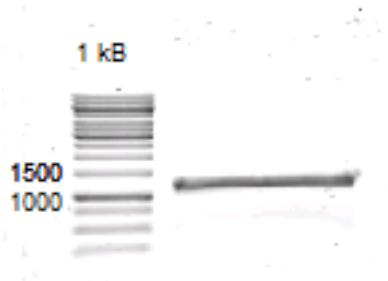

Figure 39. Agarose gel of the amplified fragment showing a sharp band at approximately 1400 bp.

Parallel to the amplification and purification of our gene of interest, the backbone for the entry vector, pENTR1A (2294 bp) (Figure 40), was prepared. The restriction enzyme EcoRV (Fermentas) was applied for generating blunt ends of the vector backbone. Additionally, the concentration of DNA was measured via NanoDrop, resulting in 78.36 ng/µl.

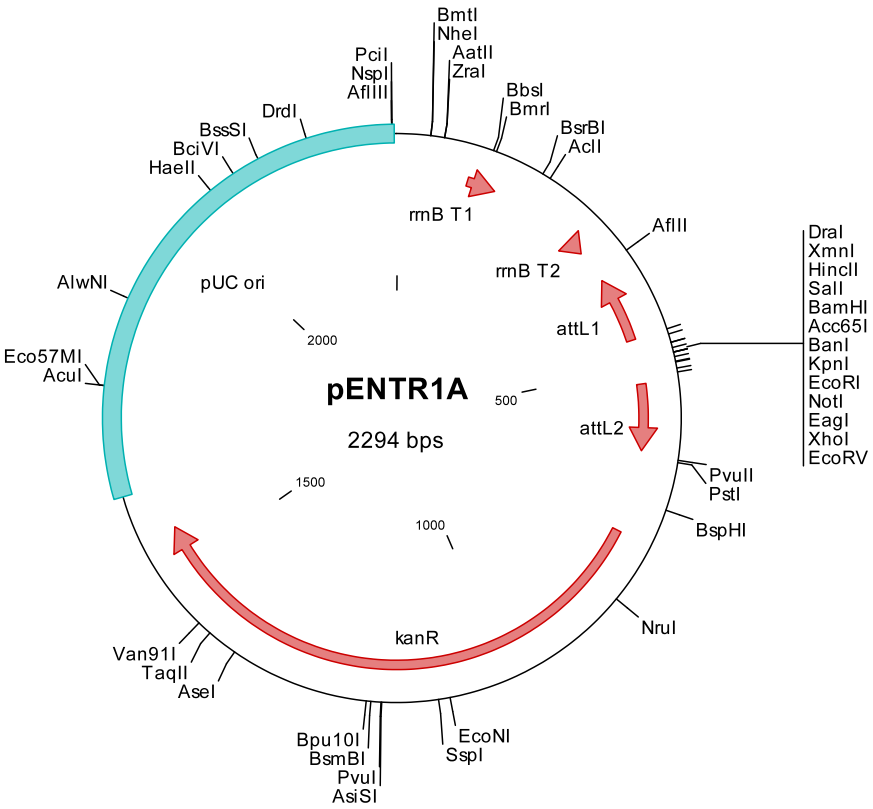

Figure 40. Vector pENTR1A (2294 bp) was used as vector backbone for the entry clone.

For the ligation of the gene of interest and the vector backbone for the entry clone, two different approaches were performed, one with a three times molar excess of the insert DNA and another approach with a five times molar excess of the insert DNA. Both approaches were afterwards transformed into competent E. coli cells and subsequently plated on LB plates containing kanamycin for the selection of cells containing the desired plasmid with our gene of interest. The following day, ten colonies were picked and allowed to grow in fresh LB medium containing kanamycin for 24 hours. For a quick detection of positive clones, we performed a boiling lysis plasmid preparation and a single restriction digest with PstI (Fermentas) in orange buffer (Fermentas). Digestion of a positive clone should give rise to two fragments (527 bp and 3066 bp). As presented in Figure 41, we identified two positive clones (clone 4 and clone 7) with fragments of the expected size. For all further steps within the construction of the lentivirus, clone number 4 (pINHBA-ENTR1A (3593 bp), Figure 42) was chosen and a plasmid miniprep for DNA purification of this bacterial culture was performed. For a long-term storage of our positive entry clone, glycerol stocks of the bacterial culture were also made.

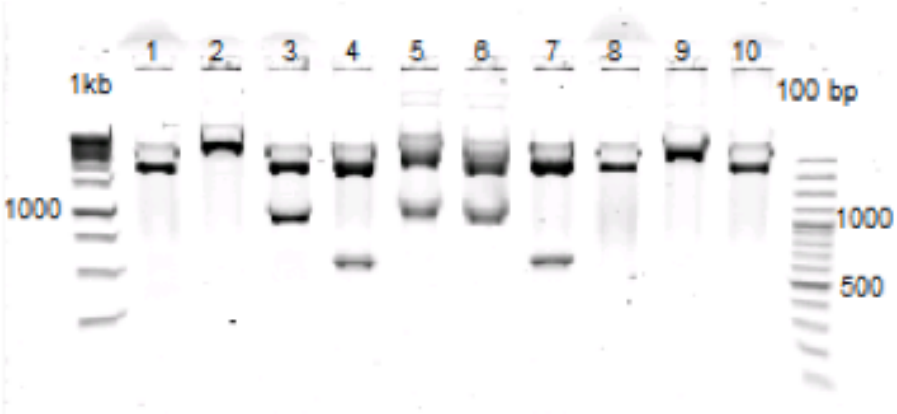

Figure 41. Agarose gel showing the results of the restriction digest with PstI. Clone 4 and clone 7 show bands of the expected size (527 bp and 3066 bp) and were identified as positive clones.

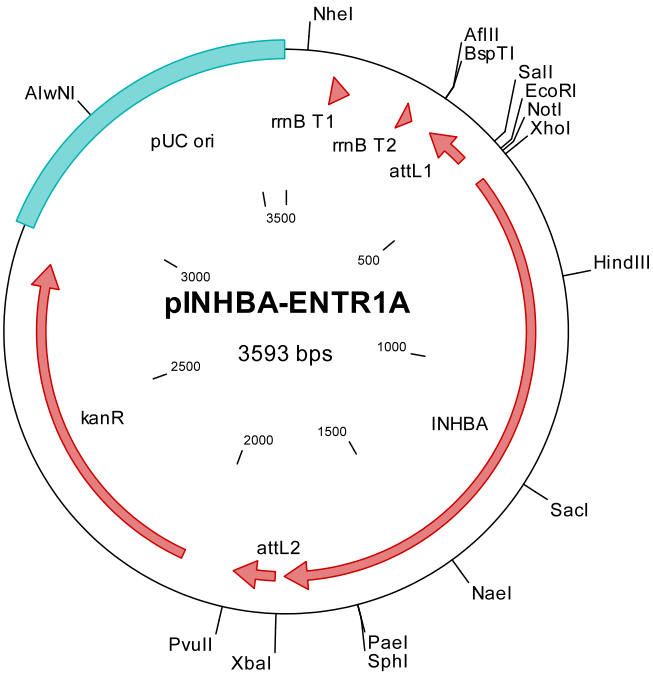

Figure 42. Ligation of the gene of intererst, INHBA, and the entry vector, pENTR1A, resulted in the entry clone pINHBA-ENTR1A (3593 bp), which was subsequently used for the LR recombination reaction.

6.8.2 Construction of the Expression Clone

The circular destination vector pLenti6/ubC/V5/Dest (9319 bp) (Figure 43), containing attR recombination sites and an ampicillin resistance cassette, and our previously verified entry clone were used for the LR recombination reaction. The resulting circular expression clone should then have a size of 9028 bp. Transformation into Stbl3 E. coli cells was performed and subsequently plated on LB agar plates containing ampicillin. Two colonies were picked and grown in fresh LB medium containing ampicillin and the culture subsequently used for plasmid minipreps to obtain purified plasmid DNA. The measurement of the concentration of the purified DNA resulted in 16.61 ng/µl for clone number 1 and 18.44 ng/µl for clone number 2.

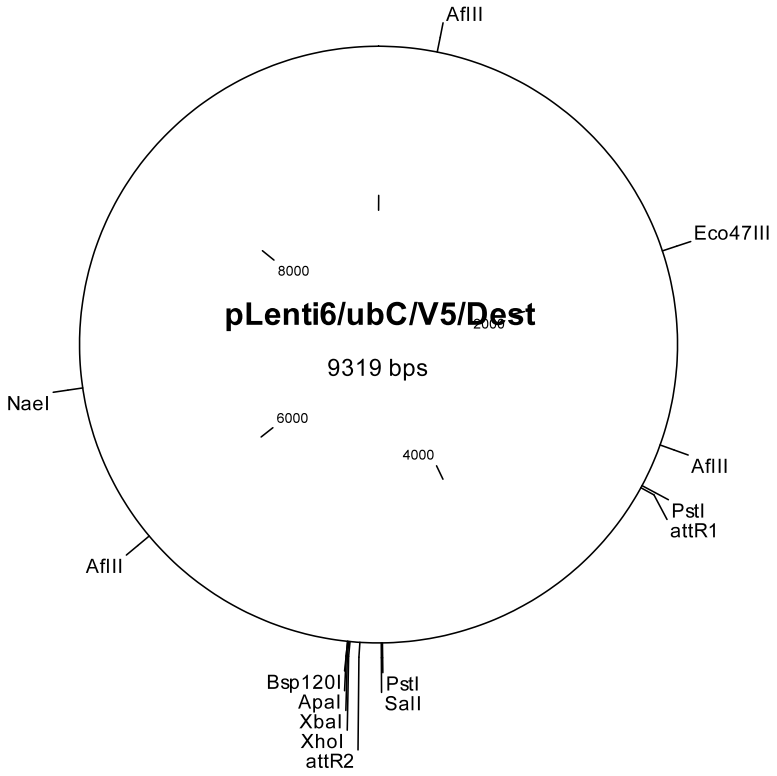

Figure 43. Destination vector pLenti6/ubC/V5/Dest (9319 bp) was used as vector backbone for the expression clone.

Two different digestions with restriction enzymes identified the chosen colonies as positive expression clones (Figure 45). First, a cut with XhoI (Fermentas), AflII (Fermentas)and Tango buffer for double digestion (Fermentas) was carried out, which should give rise to five fragments of different size (309, 1155, 1362, 2546 and 3656 bp). The smallest fragment (309 bp) can't be identified on the agarose gel, whereas the other fragments show the expected size. For the second approach, we used PstI for the digestion, which should give rise to two fragments (982 and 8042 bp). As seen in Figure 45, both fragments can be identified, thus confirming both clones as positive expression clones. For further steps within the construction of the lentivirus, expression clone number 1, pINHBA-Dest (9028 bp), was chosen and bacterial culture of this clone was stored frozen as glycerol stocks for long-term storage.

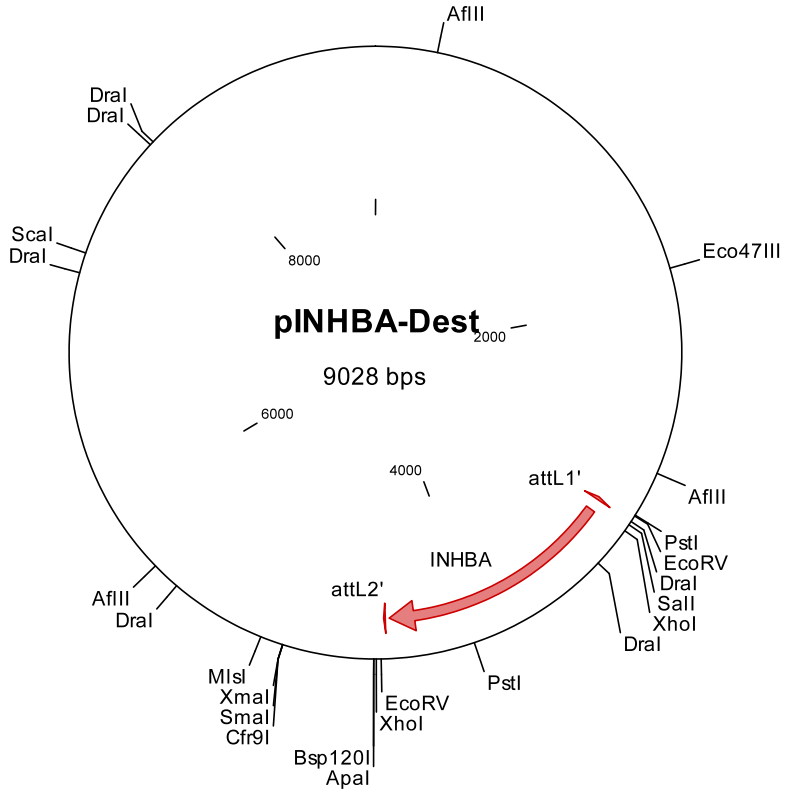

Figure 44. LR recombination reaction of pINHBA-ENTR1A (3593 bp) and pLenti6/ubC/V5/Dest (9319 bp) results in the expression clone pINHBA-Dest (9028 bp).

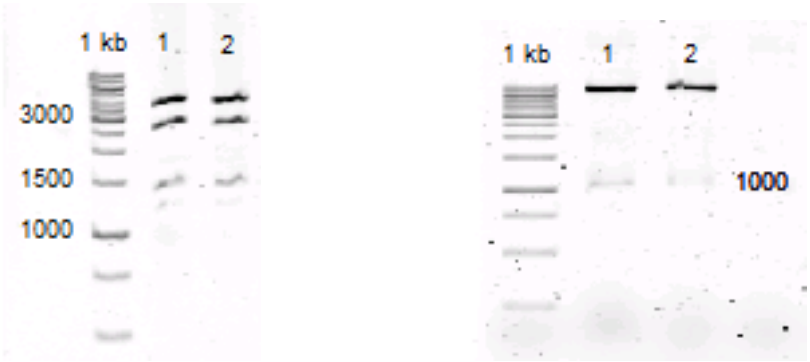

Figure 45. Restriction digests of the two selected expression clones. Left: cut with XhoI and AflII. Right: cut with PstI.

6.8.3 Outlook

By performing different restriction digests, we could confirm that our gene of interest was finally integrated in an expression clone (pINHBA-Dest). Further steps within the construction of the lentivirus were no longer part of this project, but planned further steps are described below.

For the demonstration of the biological activity of the expression clone, we will soon transfect our expression clone into Hek293 cells that will subsequently produce and secrete activin A into the medium. The cytokine can then be harvested as supernatant and used for the treatment of HepG2 cells. In this way, the biological activity will be demonstrated, since it was previously reported that treatment of HepG2 cells with activin A phosphorylates the SMAD2 pathway (229). After verifying the biological activity, the generated expression clone will be transfected as a complex with lentiviral packaging mix into 293FT cells for the production of lentiviral particles, which will then be harvested as viral supernatants 48 hours after transfection.

7 Discussion

Malignant Pleural Mesothelioma is a highly aggressive and lethal type of cancer with poor prognosis that arises from the serous lining of the lungs, the two-layered pleura. A history of past exposure to asbestos is considered to be the main cause for this disease, whereas inhaled asbestos fibres have been described as inducer of genetic alterations, necrosis and inflammation (150, 154-156). So far, no effective treatment for MPM has been established and since the increasing incidence of MPM is expected to peak within the next 20 years, novel approaches to fight Mesothelioma are urgently needed.

Previous studies demonstrated a response of MPM cells to the transforming growth factor TGF-β (171) and an inhibition of cell proliferation and tumor growth by in vitro and in vivo treatment of MPM cells with antisense oligodeoxynucleotides to TGF-β (171, 172), but the contribution of activin signals to MPM cells remained to be elucidated. Increased expression levels of activin A have already been described in association with inflammation (42, 51), wound repair (44-47) and various tumors, like oral squamous cell carcinoma (140),esophageal adenocarcinoma (144) and lung adenocarcinoma (145). For many carcinomas, an association between overexpression of activin A, metastasis, a shorter disease-free survival rate and poor prognosis for the patients have also been described so far, whereas a down-regulation of the gene expression of INHBA using siRNA reduced cell proliferation of cancer cells from these malignancies (140, 144, 145).

With this study, we could demonstrate that activin A is overexpressed in all tested MPM cell lines in comparison to the non-malignant cell line Met5a, which was used as control. We could further show, that activin A signalling plays an important role for MPM cells, since blocking of activin receptors with small molecule inhibitors as well as a specific silencing of INHBA with RNA interference results in reduced cell viability and clonogenicity. Immunohistochemical staining of tumor tissue samples derived from patients showed an intense cytoplasmatic staining for activin A. Moreover, a synergistic effect of silenced INHBA expression and cell treatment with the chemotherapeutic compound cisplatin could also be detected, thus suggesting activin A as a novel candidate for therapeutical application.

7.1.1 Expression Analysis

Since the role of activin signals in MPM has not been investigated so far, the first step within this study was to determine the mRNA expression levels of the four mammalian activin subunits

(expressed from the genes INHBA, INHBB, INHBC and INHBE), the activin receptors type I and type II and the various activin antagonizing factors. For this purpose, nine MPM cell lines, of which two have been established by our group, were analyzed in comparison to Met5a, which has previously been used as non-malignant control in studies concerning thoracic tumors (230-232).

Gene expression levels were first determined at thirty cycles via RT-PCR and with taq-polymerase. The results of these expression analysis revealed that activin A, B and E can be detected at thirty cycles in nearly all tested cell lines, whereas activin C could not be detected at all. This is not an unusual phenomenon, since activin C expressed in the human body is very restricted (21). The activin receptors type I and type II were detected in all MPM cell lines, as well as in the control cell line Met5a. Follistatin, FSTL1 and FSTL3 were detectable in many cell lines at thirty cycles, whereas INHA, Cripto and Nodal were only expressed in some cell lines.

Since these expression analysis were restricted to thirty cycles in our study and conventional RT-PCR does not allow to quantify the expression levels, additional expression analysis with quantitative RT-PCR were performed. For the calculations of the log 2 ratios of the expression levels obtained from quantitative RT-PCR, we determined the ct values for three different house-keeping genes (B2M, GAPDH and ACTB). Since B2M turned out to be inappropriate for our study due to the strong variations of the ct values in the different cell lines, we decided to refer our calculations to the average expression levels of GAPDH and ACTB, because both showed only slight variations in their expression.

The expression analysis of the activin subunits by qRT-PCR using TaqMan probes revealed, that there is a higher expression of INHBA and INHBC in all MPM cell lines, compared to the non-malignant cell line Met5a. Like it was expected from the results of the RT-PCR, INHBC showed very high ct values, thus indicating that INHBC is only expressed in MPM cell lines at relatively low levels. The activin subunit beta B was found to be highly expressed in nearly all cell lines, except the cisplatin resistant cell line p31cis, which showed a lower expression in comparison to the Met5a, whereas the expression of INHBE was upregulated in some cell lines and downregulated in others.

The activin antagonist Follistatin was strongly upregulated in some cell lines in comparison to the cell line Met5a, but also downregulated in other cell lines. Overexpression of Follistatin and also activin A has previously been reported for oral squamous cell carcinoma (140). Follistatin related genes like FSTL1 and FSTL3 showed only low expression in MPM cell lines and were downregulated in most of them.

The cell surface protein Cripto was downregulated in most MPM cell lines, whereas Nodal was upregulated in most cell lines. Since we do not possess a TaqMan probe for Nodal, it was the only activin-related factor analyzed via SYBR-Green qRT-PCR, which could be the reason for the relative high variations in the two analysis performed.

Moreover, the expression levels of the activin receptors type I (ALK4 and ALK7) and type II (ACVR2 and ACVR2B) were also determined via qRT-PCR in comparison to the Met5a. Surprisingly, the expression of type I receptors was downregulated and the expression of type II receptors was upregulated in nearly all MPM cell lines in comparison to the Met5a. In a previous study concerning activin A and activin receptors in thyroid cancer (233), a downregulation of type I receptors has also been described.

As another step in expression analysis of MPM cell lines, we wanted to determine whether INHBA gene expression can be epigenetically regulated via promotor demethylation and/or histone acetylation. For this purpose, cells were treated either with 5-azacytidine (5 μM) or Trichostatin A (300 nM) alone or with a combination of both agents. The effect of 5-AZA on INHBA gene expression was determined for three MPM cell lines. Two of them have a rather high baseline expression of INHBA, whereas the third one shows a low baseline INHBA expression. Unfortunately, we could not obtain any clear results and no correlation between promotor demethylation and INHBA expression could be made. Similar unconvincing results were examined in the expression analysis after cell treatment with TSA. But in contrast to the treatment with 5-AZA, we could see a trend in the INHBA gene expression after treatment with TSA in two of the five tested cell lines. Cell lines CRL5820and I2 showed reduced expression levels for INHBA 12 hours after the treatment with TSA and an even stronger downregulation of the gene expression after 24 hours. One cell line responded to the treatment with TSA in an upregulated expression of INHBA, whereas in the other two cell lines, the INHBA expression was downregulated after 12 hours, but upregulated after 24 hours. Combination treatments with both agents turned out to be rather toxic and we therefore failed in isolating RNA from cells treated with 5-AZA as well as TSA.

Previous studies with lung adenocarcinoma (145) and esophageal adenocarcinoma (144) have also investigated the consequences of promotor demethylation or histone acetylation on the gene expression of INHBA by using 5-aza-2'deoxycytidine or Trichostatin A. In contrast to our results, they found an upregulated expression of INHBA caused by treatment with both substances alone or in combination. They also reported that these effects differed in the tested cell lines, since some cell lines only slightly responded to the treatment with those substances, whereas for other cell lines, the effect was more prominent. Beside the cell type, the baseline expression level of INHBA could also be a factor whether epigenetically regulating substances can influence INHBA expression or not.

7.1.2 Stimulation of MPM Cells with Activin A

Although our expression analysis revealed an overexpression of activin A in all tested MPM cell lines in contrast to the non-malignant but transformed cell line Met5a, a further stimulation of cell proliferation by exogenous treatment with recombinant activin A could also be detected. In the MTT assay, significant elevated cell proliferation rates were measured when cells were treated with activin A and even under serum starvation conditions with reduced concentration of FCS added to the medium, the proliferative effect of activin A was still detectable. The stimulatory effect of activin A at a final concentration of 20 ng/ml on MPM cells was also demonstrated in respect of migration. In the scratch assay, where the migration of cells leads to closure of a scratch in the monolayer applied with a pipette tip, higher cell motility was detected when cells where treated with activin A and the scratch was closed much earlier in contrast to the scratch in the control. The strong stimulatory effect was further confirmed in the clonogenic assay, since the ability to survive and form colonies was strongly upregulated when cells were treated with activin A. In three of the tested cell lines, activin A increased the clonogenicity up to about 150% in contrast to the controls, which were treated with equal amounts of PBS.

In order to confirm, that our results concerning the stimulatory effect of activin A are tissue-dependend and specific for MPM cells and not a general phenomenon, we also treated HepG2 cells with activin A, since it was previously reported that the hepatocarcinoma cell line HepG2 shows a downregulation of viability after treatment with recombinant activin A in vitro (229). As expected, our experiments with HepG2 cells showed the same results as presented in the study mentioned above. Not only for hepatocarcinoma, but also for many other tumors, like breast cancer (121-124), prostate cancer (125-127) and pituitary adenocarcinoma (128, 129), activin was described as a negative regulator of proliferation.

Moreover, we also examined the effects of treatment with recombinant activin A at higher doses, for example 50 ng/ml or 100 ng/ml, but the proliferative effects could no longer be observed (data not shown). In the MTT assay and also in the clonogenic assay, higher concentrations of activin A added to the medium did not result in a further stimulation of cell viability and clonogenicity. These findings suggest, that activin A might function in a dose-dependend manner, as it was previously described as a characteristic for the TGF-β superfamily (234). Similar findings were already described for activin A in esophageal adenocarcinoma and lung adenocarcinoma, where the stimulatory effect of activin A could also only be detected up to a certain concentration level (144, 145). So like TGF-β, activin A could have a tumor suppressive as well as an oncogenic effect, depending on its concentration and the type of cells or tissue. The stimulatory effect of activin A could also depend on the baseline expression level of INHBA. For

example, the cell line I2, which has a high expression level of INHBA, shows a less prominent proliferative effect after stimulation with recombinant activin A in contrast to the cell line M38K, which has a low baseline expression level of INHBA and responds with a highly significant upregulation of viability when treated with activin A.

Furthermore, we could also demonstrate the functionality of the canonical TGF-β/activin axis. In all tested cell lines, incubation of cells with recombinant activin A (20 ng/ml) for 30 minutes resulted in an activation of the SMAD-pathway via phosphorylation of SMAD2. This effect was previously reported for HepG2 cells (229), but has not been shown for Malignant Pleural Mesothelioma or other thoracic tumors so far.

The monomeric protein Follistatin is known as a modulator of activin signalling, since it has the ability to bind to activin A and therefore regulate its function. Although previous studies with other thoracic tumors, like esophageal adenocarcinoma (144) or lung adenocarcinoma (145), reported an inhibition of cell proliferation after treatment with Follistatin at different concentrations, we could not show this effect for Malignant Pleural Mesothelioma. Cell treatment with Follistatin at a final concentration of 20 ng/ml did not result in a reduced cell viability or clonogenicity (data not shown). This might be due to technical problems in our study or it could also mean that like for activin A, the effect of follistatin differs between the various cell types. The inhibitory effect of Follistatin could also be dose-depended and might only be present at lower concentrations than 20 ng/ml, like it was tested in our study, or at much higher concentrations. Seder et al. reported, that cell treatment of esophageal adenocarcinoma or lung adenocarcinoma with Follistatin at a final concentration of 1 or 10 ng/ml only slightly reduces cell viability, whereas a final concentration of 100 ng/ml reduced cell proliferation down to about 70% (144, 145).

7.1.3 Inhibition of MPM Cell Proliferation

Since cell treatment with recombinant Follistatin did not show any convincing results in our study and no inhibition of cell proliferation could be observed, as it would be expected, we wanted to determine whether small molecule inhibitors for activin-like kinases have the ability to reduce cell proliferation of MPM cell lines.

Although both tested inhibitors (SB-431542 and A8301) target the same type I receptors of activin-like kinases (ALK4, ALK5 and ALK 7), we achieved stronger effects with the inhibitor SB-431542 at equal concentration levels. We could demonstrate that cell treatment with SB-431542 at a final concentration of 20 μM clearly reduces cell viability of MPM cell lines and that this

effect can further be increased when the concentration of FCS added to the medium is reduced from 10% down to 0.1%.
Beside the reduced cell proliferation, we could also demonstrate reduced clonogenicity, even at low concentrations of the inhibitor SB-431542, and less migration, as observed in the scratch assay or the transwell assay. But when the crystal violet was solubilized again by 2% SDS, the resulting data did not always consent with the visible numbers of colonies (data not shown). This might be due to the fact that the size of the colonies decreased when cells were treated with the inhibitor and that it was easier to unstain small colonies than big colonies, and many large colonies could not get unstained again by using SDS.
But all in all, our findings concerning the inhibitory effect of the small molecule inhibitors suggest that MPM cells depend on activin signals, especially activin A, and that they present a valuable candidate for further investigations regarding new therapy approaches.

Unfortunately, both small molecule inhibitors are not specific for activin receptors, since they do not discriminate between the receptors for activins and those for TGF-β. Both target the activin-like kinases ALK4, ALK5 and ALK7, whereas ALK4 and ALK7 are specific for activin signals and ALK5 for TGF-β. Therefore, we wanted to examine, whether the strong inhibitory effect caused by these inhibitors could also be shown when we target activin A alone. For this, the effect of siRNA targeting human INHBA was investigated within this project.
Four cell lines with a high baseline level of INHBA expression were used for silencing INHBA in vitro using RNA interference. For all cell lines, the regulatory effect of the siRNA at a final concentration of 50 nM was proven via quantitative RT-PCR and the biological consequences were investigated with regard to viability and clonogenicity, always in comparison to cells treated with scrambled-siRNA at the same concentration. The quantitative RT-PCR showed an efficiency of gene silencing with RNA interference of about 80% in all tested cell lines. The cell proliferation rate was clearly reduced and similar to cell treatment with recombinant activin A and SB-431542, the effect on viability was even stronger when the concentration of FCS added to the medium was reduced down to 0.1%. When MPM cell lines were treated with siRNA targeting INHBA, they showed a reduced ability to survive and form colonies when seeded at a very low density. Less colonies were formed and they also seemed to be smaller in size.

The strong growth inhibitory effect of siRNA targeting INHBA demonstrates, that the effect of the two tested small molecule inhibitors can not only be caused by the importance of TGF-β for MPM cells, but also by the effects on the activin receptors.

7.1.4 Activin A as a Valuable Candidate for Therapeutic Application?

Since we could show an inhibitory effect of siRNA targeting human INHBA on MPM cells, we wanted to examine whether the efficiency of currently used chemotherapeutic compounds like cisplatin could be enhanced by simultaneously silencing INHBA in vitro. Therefore, siINHBA was used in combination with cisplatin for cell treatment of MPM cell lines and viability was measured 72 hours later, resulting in a synergistic effect of RNA interference and cisplatin. But unfortunately, siRNA targeting INHBA cannot easily be used for tumor treatment in humans since INHBA is expressed in nearly all kinds of tissues and has various functions and therefore, a way for tumor-specific targeting of INHBA would probably have to be found.

Immunohistochemical stainings of tumor tissue samples derived from patients showed an intense cytoplasmatic staining for activin A in a large fraction of the stained panel. The results of the immunohistochemistry have not been completely evaluated so far and a correlation of the results with histologic subtype and the clinical data still has to be made. But since the expression of activin A on the protein level was only detectable with immunohistochemistry for the tumor cells and not the surrounding stromal cells, activin A might turn out to be a poor prognostic factor for MPM. These findings would be consistent with the results of previous studies with oral squamous cell carcinoma (140), esophageal squamous cell carcinoma (142) and lung adenocarcinoma (145), that reported an association between an intense cytoplasmatic staining for activin A in the tumor cells, tumor progression and poor prognosis for the patients.

Nevertheless, overexpression of activin A can't be the only mechanism underlying the malignant growth and spreading of MPM cells, since the inhibition of INHBA expression using siRNA did not result in an entire arrest of MPM cell growth and some immunohistochemical stained tissue samples did not show an expression of activin A.
All in all we can say, that our results provide evidence that activin A represents an important factor for Malignant Pleural Mesothelioma and that it therefore might be a valuable candidate for therapeutic applications, especially in combination with other treatments.

8 Abbreviations

5-AZA	5-azacytidine
ACTB	beta-actin
ActR	activin receptor
ACVR2	activin receptor 2
ACVR2B	activin receptor 2B
ALK	activin receptor-like kinase
B2M	beta-2 microglobulin
BSA	bovine serum albumin
cisplatin	cis-diamminedichloroplatinum(II)
DAB	3,3'-diaminobenzidine tetrahydrochloride
DMSO	Dimethyl sulfoxide
EDTA	ethylenediaminetetraacetic acid
FACS	fluorescence-activated cell sorting
FCS	fetal calf serum
FLRG	follistatin-related gene
GAPDH	glyceraldehyde-3 phosphate dehydrogenase
H&E	hematoxylin and eosin
HRP	horseradish peroxidase
INHA	Inhibina alpha
MEME	Minimum essential Eagle medium
MPM	Malignant Pleural Mesothelioma
NSCLC	non-small cell lung cancer
TGF-β	Transforming growth factor beta
MTT	dimethyl thiazolyl diphenyl tetrazolium salt
PBS	phosphate buffered saline
PVDF	Polyvinylidene fluoride
RPMI	Roswell Park Memorial Institute medium
RT-PCR	reverse transcriptase polymerase chain reaction
SDS	sodium dodecyl sulfate
SDS-PAGE	sodium dodecyl sulphate polyacrylamide gel electrophoresis
siRNA	small interfering RNA
SV40	Simian Virus 40
TBS	Tris buffered saline

TBST	Tris buffered saline with 0.1% Tween-20
TDGF1	teratocarcinoma-derived growth factor 1
TE	Tris EDTA buffer solution
TEMED	N,N,N',N'–tetramethylethylenediamine
TSA	Trichostatin A

9 List of Figures

Ich habe mich bemüht, sämtliche Inhaber der Bildrechte ausfindig zu machen und ihre Zustimmung zur Verwendung der Bilder in dieser Arbeit eingeholt. Sollte dennoch eine Urheberrechtsverletzung bekannt werden, ersuche ich um Meldung bei mir.

10 List of Tables

11 References

1. Hazarika M, White RM, Jr., Booth BP, Wang YC, Ham DY, Liang CY, et al. Pemetrexed in malignant pleural mesothelioma. Clin Cancer Res 2005 Feb 1;11(3):982-92.
2. Tsuchida K, Nakatani M, Matsuzaki T, Yamakawa N, Liu Z, Bao Y, et al. Novel factors in regulation of activin signaling. Mol Cell Endocrinol 2004 Oct 15;225(1-2):1-8.
3. Rudd RM. Malignant mesothelioma. Br Med Bull 2010;93:105-23.
4. Schmierer B, Hill CS. TGFbeta-SMAD signal transduction: molecular specificity and functional flexibility. Nat Rev Mol Cell Biol 2007 Dec;8(12):970-82.
5. Carbone M, Ly BH, Dodson RF, Pagano I, Morris PT, Dogan UA, et al. Malignant mesothelioma: Facts, myths and hypotheses. J Cell Physiol 2011 Mar 16.
6. Kartalou M, Essigmann JM. Mechanisms of resistance to cisplatin. Mutat Res 2001 Jul 1;478(1-2):23-43.
7. Phillips DJ, de Kretser DM. Follistatin: a multifunctional regulatory protein. Front Neuroendocrinol 1998 Oct;19(4):287-322.
8. Sterman DH, Albelda SM. Advances in the diagnosis, evaluation, and management of malignant pleural mesothelioma. Respirology 2005 Jun;10(3):266-83.
9. Hazarika M, White RM, Johnson JR, Pazdur R. FDA drug approval summaries: pemetrexed (Alimta). Oncologist 2004;9(5):482-8.
10. Rodgarkia-Dara C, Vejda S, Erlach N, Losert A, Bursch W, Berger W, et al. The activin axis in liver biology and disease. Mutat Res 2006 Nov-Dec;613(2-3):123-37.
11. Ling N, Ying SY, Ueno N, Shimasaki S, Esch F, Hotta M, et al. Pituitary FSH is released by a heterodimer of the beta-subunits from the two forms of inhibin. Nature 1986 Jun 19-25;321(6072):779-82.
12. Ling N, Ying SY, Ueno N, Shimasaki S, Esch F, Hotta M, et al. A homodimer of the beta-subunits of inhibin A stimulates the secretion of pituitary follicle stimulating hormone. Biochem Biophys Res Commun 1986 Aug 14;138(3):1129-37.
13. Vale W, Rivier J, Vaughan J, McClintock R, Corrigan A, Woo W, et al. Purification and characterization of an FSH releasing protein from porcine ovarian follicular fluid. Nature 1986 Jun 19-25;321(6072):776-9.

14. Herpin A, Lelong C, Favrel P. Transforming growth factor-beta-related proteins: an ancestral and widespread superfamily of cytokines in metazoans. Dev Comp Immunol 2004 May 3;28(5):461-85.

15. Grusch M, Rodgarkia-Dara C, Bursch W, Schulte-Hermann R. Activins and the liver. Jakowlew S, editor. TGF-β Superfamily Members in Normal and Tumor Biology.: Totowa: Humana Press; 2008.

16. Oda S, Nishimatsu S, Murakami K, Ueno N. Molecular cloning and functional analysis of a new activin beta subunit: a dorsal mesoderm-inducing activity in Xenopus. Biochem Biophys Res Commun 1995 May 16;210(2):581-8.

17. Evans LW, Muttukrishna S, Knight PG, Groome NP. Development, validation and application of a two-site enzyme-linked immunosorbent assay for activin-AB. J Endocrinol 1997 May;153(2):221-30.

18. Mellor SL, Ball EM, O'Connor AE, Ethier JF, Cranfield M, Schmitt JF, et al. Activin betaC-subunit heterodimers provide a new mechanism of regulating activin levels in the prostate. Endocrinology 2003 Oct;144(10):4410-9.

19. Mellor SL, Cranfield M, Ries R, Pedersen J, Cancilla B, de Kretser D, et al. Localization of activin beta(A)-, beta(B)-, and beta(C)-subunits in humanprostate and evidence for formation of new activin heterodimers of beta(C)-subunit. J Clin Endocrinol Metab 2000 Dec;85(12):4851-8.

20. Vejda S, Cranfield M, Peter B, Mellor SL, Groome N, Schulte-Hermann R, et al. Expression and dimerization of the rat activin subunits betaC and betaE: evidence for the ormation of novel activin dimers. J Mol Endocrinol 2002 Apr;28(2):137-48.

21. Vejda S, Erlach N, Peter B, Drucker C, Rossmanith W, Pohl J, et al. Expression of activins C and E induces apoptosis in human and rat hepatoma cells. Carcinogenesis 2003 Nov;24(11):1801-9.

22. Wada W, Medina JJ, Kuwano H, Kojima I. Comparison of the function of the beta(C) and beta(E) subunits of activin in AML12 hepatocytes. Endocr J 2005 Apr;52(2):169-75.

23. Salvas A, Benjannet S, Reudelhuber TL, Chretien M, Seidah NG. Evidence for proprotein convertase activity in the endoplasmic reticulum/early Golgi. FEBS Lett 2005 Oct 24;579(25):5621-5.

24. Mason AJ, Farnworth PG, Sullivan J. Characterization and determination of the biological activities of noncleavable high molecular weight forms of inhibin A and activin A. Mol Endocrinol 1996 Sep;10(9):1055-65.

25. Mason AJ. Functional analysis of the cysteine residues of activin A. Mol Endocrinol 1994 Mar;8(3):325-32.
26. Massague J. TGF-beta signal transduction. Annu Rev Biochem 1998;67:753-91.
27. Attisano L, Wrana JL, Montalvo E, Massague J. Activation of signalling by the activin receptor complex. Mol Cell Biol 1996 Mar;16(3):1066-73.
28. Deli A, Kreidl E, Santifaller S, Trotter B, Seir K, Berger W, et al. Activins and activin antagonists in hepatocellular carcinoma. World J Gastroenterol 2008 Mar 21;14(11):1699-709.
29. Wrana JL, Attisano L, Wieser R, Ventura F, Massague J. Mechanism of activation of the TGF-beta receptor. Nature 1994 Aug 4;370(6488):341-7.
30. Wieser R, Wrana JL, Massague J. GS domain mutations that constitutively activate T beta R-I, the downstream signaling component in the TGF-beta receptor complex. EMBO J 1995 May 15;14(10):2199-208.
31. Massague J, Chen YG. Controlling TGF-beta signaling. Genes Dev 2000 Mar 15;14(6):627-44.
32. Heldin CH, Miyazono K, ten Dijke P. TGF-beta signalling from cell membrane to nucleus through SMAD proteins. Nature 1997 Dec 4;390(6659):465-71.
33. Welt C, Sidis Y, Keutmann H, Schneyer A. Activins, inhibins, and follistatins: from endocrinology to signaling. A paradigm for the new millennium. Exp Biol Med (Maywood) 2002 Oct;227(9):724-52.
34. Wu RY, Zhang Y, Feng XH, Derynck R. Heteromeric and homomeric interactions correlate with signaling activity and functional cooperativity of Smad3 and Smad4/DPC4. Mol Cell Biol 1997 May;17(5):2521-8.
35. Derynck R, Zhang Y, Feng XH. Smads: transcriptional activators of TGF-beta responses. Cell 1998 Dec 11;95(6):737-40.
36. Massague J. How cells read TGF-beta signals. Nat Rev Mol Cell Biol 2000 Dec;1(3):169-78.
37. Mulder KM. Role of Ras and Mapks in TGFbeta signaling. Cytokine Growth Factor Rev 2000 Mar-Jun;11(1-2):23-35.
38. Murase Y, Okahashi N, Koseki T, Itoh K, Udagawa N, Hashimoto O, et al. Possible involvement of protein kinases and Smad2 signaling pathways on osteoclast differentiation enhanced by activin A. J Cell Physiol 2001 Aug;188(2):236-42.

39. Dupont J, McNeilly J, Vaiman A, Canepa S, Combarnous Y, Taragnat C. Activin signaling pathways in ovine pituitary and LbetaT2 gonadotrope cells. Biol Reprod 2003 May;68(5):1877-87.

40. Zhang L, Deng M, Parthasarathy R, Wang L, Mongan M, Molkentin JD, et al. MEKK1 transduces activin signals in keratinocytes to induce actin stress fiber formation and migration. Mol Cell Biol 2005 Jan;25(1):60-5.

41. Tuuri T, Eramaa M, Hilden K, Ritvos O. The tissue distribution of activin beta A- and beta B-subunit and follistatin messenger ribonucleic acids suggests multiple sites of action for the activin-follistatin system during human development. J Clin Endocrinol Metab 1994 Jun;78(6):1521-4.

42. Hubner G, Brauchle M, Gregor M, Werner S. Activin A: a novel player and inflammatory marker in inflammatory bowel disease? Lab Invest 1997 Oct;77(4):311-8.

43. Yu EW, Dolter KE, Shao LE, Yu J. Suppression of IL-6 biological activities by activin A and implications for inflammatory arthropathies. Clin Exp Immunol 1998 Apr;112(1):126-32.

44. Hubner G, Werner S. Serum growth factors and proinflammatory cytokines are potent inducers of activin expression in cultured fibroblasts and keratinocytes. Exp Cell Res 1996 Oct 10;228(1):106-13.

45. Hubner G, Hu Q, Smola H, Werner S. Strong induction of activin expression after injury suggests an important role of activin in wound repair. Dev Biol 1996 Feb 1;173(2):490-8.

46. Inoue S, Orimo A, Hosoi T, Ikegami A, Kozaki K, Ouchi Y, et al. Demonstration of activin-A in arteriosclerotic lesions. Biochem Biophys Res Commun 1994 Nov 30;205(1):441-8.

47. Lai M, Sirimanne E, Williams CE, Gluckman PD. Sequential patterns of inhibin subunit gene expression following hypoxic-ischemic injury in the rat brain. Neuroscience 1996 Feb;70(4):1013-24.

48. Date M, Matsuzaki K, Matsushita M, Tahashi Y, Sakitani K, Inoue K. Differential regulation of activin A for hepatocyte growth and fibronectin synthesis in rat liver injury. J Hepatol 2000 Feb;32(2):251-60.

49. Zhang YQ, Shibata H, Schrewe H, Kojima I. Reciprocal expression of mRNA for inhibin betaC and betaA subunits in hepatocytes. Endocr J 1997 Oct;44(5):759-64.

50. Patella S, Phillips DJ, de Kretser DM, Evans LW, Groome NP, Sievert W. Characterization of serum activin-A and follistatin and their relation to virological and histological determinants in chronic viral hepatitis. J Hepatol 2001 Apr;34(4):576-83.

51. Yuen MF, Norris S, Evans LW, Langley PG, Hughes RD. Transforming growth factor-beta 1, activin and follistatin in patients with hepatocellular carcinoma and patients with alcoholic cirrhosis. Scand J Gastroenterol 2002 Feb;37(2):233-8.

52. Pirisi M, Fabris C, Luisi S, Santuz M, Toniutto P, Vitulli D, et al. Evaluation of circulating activin-A as a serum marker of hepatocellular carcinoma. Cancer Detect Prev 2000;24(2):150-5.

53. Elsammak MY, Amin GM, Khalil GM, Ragab WS, Abaza MM. Possible contribution of serum activin A and IGF-1 in the development of hepatocellular carcinoma in Egyptian patients suffering from combined hepatitis C virus infection and hepatic schistosomiasis. Clin Biochem 2006 Jun;39(6):623-9.

54. Hughes RD, Evans LW. Activin A and follistatin in acute liver failure. Eur J Gastroenterol Hepatol 2003 Feb;15(2):127-31.

55. Lin SD, Kawakami T, Ushio A, Sato A, Sato S, Iwai M, et al. Ratio of circulating follistatin and activin A reflects the severity of acute liver injury and prognosis in patients with acute liver failure. J Gastroenterol Hepatol 2006 Feb;21(2):374-80.

56. Hully JR, Chang L, Schwall RH, Widmer HR, Terrell TG, Gillett NA. Induction of apoptosis in the murine liver with recombinant human activin A. Hepatology 1994 Oct;20(4 Pt 1):854-62.

57. Schwall RH, Robbins K, Jardieu P, Chang L, Lai C, Terrell TG. Activin induces cell death in hepatocytes in vivo and in vitro. Hepatology 1993 Aug;18(2):347-56.

58. Yasuda H, Mine T, Shibata H, Eto Y, Hasegawa Y, Takeuchi T, et al. Activin A: an autocrine inhibitor of initiation of DNA synthesis in rat hepatocytes. J Clin Invest 1993 Sep;92(3):1491-6.

59. Matsuse T, Fukuchi Y, Eto Y, Matsui H, Hosoi T, Oka T, et al. Expression of immunoreactive and bioactive activin A protein in adult murine lung after bleomycin treatment. Am J Respir Cell Mol Biol 1995 Jul;13(1):17-24.

60. Matsuse T, Ikegami A, Ohga E, Hosoi T, Oka T, Kida K, et al. Expression of immunoreactive activin A protein in remodeling lesions associated with interstitial pulmonary fibrosis. Am J Pathol 1996 Mar;148(3):707-13.

61. Michel U, Ebert S, Phillips D, Nau R. Serum concentrations of activin and follistatin are elevated and run in parallel in patients with septicemia. Eur J Endocrinol 2003 May;148(5):559-64.

62. Smith C, Yndestad A, Halvorsen B, Ueland T, Waehre T, Otterdal K, et al. Potential anti-inflammatory role of activin A in acute coronary syndromes. J Am Coll Cardiol 2004 Jul 21;44(2):369-75.

63. de Kretser DM, Hedger MP, Loveland KL, Phillips DJ. Inhibins, activins and follistatin in reproduction. Hum Reprod Update 2002 Nov-Dec;8(6):529-41.

64. Maguer-Satta V, Bartholin L, Jeanpierre S, Ffrench M, Martel S, Magaud JP, et al. Regulation of human erythropoiesis by activin A, BMP2, and BMP4, members of the TGFbeta family. Exp Cell Res 2003 Jan 15;282(2):110-20.

65. McDowell N, Gurdon JB. Activin as a morphogen in Xenopus mesoderm induction. Semin Cell Dev Biol 1999 Jun;10(3):311-7.

66. Beattie GM, Lopez AD, Bucay N, Hinton A, Firpo MT, King CC, et al. Activin A maintains pluripotency of human embryonic stem cells in the absence of feeder layers. Stem Cells 2005 Apr;23(4):489-95.

67. Chen YG, Wang Q, Lin SL, Chang CD, Chuang J, Ying SY. Activin signaling and its role in regulation of cell proliferation, apoptosis, and carcinogenesis. Exp Biol Med (Maywood) 2006 May;231(5):534-44.

68. Sjoholm K, Palming J, Lystig TC, Jennische E, Woodruff TK, Carlsson B, et al. The expression of inhibin beta B is high in human adipocytes, reduced by weight loss, and correlates to factors implicated in metabolic disease. Biochem Biophys Res Commun 2006 Jun 16;344(4):1308-14.

69. Hotten G, Neidhardt H, Schneider C, Pohl J. Cloning of a new member of the TGF-beta family: a putative new activin beta C chain. Biochem Biophys Res Commun 1995 Jan 17;206(2):608-13.

70. Gold EJ, O'Bryan MK, Mellor SL, Cranfield M, Risbridger GP, Groome NP, et al. Cell-specific expression of betaC-activin in the rat reproductive tract, adrenal and liver. Mol Cell Endocrinol 2004 Jul 30;222(1-2):61-9.

71. Lau AL, Nishimori K, Matzuk MM. Structural analysis of the mouse activin beta C gene. Biochim Biophys Acta 1996 Jun 7;1307(2):145-8.

72. Gold EJ, Zhang X, Wheatley AM, Mellor SL, Cranfield M, Risbridger GP, et al. betaA- and betaC-activin, follistatin, activin receptor mRNA and betaC-activin peptide expression during rat liver regeneration. J Mol Endocrinol 2005 Apr;34(2):505-15.

73. Esquela AF, Zimmers TA, Koniaris LG, Sitzmann JV, Lee SJ. Transient down-regulation of inhibin-betaC expression following partial hepatectomy. Biochem Biophys Res Commun 1997 Jun 27;235(3):553-6.

74. Takamura K, Tsuchida K, Miyake H, Tashiro S, Sugino H. Activin and activin receptor expression changes in liver regeneration in rat. J Surg Res 2005 Jun 1;126(1):3-11.

75. Hashimoto O, Tsuchida K, Ushiro Y, Hosoi Y, Hoshi N, Sugino H, et al. cDNA cloning and expression of human activin betaE subunit. Mol Cell Endocrinol 2002 Aug 30;194(1-2):117-22.

76. Fang J, Yin W, Smiley E, Wang SQ, Bonadio J. Molecular cloning of the mouse activin beta E subunit gene. Biochem Biophys Res Commun 1996 Nov 21;228(3):669-74.

77. O'Bryan MK, Sebire KL, Gerdprasert O, Hedger MP, Hearn MT, de Kretser DM. Cloning and regulation of the rat activin betaE subunit. J Mol Endocrinol 2000 Jun;24(3):409-18.

78. Grusch M, Drucker C, Peter-Vorosmarty B, Erlach N, Lackner A, Losert A, et al. Deregulation of the activin/follistatin system in hepatocarcinogenesis. J Hepatol 2006 Nov;45(5):673-80.

79. Matzuk MM, Kumar TR, Vassalli A, Bickenbach JR, Roop DR, Jaenisch R, et al. Functional analysis of activins during mammalian development. Nature 1995 Mar 23;374(6520):354-6.

80. Ferguson CA, Tucker AS, Christensen L, Lau AL, Matzuk MM, Sharpe PT. Activin is an essential early mesenchymal signal in tooth development that is required for patterning of the murine dentition. Genes Dev 1998 Aug 15;12(16):2636-49.

81. Jhaveri S, Erzurumlu RS, Chiaia N, Kumar TR, Matzuk MM. Defective whisker follicles and altered brainstem patterns in activin and follistatin knockout mice. Mol Cell Neurosci 1998 Nov;12(4-5):206-19.

82. Schrewe H, Gendron-Maguire M, Harbison ML, Gridley T. Mice homozygous for a null mutation of activin beta B are viable and fertile. Mech Dev 1994 Jul;47(1):43-51.

83. Vassalli A, Matzuk MM, Gardner HA, Lee KF, Jaenisch R. Activin/inhibin beta B subunit gene disruption leads to defects in eyelid development and female reproduction. Genes Dev 1994 Feb 15;8(4):414-27.

84. Lau AL, Kumar TR, Nishimori K, Bonadio J, Matzuk MM. Activin betaC and betaE genes are not essential for mouse liver growth, differentiation, and regeneration. Mol Cell Biol 2000 Aug;20(16):6127-37.

85. Matzuk MM, Finegold MJ, Su JG, Hsueh AJ, Bradley A. Alpha-inhibin is a tumour-suppressor gene with gonadal specificity in mice. Nature 1992 Nov 26;360(6402):313-9.
86. Burger HG, Igarashi M. Inhibin: definition and nomenclature, including related substances. J Clin Endocrinol Metab 1988 Apr;66(4):885-6.
87. Ueno N, Ling N, Ying SY, Esch F, Shimasaki S, Guillemin R. Isolation and partial characterization of follistatin: a single-chain Mr 35,000 monomeric protein that inhibits the release of follicle-stimulating hormone. Proc Natl Acad Sci U S A 1987 Dec;84(23):8282-6.
88. de Winter JP, ten Dijke P, de Vries CJ, van Achterberg TA, Sugino H, de Waele P, et al. Follistatins neutralize activin bioactivity by inhibition of activin binding to its type II receptors. Mol Cell Endocrinol 1996 Jan 15;116(1):105-14.
89. Michel U, Rao A, Findlay JK. Rat follistatin: ontogeny of steady-state mRNA levels in different tissues predicts organ-specific functions. Biochem Biophys Res Commun 1991 Oct 15;180(1):223-30.
90. Beale G, Chattopadhyay D, Gray J, Stewart S, Hudson M, Day C, et al. AFP, PIVKAII, GP3, SCCA-1 and follisatin as surveillance biomarkers for hepatocellular cancer in non-alcoholic and alcoholic fatty liver disease. BMC Cancer 2008;8:200.
91. Sugino K, Kurosawa N, Nakamura T, Takio K, Shimasaki S, Ling N, et al. Molecular heterogeneity of follistatin, an activin-binding protein. Higher affinity of the carboxyl-terminal truncated forms for heparan sulfate proteoglycans on the ovarian granulosa cell. J Biol Chem 1993 Jul 25;268(21):15579-87.
92. Shimasaki S, Koga M, Esch F, Mercado M, Cooksey K, Koba A, et al. Porcine follistatin gene structure supports two forms of mature follistatin produced by alternative splicing. Biochem Biophys Res Commun 1988 Apr 29;152(2):717-23.
93. Shimasaki S, Koga M, Esch F, Cooksey K, Mercado M, Koba A, et al. Primary structure of the human follistatin precursor and its genomic organization. Proc Natl Acad Sci U S A 1988 Jun;85(12):4218-22.
94. Tashiro K, Yamada R, Asano M, Hashimoto M, Muramatsu M, Shiokawa K. Expression of mRNA for activin-binding protein (follistatin) during early embryonic development of Xenopus laevis. Biochem Biophys Res Commun 1991 Jan 31;174(2):1022-7.
95. Harrison CA, Gray PC, Vale WW, Robertson DM. Antagonists of activin signaling: mechanisms and potential biological applications. Trends Endocrinol Metab 2005 Mar;16(2):73-8.

96. Tsuchida K, Arai KY, Kuramoto Y, Yamakawa N, Hasegawa Y, Sugino H. Identification and characterization of a novel follistatin-like protein as a binding protein for the TGF-beta family. J Biol Chem 2000 Dec 29;275(52):40788-96.

97. Harrington AE, Morris-Triggs SA, Ruotolo BT, Robinson CV, Ohnuma S, Hyvonen M. Structural basis for the inhibition of activin signalling by follistatin. EMBO J 2006 Mar 8;25(5):1035-45.

98. Keutmann HT, Schneyer AL, Sidis Y. The role of follistatin domains in follistatin biological action. Mol Endocrinol 2004 Jan;18(1):228-40.

99. Schneyer AL, Rzucidlo DA, Sluss PM, Crowley WF, Jr. Characterization of unique binding kinetics of follistatin and activin or inhibin in serum. Endocrinology 1994 Aug;135(2):667-74.

100. Inouye S, Guo Y, DePaolo L, Shimonaka M, Ling N, Shimasaki S. Recombinant expression of human follistatin with 315 and 288 amino acids: chemical and biological comparison with native porcine follistatin. Endocrinology 1991 Aug;129(2):815-22.

101. Hashimoto O, Kawasaki N, Tsuchida K, Shimasaki S, Hayakawa T, Sugino H. Difference between follistatin isoforms in the inhibition of activin signalling: activin neutralizing activity of follistatin isoforms is dependent on their affinity for activin. Cell Signal 2000 Aug;12(8):565-71.

102. Sumitomo S, Inouye S, Liu XJ, Ling N, Shimasaki S. The heparin binding site of follistatin is involved in its interaction with activin. Biochem Biophys Res Commun 1995 Mar 8;208(1):1-9.

103. Nakamura T, Sugino K, Titani K, Sugino H. Follistatin, an activin-binding protein, associates with heparan sulfate chains of proteoglycans on follicular granulosa cells. J Biol Chem 1991 Oct 15;266(29):19432-7.

104. Hashimoto O, Nakamura T, Shoji H, Shimasaki S, Hayashi Y, Sugino H. A novel role of follistatin, an activin-binding protein, in the inhibition of activin action in rat pituitary cells. Endocytotic degradation of activin and its acceleration by follistatin associated with cell-surface heparan sulfate. J Biol Chem 1997 May 23;272(21):13835-42.

105. Schneyer AL, Hall HA, Lambert-Messerlian G, Wang QF, Sluss P, Crowley WF, Jr. Follistatin-activin complexes in human serum and follicular fluid differ immunologically and biochemically. Endocrinology 1996 Jan;137(1):240-7.

106. Schneyer A, Schoen A, Quigg A, Sidis Y. Differential binding and neutralization of activins A and B by follistatin and follistatin like-3 (FSTL-3/FSRP/FLRG). Endocrinology 2003 May;144(5):1671-4.

107. Iemura S, Yamamoto TS, Takagi C, Uchiyama H, Natsume T, Shimasaki S, et al. Direct binding of follistatin to a complex of bone-morphogenetic protein and its receptor inhibits ventral and epidermal cell fates in early Xenopus embryo. Proc Natl Acad Sci U S A 1998 Aug 4;95(16):9337-42.

108. Amthor H, Nicholas G, McKinnell I, Kemp CF, Sharma M, Kambadur R, et al. Follistatin complexes Myostatin and antagonises Myostatin-mediated inhibition of myogenesis. Dev Biol 2004 Jun 1;270(1):19-30.

109. Glister C, Kemp CF, Knight PG. Bone morphogenetic protein (BMP) ligands and receptors in bovine ovarian follicle cells: actions of BMP-4, -6 and -7 on granulosa cells and differential modulation of Smad-1 phosphorylation by follistatin. Reproduction 2004 Feb;127(2):239-54.

110. Lee SJ, McPherron AC. Regulation of myostatin activity and muscle growth. Proc Natl Acad Sci U S A 2001 Jul 31;98(16):9306-11.

111. Hayette S, Gadoux M, Martel S, Bertrand S, Tigaud I, Magaud JP, et al. FLRG (follistatin-related gene), a new target of chromosomal rearrangement in malignant blood disorders. Oncogene 1998 Jun 4;16(22):2949-54.

112. Mukherjee A, Sidis Y, Mahan A, Raher MJ, Xia Y, Rosen ED, et al. FSTL3 deletion reveals roles for TGF-beta family ligands in glucose and fat homeostasis in adults. Proc Natl Acad Sci U S A 2007 Jan 23;104(4):1348-53.

113. Nakao A, Afrakhte M, Moren A, Nakayama T, Christian JL, Heuchel R, et al. Identification of Smad7, a TGFbeta-inducible antagonist of TGF-beta signalling. Nature 1997 Oct 9;389(6651):631-5.

114. Hayashi H, Abdollah S, Qiu Y, Cai J, Xu YY, Grinnell BW, et al. The MAD-related protein Smad7 associates with the TGFbeta receptor and functions as an antagonist of TGFbeta signaling. Cell 1997 Jun 27;89(7):1165-73.

115. Adamson ED, Minchiotti G, Salomon DS. Cripto: a tumor growth factor and more. J Cell Physiol 2002 Mar;190(3):267-78.

116. Gray PC, Harrison CA, Vale W. Cripto forms a complex with activin and type II activin receptors and can block activin signaling. Proc Natl Acad Sci U S A 2003 Apr 29;100(9):5193-8.

117. Adkins HB, Bianco C, Schiffer SG, Rayhorn P, Zafari M, Cheung AE, et al. Antibody blockade of the Cripto CFC domain suppresses tumor cell growth in vivo. J Clin Invest 2003 Aug;112(4):575-87.

118. Yeo C, Whitman M. Nodal signals to Smads through Cripto-dependent and Cripto-independent mechanisms. Mol Cell 2001 May;7(5):949-57.

119. Shen MM. Nodal signaling: developmental roles and regulation. Development 2007 Mar;134(6):1023-34.

120. Chen W, Woodruff TK, Mayo KE. Activin A-induced HepG2 liver cell apoptosis: involvement of activin receptors and smad proteins. Endocrinology 2000 Mar;141(3):1263-72.

121. Liu QY, Niranjan B, Gomes P, Gomm JJ, Davies D, Coombes RC, et al. Inhibitory effects of activin on the growth and morpholgenesis of primary and transformed mammary epithelial cells. Cancer Res 1996 Mar 1;56(5):1155-63.

122. Reis FM, Luisi S, Carneiro MM, Cobellis L, Federico M, Camargos AF, et al. Activin, inhibin and the human breast. Mol Cell Endocrinol 2004 Oct 15;225(1-2):77-82.

123. Burdette JE, Jeruss JS, Kurley SJ, Lee EJ, Woodruff TK. Activin A mediates growth inhibition and cell cycle arrest through Smads in human breast cancer cells. Cancer Res 2005 Sep 1;65(17):7968-75.

124. Katik I, Mackenzie-Kludas C, Nicholls C, Jiang FX, Zhou S, Li H, et al. Activin inhibits telomerase activity in cancer. Biochem Biophys Res Commun 2009 Nov 27;389(4):668-72.

125. Wang QF, Tilly KI, Tilly JL, Preffer F, Schneyer AL, Crowley WF, Jr., et al. Activin inhibits basal and androgen-stimulated proliferation and induces apoptosis in the human prostatic cancer cell line, LNCaP. Endocrinology 1996 Dec;137(12):5476-83.

126. Risbridger GP, Mellor SL, McPherson SJ, Schmitt JF. The contribution of inhibins and activins to malignant prostate disease. Mol Cell Endocrinol 2001 Jun 30;180(1-2):149-53.

127. Dowling CR, Risbridger GP. The role of inhibins and activins in prostate cancer pathogenesis. Endocr Relat Cancer 2000 Dec;7(4):243-56.

128. Danila DC, Inder WJ, Zhang X, Alexander JM, Swearingen B, Hedley-Whyte ET, et al. Activin effects on neoplastic proliferation of human pituitary tumors. J Clin Endocrinol Metab 2000 Mar;85(3):1009-15.

129. Danila DC, Zhang X, Zhou Y, Haidar JN, Klibanski A. Overexpression of wild-type activin receptor alk4-1 restores activin antiproliferative effects in human pituitary tumor cells. J Clin Endocrinol Metab 2002 Oct;87(10):4741-6.

130. Zheng W, Luo MP, Welt C, Lambert-Messerlian G, Sung CJ, Zhang Z, et al. Imbalanced expression of inhibin and activin subunits in primary epithelial ovarian cancer. Gynecol Oncol 1998 Apr;69(1):23-31.
131. Welt CK, Lambert-Messerlian G, Zheng W, Crowley WF, Jr., Schneyer AL. Presence of activin, inhibin, and follistatin in epithelial ovarian carcinoma. J Clin Endocrinol Metab 1997 Nov;82(11):3720-7.
132. Petraglia F, Florio P, Luisi S, Gallo R, Gadducci A, Vigano P, et al. Expression and secretion of inhibin and activin in normal and neoplastic uterine tissues. High levels of serum activin A in women with endometrial and cervical carcinoma. J Clin Endocrinol Metab 1998 Apr;83(4):1194-200.
133. Reis FM, Cobellis L, Tameirao LC, Anania G, Luisi S, Silva IS, et al. Serum and tissue expression of activin a in postmenopausal women with breast cancer. J Clin Endocrinol Metab 2002 May;87(5):2277-82.
134. Tanaka T, Toujima S, Umesaki N. Activin A inhibits growth-inhibitory signals by TGF-beta1 in differentiated human endometrial adenocarcinoma cells. Oncol Rep 2004 Apr;11(4):875-9.
135. Ferreira MC, Witz CA, Hammes LS, Kirma N, Petraglia F, Schenken RS, et al. Activin A increases invasiveness of endometrial cells in an in vitro model of human peritoneum. Mol Hum Reprod 2008 May;14(5):301-7.
136. Devouassoux-Shisheboran M, Mauduit C, Tabone E, Droz JP, Benahmed M. Growth regulatory factors and signalling proteins in testicular germ cell tumours. APMIS 2003 Jan;111(1):212-24; discussion 24.
137. Takeno A, Takemasa I, Doki Y, Yamasaki M, Miyata H, Takiguchi S, et al. Integrative approach for differentially overexpressed genes in gastric cancer by combining large-scale gene expression profiling and network analysis. Br J Cancer 2008 Oct 21;99(8):1307-15.
138. Wang Q, Wen YG, Li DP, Xia J, Zhou CZ, Yan DW, et al. Upregulated INHBA expression is associated with poor survival in gastric cancer. Med Oncol 2010 Dec 4.
139. Shimizu S, Seki N, Sugimoto T, Horiguchi S, Tanzawa H, Hanazawa T, et al. Identification of molecular targets in head and neck squamous cell carcinomas based on genome-wide gene expression profiling. Oncol Rep 2007 Dec;18(6):1489-97.
140. Chang KP, Kao HK, Liang Y, Cheng MH, Chang YL, Liu SC, et al. Overexpression of activin A in oral squamous cell carcinoma: association with poor prognosis and tumor progression. Ann Surg Oncol 2010 Jul;17(7):1945-56.

141. Yoshinaga K, Mimori K, Yamashita K, Utsunomiya T, Inoue H, Mori M. Clinical significance of the expression of activin A in esophageal carcinoma. Int J Oncol 2003 Jan;22(1):75-80.

142. Yoshinaga K, Yamashita K, Mimori K, Tanaka F, Inoue H, Mori M. Activin a causes cancer cell aggressiveness in esophageal squamous cell carcinoma cells. Ann Surg Oncol 2008 Jan;15(1):96-103.

143. Puhringer-Oppermann F, Sarbia M, Ott N, Brucher BL. The predictive value of genes of the TGF-beta1 pathway in multimodally treated squamous cell carcinoma of the esophagus. Int J Colorectal Dis 2010 Apr;25(4):515-21.

144. Seder CW, Hartojo W, Lin L, Silvers AL, Wang Z, Thomas DG, et al. INHBA overexpression promotes cell proliferation and may be epigenetically regulated in esophageal adenocarcinoma. J Thorac Oncol 2009 Apr;4(4):455-62.

145. Seder CW, Hartojo W, Lin L, Silvers AL, Wang Z, Thomas DG, et al. Upregulated INHBA expression may promote cell proliferation and is associated with poor survival in lung adenocarcinoma. Neoplasia 2009 Apr;11(4):388-96.

146. Wagner JC, Sleggs CA, Marchand P. Diffuse pleural mesothelioma and asbestos exposure in the North Western Cape Province. Br J Ind Med 1960 Oct;17:260-71.

147. Peto J, Hodgson JT, Matthews FE, Jones JR. Continuing increase in mesothelioma mortality in Britain. Lancet 1995 Mar 4;345(8949):535-9.

148. Bianchi C, Bianchi T. Malignant mesothelioma: global incidence and relationship with asbestos. Ind Health 2007 Jun;45(3):379-87.

149. Larson T, Melnikova N, Davis SI, Jamison P. Incidence and descriptive epidemiology of mesothelioma in the United States, 1999-2002. Int J Occup Environ Health 2007 Oct-Dec;13(4):398-403.

150. Yang H, Testa JR, Carbone M. Mesothelioma epidemiology, carcinogenesis, and pathogenesis. Curr Treat Options Oncol 2008 Jun;9(2-3):147-57.

151. Selikoff IJ, Hammond EC, Seidman H. Latency of asbestos disease among insulation workers in the United States and Canada. Cancer 1980 Dec 15;46(12):2736-40.

152. Carbone M, Kratzke RA, Testa JR. The pathogenesis of mesothelioma. Semin Oncol 2002 Feb;29(1):2-17.

153. Antman KH. Natural history and epidemiology of malignant mesothelioma. Chest 1993 Apr;103(4 Suppl):373S-6S.

154. Olofsson K, Mark J. Specificity of asbestos-induced chromosomal aberrations in short-term cultured human mesothelial cells. Cancer Genet Cytogenet 1989 Aug;41(1):33-9.

155. BeruBe KA, Quinlan TR, Fung H, Magae J, Vacek P, Taatjes DJ, et al. Apoptosis is observed in mesothelial cells after exposure to crocidolite asbestos. Am J Respir Cell Mol Biol 1996 Jul;15(1):141-7.

156. Broaddus VC, Yang L, Scavo LM, Ernst JD, Boylan AM. Asbestos induces apoptosis of human and rabbit pleural mesothelial cells via reactive oxygen species. J Clin Invest 1996 Nov 1;98(9):2050-9.

157. Barrett JC. Cellular and molecular mechanisms of asbestos carcinogenicity: implications for biopersistence. Environ Health Perspect 1994 Oct;102 Suppl 5:19-23.

158. Hesterberg TW, Chase G, Axten C, Miller WC, Musselman RP, Kamstrup O, et al. Biopersistence of synthetic vitreous fibers and amosite asbestos in the rat lung following inhalation. Toxicol Appl Pharmacol 1998 Aug;151(2):262-75.

159. Janssen YM, Barchowsky A, Treadwell M, Driscoll KE, Mossman BT. Asbestos induces nuclear factor kappa B (NF-kappa B) DNA-binding activity and NF-kappa B-dependent gene expression in tracheal epithelial cells. Proc Natl Acad Sci U S A 1995 Aug 29;92(18):8458-62.

160. Janssen YM, Driscoll KE, Howard B, Quinlan TR, Treadwell M, Barchowsky A, et al. Asbestos causes translocation of p65 protein and increases NF-kappa B DNA binding activity in rat lung epithelial and pleural mesothelial cells. Am J Pathol 1997 Aug;151(2):389-401.

161. Yang H, Bocchetta M, Kroczynska B, Elmishad AG, Chen Y, Liu Z, et al. TNF-alpha inhibits asbestos-induced cytotoxicity via a NF-kappaB-dependent pathway, a possible mechanism for asbestos-induced oncogenesis. Proc Natl Acad Sci U S A 2006 Jul 5;103(27):10397-402.

162. Yang H, Rivera Z, Jube S, Nasu M, Bertino P, Goparaju C, et al. Programmed necrosis induced by asbestos in human mesothelial cells causes high-mobility group box 1 protein release and resultant inflammation. Proc Natl Acad Sci U S A 2010 Jul 13;107(28):12611-6.

163. Liu JY, Brass DM, Hoyle GW, Brody AR. TNF-alpha receptor knockout mice are protected from the fibroproliferative effects of inhaled asbestos fibers. Am J Pathol 1998 Dec;153(6):1839-47.

164. Walker C, Everitt J, Barrett JC. Possible cellular and molecular mechanisms for asbestos carcinogenicity. Am J Ind Med 1992;21(2):253-73.

165. Versnel MA, Claesson-Welsh L, Hammacher A, Bouts MJ, van der Kwast TH, Eriksson A, et al. Human malignant mesothelioma cell lines express PDGF beta-receptors whereas cultured normal mesothelial cells express predominantly PDGF alpha-receptors. Oncogene 1991 Nov;6(11):2005-11.

166. Strizzi L, Catalano A, Vianale G, Orecchia S, Casalini A, Tassi G, et al. Vascular endothelial growth factor is an autocrine growth factor in human malignant mesothelioma. J Pathol 2001 Apr;193(4):468-75.

167. Masood R, Kundra A, Zhu S, Xia G, Scalia P, Smith DL, et al. Malignant mesothelioma growth inhibition by agents that target the VEGF and VEGF-C autocrine loops. Int J Cancer 2003 May 1;104(5):603-10.

168. Dazzi H, Hasleton PS, Thatcher N, Wilkes S, Swindell R, Chatterjee AK. Malignant pleural mesothelioma and epidermal growth factor receptor (EGF-R). Relationship of EGF-R with histology and survival using fixed paraffin embedded tissue and the F4, monoclonal antibody. Br J Cancer 1990 Jun;61(6):924-6.

169. Tolnay E, Kuhnen C, Wiethege T, Konig JE, Voss B, Muller KM. Hepatocyte growth factor/scatter factor and its receptor c-Met are overexpressed and associated with an increased microvessel density in malignant pleural mesothelioma. J Cancer Res Clin Oncol 1998;124(6):291-6.

170. Liu Z, Klominek J. Chemotaxis and chemokinesis of malignant mesothelioma cells to multiple growth factors. Anticancer Res 2004 May-Jun;24(3a):1625-30.

171. Fitzpatrick DR, Bielefeldt-Ohmann H, Himbeck RP, Jarnicki AG, Marzo AL, Robinson BW. Transforming growth factor-beta: antisense RNA-mediated inhibition affects anchorage-independent growth, tumorigenicity and tumor-infiltrating T-cells in malignant mesothelioma. Growth Factors 1994;11(1):29-44.

172. Marzo AL, Fitzpatrick DR, Robinson BW, Scott B. Antisense oligonucleotides specific for transforming growth factor beta2 inhibit the growth of malignant mesothelioma both in vitro and in vivo. Cancer Res 1997 Aug 1;57(15):3200-7.

173. Hillegass JM, Shukla A, Lathrop SA, MacPherson MB, Beuschel SL, Butnor KJ, et al. Inflammation precedes the development of human malignant mesotheliomas in a SCID mouse xenograft model. Ann N Y Acad Sci 2010 Aug;1203:7-14.

174. Merritt RE, Yamada RE, Wasif N, Crystal RG, Korst RJ. Effect of inhibition of multiple steps of angiogenesis in syngeneic murine pleural mesothelioma. Ann Thorac Surg 2004 Sep;78(3):1042-51; discussion -51.

175. Hesterberg TW, Barrett JC. Induction by asbestos fibers of anaphase abnormalities: mechanism for aneuploidy induction and possibly carcinogenesis. Carcinogenesis 1985 Mar;6(3):473-5.

176. Murthy SS, Testa JR. Asbestos, chromosomal deletions, and tumor suppressor gene alterations in human malignant mesothelioma. J Cell Physiol 1999 Aug;180(2):150-7.

177. Sekido Y, Pass HI, Bader S, Mew DJ, Christman MF, Gazdar AF, et al. Neurofibromatosis type 2 (NF2) gene is somatically mutated in mesothelioma but not in lung cancer. Cancer Res 1995 Mar 15;55(6):1227-31.

178. Bianchi AB, Mitsunaga SI, Cheng JQ, Klein WM, Jhanwar SC, Seizinger B, et al. High frequency of inactivating mutations in the neurofibromatosis type 2 gene (NF2) in primary malignant mesotheliomas. Proc Natl Acad Sci U S A 1995 Nov 21;92(24):10854-8.

179. Lechner JF, Tesfaigzi J, Gerwin BI. Oncogenes and tumor-suppressor genes in mesothelioma--a synopsis. Environ Health Perspect 1997 Sep;105 Suppl 5:1061-7.

180. Cheng JQ, Jhanwar SC, Klein WM, Bell DW, Lee WC, Altomare DA, et al. p16 alterations and deletion mapping of 9p21-p22 in malignant mesothelioma. Cancer Res 1994 Nov 1;54(21):5547-51.

181. Hirao T, Bueno R, Chen CJ, Gordon GJ, Heilig E, Kelsey KT. Alterations of the p16(INK4) locus in human malignant mesothelial tumors. Carcinogenesis 2002 Jul;23(7):1127-30.

182. Altomare DA, You H, Xiao GH, Ramos-Nino ME, Skele KL, De Rienzo A, et al. Human and mouse mesotheliomas exhibit elevated AKT/PKB activity, which can be targeted pharmacologically to inhibit tumor cell growth. Oncogene 2005 Sep 8;24(40):6080-9.

183. Taniguchi T, Karnan S, Fukui T, Yokoyama T, Tagawa H, Yokoi K, et al. Genomic profiling of malignant pleural mesothelioma with array-based comparative genomic hybridization shows frequent non-random chromosomal alteration regions including JUN amplification on 1p32. Cancer Sci 2007 Mar;98(3):438-46.

184. Wong L, Zhou J, Anderson D, Kratzke RA. Inactivation of p16INK4a expression in malignant mesothelioma by methylation. Lung Cancer 2002 Nov;38(2):131-6.

185. Yang CT, You L, Yeh CC, Chang JW, Zhang F, McCormick F, et al. Adenovirus-mediated p14(ARF) gene transfer in human mesothelioma cells. J Natl Cancer Inst 2000 Apr 19;92(8):636-41.

186. Frizelle SP, Grim J, Zhou J, Gupta P, Curiel DT, Geradts J, et al. Re-expression of p16INK4a in mesothelioma cells results in cell cycle arrest, cell death, tumor suppression and tumor regression. Oncogene 1998 Jun 18;16(24):3087-95.

187. Balsara BR, Bell DW, Sonoda G, De Rienzo A, du Manoir S, Jhanwar SC, et al. Comparative genomic hybridization and loss of heterozygosity analyses identify a common region of deletion at 15q11.1-15 in human malignant mesothelioma. Cancer Res 1999 Jan 15;59(2):450-4.

188. Bjorkqvist AM, Tammilehto L, Anttila S, Mattson K, Knuutila S. Recurrent DNA copy number changes in 1q, 4q, 6q, 9p, 13q, 14q and 22q detected by comparative genomic hybridization in malignant mesothelioma. Br J Cancer 1997;75(4):523-7.

189. Dhaene K, Hubner R, Kumar-Singh S, Weyn B, Van Marck E. Telomerase activity in human pleural mesothelioma. Thorax 1998 Nov;53(11):915-8.

190. Dhaene K, Wauters J, Weyn B, Timmermans JP, van Marck E. Expression profile of telomerase subunits in human pleural mesothelioma. J Pathol 2000 Jan;190(1):80-5.

191. Narasimhan SR, Yang L, Gerwin BI, Broaddus VC. Resistance of pleural mesothelioma cell lines to apoptosis: relation to expression of Bcl-2 and Bax. Am J Physiol 1998 Jul;275(1 Pt 1):L165-71.

192. Soini Y, Kinnula V, Kaarteenaho-Wiik R, Kurttila E, Linnainmaa K, Paakko P. Apoptosis and expression of apoptosis regulating proteins bcl-2, mcl-1, bcl-X, and bax in malignant mesothelioma. Clin Cancer Res 1999 Nov;5(11):3508-15.

193. Robinson BW, Lake RA. Advances in malignant mesothelioma. N Engl J Med 2005 Oct 13;353(15):1591-603.

194. Cicala C, Pompetti F, Carbone M. SV40 induces mesotheliomas in hamsters. Am J Pathol 1993 May;142(5):1524-33.

195. Carbone M, Rizzo P, Grimley PM, Procopio A, Mew DJ, Shridhar V, et al. Simian virus-40 large-T antigen binds p53 in human mesotheliomas. Nat Med 1997 Aug;3(8):908-12.

196. De Luca A, Baldi A, Esposito V, Howard CM, Bagella L, Rizzo P, et al. The retinoblastoma gene family pRb/p105, p107, pRb2/p130 and simian virus-40 large T-antigen in human mesotheliomas. Nat Med 1997 Aug;3(8):913-6.

197. Foddis R, De Rienzo A, Broccoli D, Bocchetta M, Stekala E, Rizzo P, et al. SV40 infection induces telomerase activity in human mesothelial cells. Oncogene 2002 Feb 21;21(9):1434-42.
198. Butel JS, Jafar S, Wong C, Arrington AS, Opekun AR, Finegold MJ, et al. Evidence of SV40 infections in hospitalized children. Hum Pathol 1999 Dec;30(12):1496-502.
199. Testa JR, Carbone M, Hirvonen A, Khalili K, Krynska B, Linnainmaa K, et al. A multi-institutional study confirms the presence and expression of simian virus 40 in human malignant mesotheliomas. Cancer Res 1998 Oct 15;58(20):4505-9.
200. Shivapurkar N, Wiethege T, Wistuba, II, Salomon E, Milchgrub S, Muller KM, et al. Presence of simian virus 40 sequences in malignant mesotheliomas and mesothelial cell proliferations. J Cell Biochem 1999 Dec;76(2):181-8.
201. Ramael M, Nagels J, Heylen H, De Schepper S, Paulussen J, De Maeyer M, et al. Detection of SV40 like viral DNA and viral antigens in malignant pleural mesothelioma. Eur Respir J 1999 Dec;14(6):1381-6.
202. Mayall FG, Jacobson G, Wilkins R. Mutations of p53 gene and SV40 sequences in asbestos associated and non-asbestos-associated mesotheliomas. J Clin Pathol 1999 Apr;52(4):291-3.
203. Kroczynska B, Cutrone R, Bocchetta M, Yang H, Elmishad AG, Vacek P, et al. Crocidolite asbestos and SV40 are cocarcinogens in human mesothelial cells and in causing mesothelioma in hamsters. Proc Natl Acad Sci U S A 2006 Sep 19;103(38):14128-33.
204. Robinson C, van Bruggen I, Segal A, Dunham M, Sherwood A, Koentgen F, et al. A novel SV40 TAg transgenic model of asbestos-induced mesothelioma: malignant transformation is dose dependent. Cancer Res 2006 Nov 15;66(22):10786-94.
205. Pietruska JR, Kane AB. SV40 oncoproteins enhance asbestos-induced DNA double-strand breaks and abrogate senescence in murine mesothelial cells. Cancer Res 2007 Apr 15;67(8):3637-45.
206. van Ruth S, Baas P, Zoetmulder FA. Surgical treatment of malignant pleural mesothelioma: a review. Chest 2003 Feb;123(2):551-61.
207. Pass HI, Lott D, Lonardo F, Harbut M, Liu Z, Tang N, et al. Asbestos exposure, pleural mesothelioma, and serum osteopontin levels. N Engl J Med 2005 Oct 13;353(15):1564-73.
208. O'Byrne KJ, Edwards JG, Waller DA. Clinico-pathological and biological prognostic factors in pleural malignant mesothelioma. Lung Cancer 2004 Aug;45 Suppl 1:S45-8.

209. Herndon JE, Green MR, Chahinian AP, Corson JM, Suzuki Y, Vogelzang NJ. Factors predictive of survival among 337 patients with mesothelioma treated between 1984 and 1994 by the Cancer and Leukemia Group B. Chest 1998 Mar;113(3):723-31.

210. Steele JP, Klabatsa A, Fennell DA, Pallaska A, Sheaff MT, Evans MT, et al. Prognostic factors in mesothelioma. Lung Cancer 2005 Jul;49 Suppl 1:S49-52.

211. Vogelzang NJ, Rusthoven JJ, Symanowski J, Denham C, Kaukel E, Ruffie P, et al. Phase III study of pemetrexed in combination with cisplatin versus cisplatin alone in patients with malignant pleural mesothelioma. J Clin Oncol 2003 Jul 15;21(14):2636-44.

212. Sugarbaker DJ, Jaklitsch MT, Liptay MJ. Mesothelioma and radical multimodality therapy: who benefits? Chest 1995 Jun;107(6 Suppl):345S-50S.

213. Sugarbaker DJ, Flores RM, Jaklitsch MT, Richards WG, Strauss GM, Corson JM, et al. Resection margins, extrapleural nodal status, and cell type determine postoperative long-term survival in trimodality therapy of malignant pleural mesothelioma: results in 183 patients. J Thorac Cardiovasc Surg 1999 Jan;117(1):54-63; discussion -5.

214. Sugarbaker DJ, Heher EC, Lee TH, Couper G, Mentzer S, Corson JM, et al. Extrapleural pneumonectomy, chemotherapy, and radiotherapy in the treatment of diffuse malignant pleural mesothelioma. J Thorac Cardiovasc Surg 1991 Jul;102(1):10-4; discussion 4-5.

215. Sugarbaker DJ, Garcia JP, Richards WG, Harpole DH, Jr., Healy-Baldini E, DeCamp MM, Jr., et al. Extrapleural pneumonectomy in the multimodality therapy of malignant pleural mesothelioma. Results in 120 consecutive patients. Ann Surg 1996 Sep;224(3):288-94; discussion 94-6.

216. Linden CJ, Mercke C, Albrechtsson U, Johansson L, Ewers SB. Effect of hemithorax irradiation alone or combined with doxorubicin and cyclophosphamide in 47 pleural mesotheliomas: a nonrandomized phase II study. Eur Respir J 1996 Dec;9(12):2565-72.

217. Gordon W, Jr., Antman KH, Greenberger JS, Weichselbaum RR, Chaffey JT. Radiation therapy in the management of patients with mesothelioma. Int J Radiat Oncol Biol Phys 1982 Jan;8(1):19-25.

218. Berghmans T, Paesmans M, Lalami Y, Louviaux I, Luce S, Mascaux C, et al. Activity of chemotherapy and immunotherapy on malignant mesothelioma: a systematic review of the literature with meta-analysis. Lung Cancer 2002 Nov;38(2):111-21.

219. Rosenberg B, Vancamp L, Krigas T. Inhibition of Cell Division in Escherichia Coli by Electrolysis Products from a Platinum Electrode. Nature 1965 Feb 13;205:698-9.

220. Uchida K, Tanaka Y, Nishimura T, Hashimoto Y, Watanabe T, Harada I. Effect of serum on inhibition of DNA synthesis in leukemia cells by cis- and trans-(Pt (NH3) 2C1(2)). Biochem Biophys Res Commun 1986 Jul 31;138(2):631-7.
221. Mello JA, Lippard SJ, Essigmann JM. DNA adducts of cis-diamminedichloroplatinum(II) and its trans isomer inhibit RNA polymerase II differentially in vivo. Biochemistry 1995 Nov 14;34(45):14783-91.
222. Sorenson CM, Barry MA, Eastman A. Analysis of events associated with cell cycle arrest at G2 phase and cell death induced by cisplatin. J Natl Cancer Inst 1990 May 2;82(9):749-55.
223. Sorenson CM, Eastman A. Influence of cis-diamminedichloroplatinum(II) on DNA synthesis and cell cycle progression in excision repair proficient and deficient Chinese hamster ovary cells. Cancer Res 1988 Dec 1;48(23):6703-7.
224. Williams CJ, Whitehouse JM. Cis-platinum: a new anticancer agent. Br Med J 1979 Jun 23;1(6179):1689-91.
225. Wang Y, Zhao R, Chattopadhyay S, Goldman ID. A novel folate transport activity in human mesothelioma cell lines with high affinity and specificity for the new-generation antifolate, pemetrexed. Cancer Res 2002 Nov 15;62(22):6434-7.
226. Adjei AA. Pemetrexed: a multitargeted antifolate agent with promising activity in solid tumors. Ann Oncol 2000 Oct;11(10):1335-41.
227. Livak KJ, Schmittgen TD. Analysis of relative gene expression data using real-time quantitative PCR and the 2(-Delta Delta C(T)) Method. Methods 2001 Dec;25(4):402-8.
228. Gallagher S, Winston SE, Fuller SA, Hurrell JG. Immunoblotting and immunodetection. Curr Protoc Mol Biol 2008 Jul;Chapter 10:Unit 10 8.
229. Razanajaona D, Joguet S, Ay AS, Treilleux I, Goddard-Leon S, Bartholin L, et al. Silencing of FLRG, an antagonist of activin, inhibits human breast tumor cell growth. Cancer Res 2007 Aug 1;67(15):7223-9.
230. Tabet L, Bussy C, Amara N, Setyan A, Grodet A, Rossi MJ, et al. Adverse effects of industrial multiwalled carbon nanotubes on human pulmonary cells. J Toxicol Environ Health A 2009;72(2):60-73.
231. Nymark P, Lindholm PM, Korpela MV, Lahti L, Ruosaari S, Kaski S, et al. Gene expression profiles in asbestos-exposed epithelial and mesothelial lung cell lines. BMC Genomics 2007;8:62.

232. Pelin K, Kivipensas P, Linnainmaa K. Effects of asbestos and man-made vitreous fibers on cell division in cultured human mesothelial cells in comparison to rodent cells. Environ Mol Mutagen 1995;25(2):118-25.
233. Schulte KM, Jonas C, Krebs R, Roher HD. Activin A and activin receptors in thyroid cancer. Thyroid 2001 Jan;11(1):3-14.
234. Bachman KE, Park BH. Duel nature of TGF-beta signaling: tumor suppressor vs. tumor promoter. Curr Opin Oncol 2005 Jan;17(1):49-54.

12 Curriculum Vitae

Julia Münzker

Date of Birth: 06. 07. 1987

Place of Birth: Vienna

Citizenship: Austrian

E-mail: julia.muenzker@gmail.com

Education:

since 03/2010	diploma student Institute of Cancer Research and Division of Thoracic Surgery, Medical University of Vienna Supervision by Priv. Doz. Michael Grusch and Dr. Mir Ali Reza Hoda
since 03/2007	Diploma study in Biology University of Vienna Specialization: Anthropology (Human Genetics)
10/2005-02/2007	Diploma study in Pharmacy University of Vienna
since 10/2005	Diploma study in Nutritional Sciences University of Vienna
06/2005	Matura, AHS *Maria Regina,* Vienna

Work Experience:

07/2009	Group of Univ.-Prof. Dr Werner Sieghart Medical University of Vienna, Center for Brain Research, Department of Biochemistry and Molecular Biology

Oral Presentations:

07/2011 Deregulation of Activin Signals Contributes to Aggressiveness of Malignant Pleural Mesothelioma Cells. 14th World Concerence on Lung Cancer, IASLC Amsterdam – July 2011